Development of Lipid-Modified Chitinase as a New Antifungal Reagent

プゴフ, サントソ

Development of Lipid-Modified Chitinase as a New Antifungal Reagent

Pugoh Santoso

Department of Chemical Systems & Engineering

Faculty of Engineering

Kyushu University

2022

TABLE OF CONTENTS

Chapter 1 Introduction

1.1 Amphotericin B

Globally, the threat of an alarming increase in fungal infection in various sectors of human health, livestock, and agriculture has exhibited a scary condition. Concerning the human health sector, infectious diseases caused by fungal pathogens accounted for around 1.5 million deaths yearly[1,2]. Individuals immunocompromised and aspergillosis fatally infected by *Candida* and *Aspergillus* species are the most likely to be contributing to a high mortality rate and morbidity rate for decades[3]. In addition, the emergence of antifungal drug-resistant fungi is also a critical issue, and recent studies showed that *A. fumigatus* might be resistant to several commercial antifungal drugs [4,5]. Azole and polyenes groups are widely used to fight fungal infection because they have a broad spectrum of antifungal activity; however, these antifungal drugs are reported to have limitations in dealing with fungal infections[6,7]. For instance, fluconazole only shows its action against the *Blastomyces, Cryptococcus, Histoplasma, Candida*, and *Coccidioides* species, but their activity is low on molds[8,9]. Lastly, amphotericin B (AMB) is the polyenes group where it is widely used to treat a systemic infection.

AMB is a natural antibiotic originating from the actinomycete *Streptomyces nodosus*. It was beginning isolated in 1955 and introduced by Bristol–Myers Squibb in 1958 and was recognized by US Food and Drug Administration (FDA) as the first antifungal in 1965[6]. The most crucial constituent of AMB is its amphiphilic and amphoteric behavior resulting from its polar and polar sides of the lactone ring and ionizable carboxyl and amine groups. It forms soluble salts in acidic and

alkaline media. It is classified in the biopharmaceutics classification system (BCS) class due to its low solubility and permeability. The toxicity, spectrum, and feasible commercial formulations of AmB are described in Fig. 1.1. AMB cooperates with ergosterol in the cell membrane of sensitive fungi, changing its structure and permeability. In addition, the inhibitory effect on *Aspergillus, Cryptococcus neoformans*, *C. albicans,* and *Coccidioides* has also been recognized. It has a high affinity for binding to fungal cell membrane sterols, especially ergosterol (up to 30%, mol/mol), and this consequence responsible for its severe nephrotoxicity because of the interaction with a cholesterol-rich membrane of kidney cells.

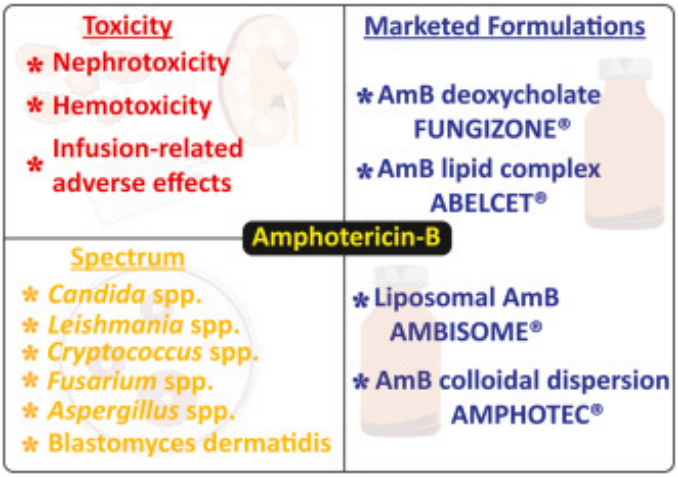

Fig. 1.1 Toxicity, spectrum, and available marketed AMB formulations. Reproduce with permission from Ref. 13. Copyright 2022 Elsevier.

The chemical structure and possible mechanisms of action of AMB on fungal cells are illustrated in Fig. 1.2. Today, the utilization of nanotechnology in the development of Drug Delivery Systems (DDS) for the treatment of various diseases have been shown favorable results. These nanoscale vector systems offer multiple gains over traditional delivery systems, such as protecting encapsulated drugs from degradation and metabolism, enhanced residence time, and improved targeting of specific cells or organs. In line with this situation, the AMB formulations based on nanoparticles (NPs) significantly

diminished the side effects and increased the therapeutic index. NPs including lipid-based, conjugated polymeric NPs dispensing systems, nano-emulsions, and nano-suspensions, based on metals NP and microneedles are considered the most promising DDS for AMB. Consideration of the emergence of antifungal drug resistance-fungi, it is abundantly evident that novel antifungal therapies are urgently needed to combat the pathogenic fungi since there is currently a lack of antimycotics available on the market. For the problem above, the biologically active protein is the best consideration for tackling the problem because it shows an expected low negative effect on human cells.

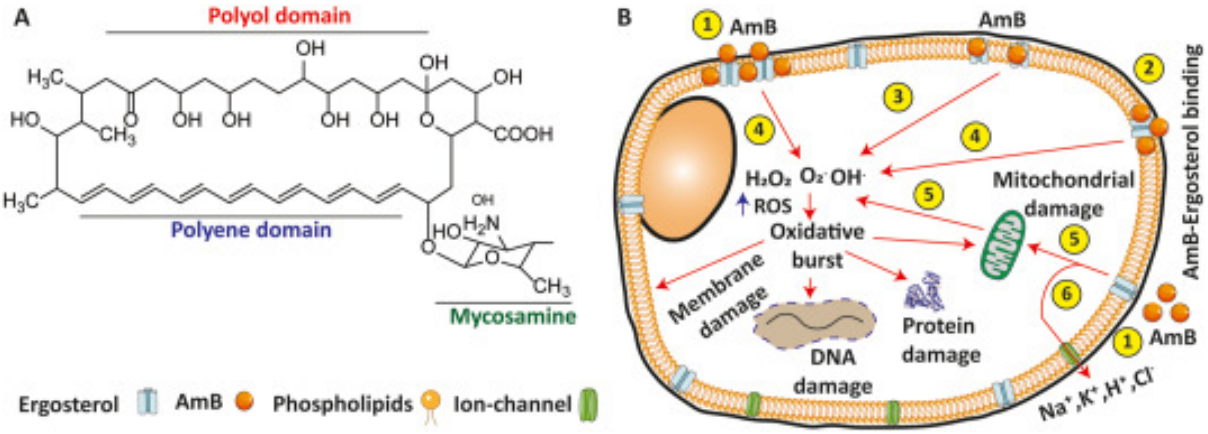

Fig. 1. 2 Chemical structure (A) and mechanism of AMB on the fungal cell (B). AMB generates its action in several ways. On the cell membrane: (1) It interacts with the membrane ergosterol and provides rapid fixation of the ergosterol and (2) interrupts the stability of the membrane. Inside the cell: induces an oxidizing agent bursting as pro-oxidant production and (3) increases reactive oxygen species in the cell. (4) The fabrication of oxygen species (ROS) obtained during the respiratory chain reaction, suggested that AMB influences mitochondrial function and (5) stimulates the oxidative burst. Likewise, (5) AMB can modify cellular ion homeostasis and allow infiltration of monovalent Na^+, K^+, H^+, and Cl^- ions. therefore, the increased level of These free radicals and this ionic imbalance produces multiple deleterious effects on the vital components of the cell (membrane, mitochondria, proteins, and DNA), leading to cell death. Reproduce with permission from Ref. [10]. Copyright 2022 Elsevier.

1.2 Chitinase-based antifungal drug

Over the last several years, there has been a consistent rise in the number of illnesses treated using biologics. Because of the high specificities given by their complex structures, biologics have risen in popularity as a class of therapeutics in recent years. This is mainly because they result in lower toxicity and side effects. Biologically active protein, like an enzyme, is a promising agent that can treat a disease with a low adverse impact because its mode of action is specific to a substrate. Among the biologically active protein based on enzymes, chitinase is currently one of the potential candidates as an antifungal agent targeting the degradation of chitin on the cell walls of fungi. Recently, research on the use of chitinases in medical applications has been described, which has shown encouraging findings, such as the supernatant of chitinase-producing *Bacillus sp*. A14 showed intense antifungal activity against *Fusarium* sp[11]. A class IV chitinase isolated from *Anacardium occidentale* L. was reported to exhibit antifungal activity toward the phytopathogenic fungus *Lasiodiplodia theobromae*, potentially inhibiting its growth by degrading the hyphae[16]. Notably, Medhat and George reported that *Trichoderma viride* chitinase was nontoxic to the human HeLa and HepG2 cell lines, even at a high concentration of chitinase (>120 μg/mL). This chitinase was reported to inhibit the growth of *Fusarium oxysporum* f. sp. *lycopersici race* 3 at 2.13 mg/mL[12].

1.2.1 Classification of chitinase

Chitinase (EC.3.2.1.14), a glycoside hydrolase enzyme, that degrades the β-1,4-linkages in chitin, has been gaining significant attention as an alternative to commercial antifungal agents due to its specific action on the chitin in the fungal cell walls. Chitin is nature's second most prevalent

biopolymer, and it is found in fungi cell wall structures in large quantities. Chitinase and other proteins are produced by the majority of living organisms in nature in order to defend themselves against fungi and insects by destabilizing their chitin barriers. Chitin is a structurally important component of filamentous fungi's cell walls, and it may account for as much as 20% of the wall's total weight when combined with carbohydrates and proteins[13]. In the fungal cell wall, a chitin-rich core is supported by branching β -(1,3): β -(1,6) glucans and an outside layer of proteins and/or polysaccharides, resulting in a three-layered structure: Fungal species all have a common core, however, the outer layer composition changes depending on growing circumstances and life cycle stage[14].

The amino acid sequences and domain designs of chitinases are used to classify them. Chitin polymers are degraded by glycosidases from families 18 and 19. For GH family 18, there are two subfamilies of chitinase isolated from bacteria, A and B, which are characterized by the chitin insertion domain (CID) in subfamily A, and three subfamilies of chitinase produced by the fungi, A, B, and C. Meanwhile, the GH 18 family isolated from plants that generate chitinase is classified into III and V groups. Many physiological activities have been linked to GH18 chitinases, including tissue breakdown, developmental control, pathogenicity, and immunological defense[15]. GH family 19 also includes a lot of information from plant-derived chitinases, such as classes I, II, and IV, which are all dependent on the existence of the chitin-binding domain (CBD). Depending on their method of action, chitinases are classified as endo-chitinase or Exo-chitinase[16]. The endo-hydrolysis of N-acetyl-D-glucosaminide-(1–4) links in chitin and chitodextrins are catalyzed by endo-chitinase (EC 3.2.1.14). Exo-chitinase, on the other hand, may be classified into two classes depending on whether it works on

reducing or non-reducing chitin and chitodextrin chains. The variety of chitinases that have been examined is rather extensive, with molecular sizes ranging from around 14 to 150 kDa, pH ranges from 1.0 to 10.5, optimal temperatures ranging from 18 to 90°C, and multi-domain structures[14].

1.2.2 Strategy to increase the performance of chitinase

Chitinase isolated from *Pteris ryukyuensis* (PrChiA) has been well studied by Dr. Toki Taira and his colleagues. This enzyme has two chitin-binding domains, namely LysM-1 and LysM-2, and a catalytic domain (CatD) connected with a linker of amino acids[17]. The LysM domains of PrChiA function as a chitin-binding domain (ChBD). Takashima *et al*. revealed that tandemly arranged LysM without the CatD has been shown to exhibit antifungal activity[17]. They have proposed a mechanism for how tandem LysM multimers achieve the lysis of *T. viride* at the tips of hyphae. The key point of the proposed mechanism is the bridging of different chitin chains by the LysM multimers[17]. The bridging of chitin chains by a LysM multimer prevents the cell wall at the tip of hyphae from stretching, and as the cell growth continues, the internal cell pressure increases. When the internal cell pressure reaches the limit of the cell, the rupture will occur at the tip of the hyphae to lyse the cells. In this model, a covalently connected multimer of LysM is essential. However, the antifungal activity of PrChiA and its domains is not sufficient for use as a practical antifungal agent, and they need to be administered at high concentrations to exert antifungal activity. To improve the antifungal activity of chitinase, Minamihata *et al.* [18] prepared a LysM-grafted CatD polymer, which had increased activity[18]. The CatD was genetically engineered, and peptide tags containing a tyrosine residue (Y-tag) and tyrosine and lysine residues (KY-tag) were introduced to the N- and C-termini, respectively.

The Tyr residues in the peptide tags were recognized by horseradish peroxidase and formed radicals, and subsequently, a CatD polymer was formed by the coupling of the Tyr radicals. Then, LysM with a peptide tag containing a microbial transglutaminase-reactive glutamine residue (Q-tag) was grafted onto the CatD polymer. The LysM-grafted CatD polymer showed superior activity compared with wild-type ChiA, demonstrating that the engineering of chitinase can be used to improve antifungal activity. From this finding, the conjugation catalyzed by biocatalyst, specifically microbial transglutaminase, gave a promising result with the expected enhancement performance of chitinase.

Microbial transglutaminase (EC 2.3.2.13) is a transferase enzyme that catalyzes the reaction between an acyl donor of a glutamine residue with an acceptor donor of a lysine residue in all proteins to form γ-glutamyl-ε-lysine isopeptide linkage (Fig 1.3). The mechanism of reaction catalyzed by microbial transglutaminase (MTG) is a nucleophilic substitution (SN1) reaction that produces two intermediate products to form γ-glutamyl-ε-lysine isopeptide linkage as the target product. The mechanism reaction started from the sulfur atom of microbial transglutaminase as a nucleophilic, which riches the free electron. This nucleophilic attacks the electrophile of carbonyl groups on glutamine, and it causes the oxygen electron of a carbonyl group (glutamine) to be negatively charged; then, the first intermediate product is formed with the positively charged on the sulfur atom, and the ammonia is released. In this process, the electron from oxygen forms a double bond then the nucleophilic nitrogen atom attacks the electrophile of the hydrogen atom, which binds to the sulfur.

The second mechanism reaction is the formation of the second intermediate product by using the nucleophile, ε-amino group of lysine (K), attacking the electrophile of carbonyl to the first intermediate

product. Then the oxygen atom breaks one of its double bonds, and it forms a negatively charged oxygen atom. In the second intermediate product, the electron from oxygen atoms enters to form a double bond, breaking the carbon and sulfur bonds. Furthermore, the sulfur atom's nucleophile attacks the hydrogen's neighboring electrophile that bonds with the nitrogen atom. In the final process, the reaction product of γ-glutamyl-ε-lysine isopeptide linkage is formed, and the microbial transglutaminase is released to its initial state.

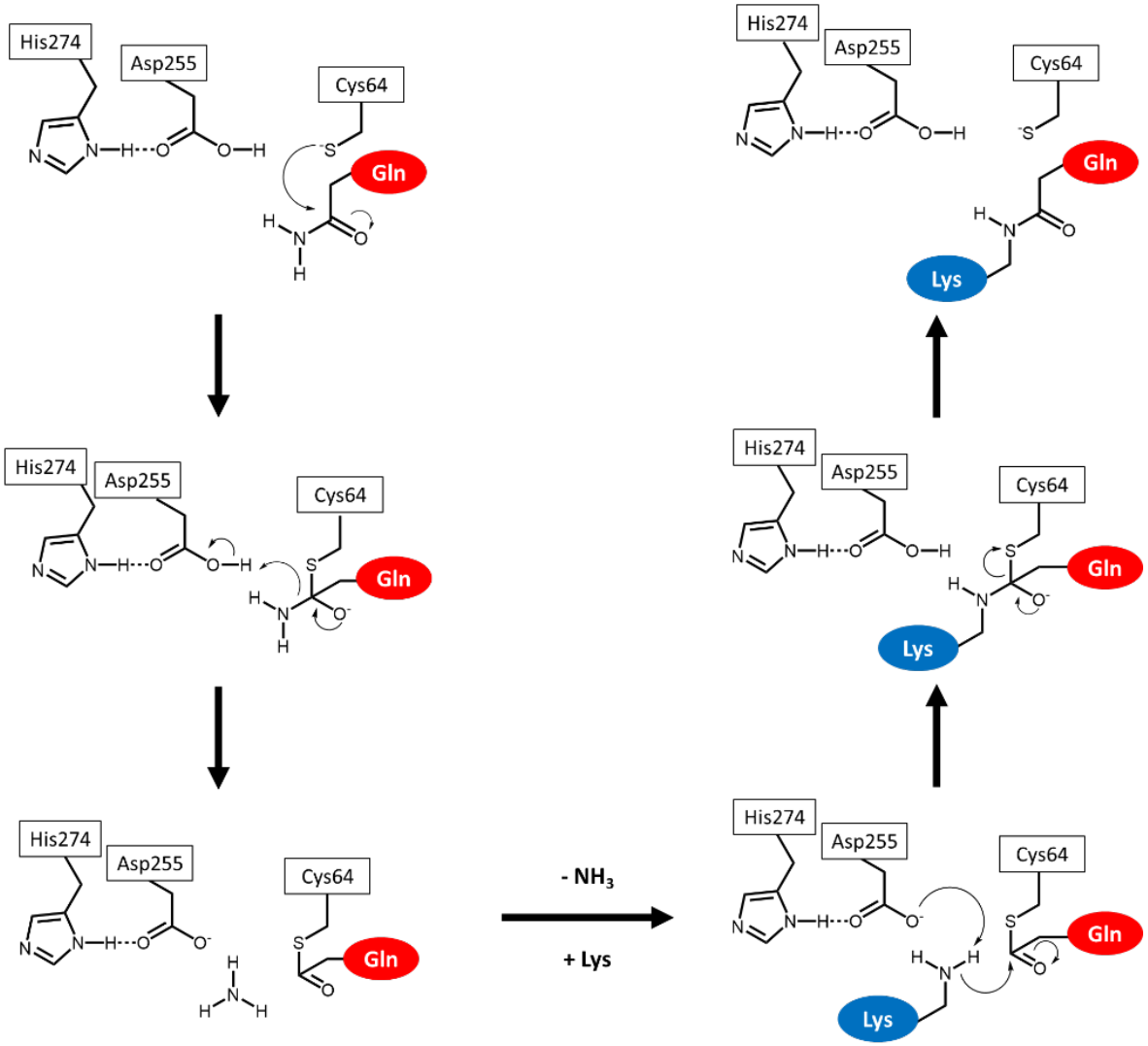

Fig.1.3. Mechanism reaction of iso-peptide bond formation between glutamine (Q) as acyl donors and lysine (K) as acyl acceptors.

The ability to perform conjugation, which is specifically controlled by MTG, offers a fantastic opportunity to make proteins of interest, such as chitin-binding domain-grafted chitinase for antifungal[18], polymer collagen-based hydrogels for tissue engineering and cancer therapy[19], neoepitope complexes that are potentially pathogenic in celiac disease[20], and protein identification via avidin-biotin interaction[21]. In addition to this, the use of MTG for conjugation in the realm of therapeutic or diagnostic applications against antibody conjugation investigations and thyroid-stimulating hormone will be successful with low needs for both reaction and reagents[22]. MTG has also been capable of conjugating proteins and a DNA aptamer that can detect cancer cells through the interaction with c-Met receptor[23]. Additionally, the use of MTG has been more prevalent in the field of biomedicine[24].

1.3 Aim and outline of the thesis

Although a number of publications already reported the potency of chitinase as an antifungal candidate, in fact, the antifungal activity of chitinase to inhibit fungal growth still needs a high dose, and the mechanism of action is affected by the chitin-binding domain; meanwhile, there is a class chitinase that does not have a chitin-binding domain. In addition, the rigidity of the chitin structure and the complexity of fungal cell walls make the chitinase can not work optimally. To address this limitation, the current study intends to improve the antifungal activity of chitinase by artificial lipidation approach, investigate its synergistic effect on AMB, a commercial gold-standard antifungal drug widely used to treat fungal infection, and incorporate a liposomal formulation. Furthermore, to know the localization of membrane integrity caused by the chitin-binding domain (LysM), the author

evaluated the effect of lipidated LysM using fluorescently labeled-LysM and propidium iodide staining, respectively.

The combination strategy and the application of liposomes in this study have been expected to reduce intrinsic toxicity due to the decreased AMB concentration required in the application and the encapsulation into liposomes; meanwhile, the conjugation of chitinase with lipids aimed to make chitinase easily inserts into the cell walls of fungi, and the lipid moiety binds to the fungal membrane cells. Hence, chitinase can directly bind the target, i.e., the chitin content on the fungal cell walls, resulting in increased antifungal activity. Protein lipidation is a unique cotranslational or posttranslational modification that plays a critical role in cell signaling and dynamically regulates protein functions in response to extrinsic and intrinsic cues such as biological functions, including regulation of cellular trafficking[25], signaling[26] and various transport activities[27].

Lipidation modulates the function of targeted proteins by increasing their binding affinity to biological membranes, rapidly switching their subcellular localizations, affecting folding and stability, and modulating association with other proteins. Proteins can be covalently modified by at least six types of lipids, including fatty acids, isoprenoids, sterols, phospholipids, glycosylphosphatidylinositol (GPI) anchors, and lipid-derived electrophiles (LDEs). Recent advances in detecting lipidated proteins used proteomic and targeted approaches. They have revealed that lipidation of signaling proteins is essential for regulating a wide variety of signaling pathways[28]. According to the location of the modified proteins, lipidation can be divided into two types: those that are modified in the ER lumen and secreted modified in the cytoplasm or on the cytoplasmic face of the membrane. The former type

includes glycosylphosphatidylinositol (GPI) anchor and cholesterylation, and the latter includes N-myristoylation, acylation, and prenylation. Hence, the study was segmented into three separate projects sequel to achieve the above research goals. The subsequent chapters of this thesis will provide a more in-depth discussion of each project. The current thesis has a total of 5 chapters: an overall introduction (Chapter 1), a discussion of the research accomplishments (Chapters 2, 3, and 4), and a summary (Chapter 5). A list of references is included in each chapter's conclusion.

In chapter 1, a general introduction of the current status of fungal infection was explained. In this case, the commercial antifungal drug, specifically amphotericin B, was chosen as the mode of the antifungal drug due to its broad-spectrum activity towards several fungal pathogens and its limitation. Additionally, according to the scientific literature, the author briefly introduced the application of chitinase as a safe antifungal candidate and the application of microbial transglutaminase in the bioconjugation application for pharmaceutical studies.

In chapter 2, the author discussed the role of the chitin-binding protein of chitinase from *Pteris ryukyuensis* on the synergistic effect on each antifungal activity of domain chitinase and its antifungal activity against *Trichoderma viride*. The chitinase was constructed into a chitin-binding domain (LysM), catalytic domain (CatD), inactive catalytic domain (CatD(E247Q)), and chitin-binding domain-fused catalytic domain (LysM-CatD) by adding a flexible linker containing glutamine-tag (Q-tag) at the C-terminus to construct Q-tag chitinase. In addition, the palmitic acid-peptide containing MTG-reactive lysine (lipid-K) was prepared and purified using Fmoc solid-phase peptide synthesis. The introduction of the peptide on the palmitic acid (Pal) was proposed to enhance the solubility of

Pal in the water, which can efficiently improve the conjugation process between chitinase and Pal. MTG cross-links the recombinant chitinase and K-tagged palmitic acid (Pal-K) in the conjugation reaction to yield palmitoylated chitinase. The performance and proposed mode of action of palmitoylated chitinase and chitinase combined with or without AMB in suppressing the *Trichoderma viride* growth were systematically evaluated in this chapter.

Chapter 3 discussed the effect of palmitoylation in improving the antifungal activity shown in chapter 2. To support the result of palmitoylated chitinase, the author decided to choose LysM mutant as a model chitinase because this mutant exhibited the highest antifungal activity compared with the others. The localization and membrane integrity was analyzed using fluorescently labeled-LysM and propidium iodide staining, respectively. In comparison, the LysM was conjugated with lipids comprising different alkyl chain lengths (octanoic acid, C8 and dodecanoic acid, C12) catalyzed by microbial transglutaminase. Both LysM and lipids were engineered by adding the reactive glutamine-tag (Q-tag) and lysine-tag (K-tag), cross-linked by MTG.

Chapter 4 discussed the effect of liposomal formulation of AMB integrated with palmitoylated LysM in combating *T. viride*. The behaviour of liposomal-encapsulated AMB in combination with palmitoylated chitinase was studied and explained in detail.

In chapter 5, The study's results are provided with an overview of its accomplishments. In addition, the author presented a concise view of the future possibilities of this work for use in the pharmaceutical industry in the battle against fungal infections.

References

(1) Liu, W.; Yuan, L.; Wang, S. Recent Progress in the Discovery of Antifungal Agents Targeting the Cell Wall. *J. Med. Chem.* **2020**, *63* (21), 12429–12459.

(2) Lionakis, M. S. Primary Immunodeficiencies and Invasive Fungal Infection: When to Suspect and How to Diagnose and Manage. *Curr. Opin. Infect. Dis.* **2019**, 531–537.

(3) Lee, Y.; Puumala, E.; Robbins, N.; Cowen, L. E. Antifungal Drug Resistance: Molecular Mechanisms in *Candida Albicans* and Beyond. *Chem. Rev.* **2021**, *121* (6), 3390–3411.

(4) Escribano, P.; Rodríguez-Sánchez, B.; Díaz-García, J.; Martín-Gómez, M. T.; Ibáñez-Martínez, E.; Rodríguez-Mayo, M.; Peláez, T.; García-Gómez de la Pedrosa, E.; Tejero-García, R.; Marimón, J. M.; Reigadas, E.; Rezusta, A.; Labayru-Echeverría, C.; Pérez-Ayala, A.; Ayats, J.; Cobo, F.; Pazos, C.; López-Soria, L.; Alastruey-Izquierdo, A.; Muñoz, P.; Guinea, J.; Sánchez-Yebra, W.; Sánchez-Gómez, J.; Lozano, I.; Marfil, E.; Muñoz de la Rosa, M.; García, R. T.; Castro, C.; López, C.; Castelló-Abietar, C.; Costales, I.; Serra, J. L.; Jiménez, R.; Echeverría, C. L.; Pérez, C. L.; Megías-Lobón, G.; Lorenzo, B.; Sánchez-Reus, F.; Martín, M. T.; Vidal, I.; Sánchez-Hellín, V.; Ibáñez, E.; Pemán, J.; Fajardo, M.; Gómez, E.; Serrano, J.; Rodríguez, B.; Zvezdanova, E.; Gómez-Núñez, A.; Leiva, J. G.; Machado, M.; Sánchez-Romero, I.; García-Rodríguez, J.; Luis del Pozo, J.; Vallejo, M. R.; Ruiz de Alegría-Puig, C.; Vicente, D.; Fernández-Torres, M.; Hernáez-Crespo, S. Azole Resistance Survey on Clinical Aspergillus Fumigatus Isolates in Spain. *Clin. Microbiol. Infect.* **2021**, *27* (8), 1170.e1-1170.e7.

(5) Satish, S.; Perlin, D. S. Echinocandin Resistance in Aspergillus Fumigatus Has Broad Implications for Membrane Lipid Perturbations That Influence Drug-Target Interactions . *Microbiol. Insights* **2019**, *12*, 1-4

(6) Cavassin, F. B.; Baú-Carneiro, J. L.; Vilas-Boas, R. R.; Queiroz-Telles, F. Sixty Years of Amphotericin B: An Overview of the Main Antifungal Agent Used to Treat Invasive Fungal Infections. *Infect. Dis. Ther.* **2021**, *10* (1), 115–147.

(7) Lelièvre, L.; Groh, M.; Angebault, C.; Maherault, A. C.; Didier, E.; Bougnoux, M. E. Azole Resistant Aspergillus Fumigatus: An Emerging Problem. *Med. Mal. Infect.* **2013**, *43* (4), 139–145.

(8) Pardasani, A. Oral Antifungal Agents Used in Dermatology Triazoles : Fluconazole and Itraconazole. Curr. *Probl. Dermatol.* **2000**. 12 (6), 270-275.

(9) Bartlett, J. G. Guidelines for Treatment of Candidiasis. *Infect. Dis. Clin. Pract.* **2004**, *12* (4),

245–246.

(10) Wang, X.; Mohammad, I. S.; Fan, L.; Zhao, Z.; Nurunnabi, M.; Sallam, M. A.; Wu, J.; Chen, Z.; Yin, L.; He, W. Delivery Strategies of Amphotericin B for Invasive Fungal Infections. *Acta Pharm. Sin. B* **2021**, *11* (8), 2585–2604.

(11) Cd, D.; Lb, V.; Ma, M.; Md, B. Extracellular Antifungal Activity of Chitinase-Producing Bacteria Isolated From Guano of Insectivorous Bats. *Curr. Microbiol.* **2021**, *78* (7), 2787–2798.

(12) Abu-Tahon, M. A.; Isaac, G. S. Anticancer and Antifungal Efficiencies of Purified Chitinase Produced from Trichoderma Viride under Submerged Fermentation. *J. Gen. Appl. Microbiol.* **2020**, *66* (1), 32–40.

(13) Hartl, L.; Zach, S.; Seidl-Seiboth, V. Fungal Chitinases: Diversity, Mechanistic Properties and Biotechnological Potential. *Appl. Microbiol. Biotechnol.* **2012**, *93* (2), 533–543.

(14) Berini, F.; Katz, C.; Gruzdev, N.; Casartelli, M.; Tettamanti, G.; Marinelli, F. Microbial and Viral Chitinases: Attractive Biopesticides for Integrated Pest Management. *Biotechnol. Adv.* **2018**, *36* (3), 818–838.

(15) Huang, Q. S.; Xie, X. L.; Liang, G.; Gong, F.; Wang, Y.; Wei, X. Q.; Wang, Q.; Ji, Z. L.; Chen, Q. X. The GH18 Family of Chitinases: Their Domain Architectures, Functions and Evolutions. *Glycobiology* **2012**, *22* (1), 23–34.

(16) Rajput, M.; Kumar, M.; Pareek, N. Myco-Chitinases as Versatile Biocatalysts for Translation of Coastal Residual Resources to Eco-Competent Chito-Bioactives. *Fungal Biol. Rev.* **2022**.

(17) Takashima, T.; Sunagawa, R.; Uechi, K.; Taira, T. Antifungal Activities of LysM-Domain Multimers and Their Fusion Chitinases. *Int. J. Biol. Macromol.* **2020**, *154*, 1295–1302.

(18) Minamihata, K.; Tanaka, Y.; Santoso, P.; Goto, M.; Kozome, D.; Taira, T.; Kamiya, N. Orthogonal Enzymatic Conjugation Reactions Create Chitin Binding Domain Grafted Chitinase Polymers with Enhanced Antifungal Activity. *Bioconjug. Chem.* **2021**, *32* (8), 1688–1698.

(19) Li, X.; Fan, D. Smart Collagen Hydrogels Based on 1-Ethyl-3-Methylimidazolium Acetate and Microbial Transglutaminase for Potential Applications in Tissue Engineering and Cancer Therapy. *ACS Biomater. Sci. Eng.* **2019**, *5* (7), 3523–3536.

(20) Aaron, L.; Torsten, M. Microbial Transglutaminase: A New Potential Player in Celiac Disease. *Clin. Immunol.* **2019**, *199* (December 2018), 37–43.

(21) Spolaore, B.; Damiano, N.; Raboni, S.; Fontana, A. Site-Specific Derivatization of Avidin Using Microbial Transglutaminase. *Bioconjug. Chem.* **2014**, *25* (3), 470–480.

(22) Steffen, W.; Ko, F. C.; Patel, J.; Lyamichev, V.; Albert, T. J.; Benz, J.; Rudolph, M. G.; Bergmann, F.; Streidl, T.; Kratzsch, P.; Boenitz-dulat, M.; Oelschlaegel, T.; Schraeml, M. Discovery of a Microbial Transglutaminase Enabling Highly Site-Specific Labeling of Proteins. *J. Biol. Chem.* **2017**, *292* (38), 15622–15635.

(23) Takahara, M.; Wakabayashi, R.; Minamihata, K.; Goto, M.; Kamiya, N. Primary Amine-Clustered DNA Aptamer for DNA-Protein Conjugation Catalyzed by Microbial Transglutaminase. *Bioconjug. Chem.* **2017**, *28* (12), 2954–2961.

(24) Savoca, M. P.; Tonoli, E.; Atobatele, A. G.; Verderio, E. A. M. Biocatalysis by Transglutaminases: A Review of Biotechnological Applications. *Micromachines* **2018**, *9* (11), 9–11.

(25) Resh, M. D. Trafficking and Signaling by Fatty-Acylated and Prenylated Proteins. *Nat. Chem. Biol.* **2006**, *2* (11), 584–590.

(26) Casey, P. J. Protein Lipidation in Cell Signaling. *Science (80-.).* **1995**, *268* (5208), 221–225.

(27) Stenmark, H. Rab GTPases as Coordinators of Vesicle Traffic. *Nat. Rev. Mol. Cell Biol.* **2009**, *10* (8), 513–525.

(28) Ray, A.; Jatana, N.; Thukral, L. Lipidated Proteins: Spotlight on Protein-Membrane Binding Interfaces. *Prog. Biophys. Mol. Biol.* **2017**, *128*, 74–84.

Chapter 2 Enhancement of the Antifungal Activity of Chitinase by Palmitoylation and the Synergy of Palmitoylated Chitinase with Amphotericin B

2.1 Introduction

The problems caused by fungal infections in the agriculture, livestock, and human health sectors have increased at an alarming level. Fungal infections account for approximately 1.5 million deaths worldwide[1,2]. The numbers of cases of fungal infections increase every year, and the discovery of new pathogenic strains, particularly antibiotic-resistant strains[3,4], causes problems in the treatment of infections. In the past few decades, azoles, echinocandin, and amphotericin-B (AMB) have been widely used to treat fungal infectious diseases[5]. AMB has been considered to be the gold standard of antifungal medications because it has a broad fungicidal activity spectrum[6]. The antifungal activity of AMB is a result of several different modes of action[7]. The primary mechanism is the interaction of AMB with ergosterol in the fungal cell membrane to form small pores on the plasma membrane, whereby small ions leak out through these pores, resulting in the death of the fungi. Other reported mechanisms of AMB are the sequestration[8] and extraction of ergosterol[9,10] to destabilize the plasma membrane and the induction of oxidative stress[11]. However, AMB also interacts weakly with cholesterol—an analogue of ergosterol used in mammalian cell membranes—and exerts similar destructive effects on mammalian cells, resulting in strong toxicity when prescribed at high concentrations. Therefore, it is desirable to develop safer antifungal drugs[12] or methods to combine AMB with other antifungal agents to reduce the required dosage of AMB[13,14,15].

Recently, chitinase has attracted attention as a safe alternative to existing antifungal drugs[16, 17, 18, 19, 20]. Chitinase degrades the chitin that constitutes the cell wall of fungi. Because human and animal cells do not contain chitin, the activity of chitinase is not expected to cause damage to the cells; thus, chitinase is considered to be safe for use in humans and animals. In addition, because chitinase exerts its antifungal activity by disrupting the chitin in the cell wall structures, the development of chitinase-resistant fungi is unlikely to occur. If chitinase can be used in combination with AMB to exert higher antifungal activity, the dose of AMB may be able to be decreased, resulting in a decrease in the side effects caused by AMB, and this combination may be a useful method for treating fungal infections. Other researchers also investigated the combination of AMB with some antimycotic agents[21,22]. For instance, the combination of 4-(5-methyl-1,3,4-thiadiazole-2-yl) benzene-1,3-diol (C1) with AMB to combat several pathogenic fungi has been reported in improving antifungal activity. The minimum inhibitory concentration (MIC) value of all pathogenic fungi differs depending on the concentration of C1. The MIC values of individual AMB and C1 for *Candida albicans* isolate 102 were 0.5 and 32 μg/mL, respectively. On contrary, the MIC value of AMB decreased to 0.25 μg/mL when the C1 was added at a concentration of 2 μg/mL, indicating that the antifungal activity drastically improved by combining C1and AMB[23].

PrChiA is a chitinase from the fern *Pteris ryukyuensis*, which is characterized by a tandem arrangement of two lysin motifs (LysM) at the N-terminus of the catalytic domain (CatD)[24,25]. The LysM domains of PrChiA function as a chitin-binding domain (ChBD), and tandemly arranged LysM without the CatD has been shown to exhibit antifungal activity[26]. However, the antifungal activity of

PrChiA and its domains is not sufficient for use as an antifungal agent, and they need to be administered at high concentrations to exert antifungal activity. To improve the antifungal activity of chitinase, Minamihata *et al.* previously prepared a LysM-grafted CatD polymer, which had increased activity[27]. Briefly, the CatD was genetically engineered, and peptide tags containing a tyrosine residue (Y-tag) and tyrosine and lysine residues (KY-tag) were introduced to the N- and C-termini, respectively. The Tyr residues in the peptide tags were recognized by horseradish peroxidase and formed radicals, and subsequently a CatD polymer was formed by the coupling of the Tyr radicals. Then, LysM with a peptide tag containing a microbial transglutaminase (MTG)-reactive glutamine residue (Q-tag) was grafted onto the CatD polymer. The LysM-grafted CatD polymer showed superior activity compared with wild-type ChiA, demonstrating that the engineering of chitinase can be used to improve the antifungal activity. In this context, the author aimed to combine AMB with chitinases engineered to perform well with AMB for the synergistic enhancement of antifungal activity.

To design a chitinase compatible with AMB, the author proposed to lipidate chitinase. Lipidation of a protein is expected to increase the hydrophobicity of the protein and increase its affinity to the cell membrane. Lipidation can also enhance the bioavailability of proteins because of an extension of the circulation time in vivo caused by the interaction of the lipid with albumin[28,29]. Recently, Takahara *et al.* have successfully demonstrated the lipidation of enhanced green fluorescent protein (EGFP) using an MTG-catalyzed, cross-linking reaction between a Q-tag at the C-termini of EGFP and various types of lipidated peptides containing an MTG-reactive lysine residue (Lipid-K)[30,31]. The lipidated EGFP anchored to the plasma membrane of mammalian cells with different efficiencies depending on the

type of lipid. In addition, artificially lipidated EGFP has been shown to have a prolonged half-life in vivo[32]. Because AMB is a highly hydrophobic drug, it is usually used in a micellar formulation solubilized with deoxycholic acid. Thus, it is of great interest to create a lipidated chitinase and examine whether it has a synergistic effect with the micellar formulation of AMB.

Herein, the author constructed Q-tagged LysM (LysM-Q), CatD (CatD-Q), and a chimera of LysM and CatD (LysM-CatD-Q) (Figure 1A), which were modified with a palmitoylated Lys-containing peptide (Pal-K) using the MTG reaction (Figure 1B). Palmitic acid was selected as the lipid because it has shown sufficient ability to anchor to the plasma membrane with only moderate toxicity toward mammalian cells[31]. The author anticipated that the palmitoylated chitinase domains would efficiently interact with the plasma membrane of fungi and exert antifungal effects by the anchoring of the palmitic acid motif to cells and binding the chitinase domains to and degrading the chitin in the fungal cell wall. Concomitantly, AMB would exert its antifungal effects by interacting with ergosterol in the plasma membrane of the fungi. The author evaluated possible synergistic effects between the palmitoylated chitinase domains and AMB to enhance the antifungal activity (Figure 1C).

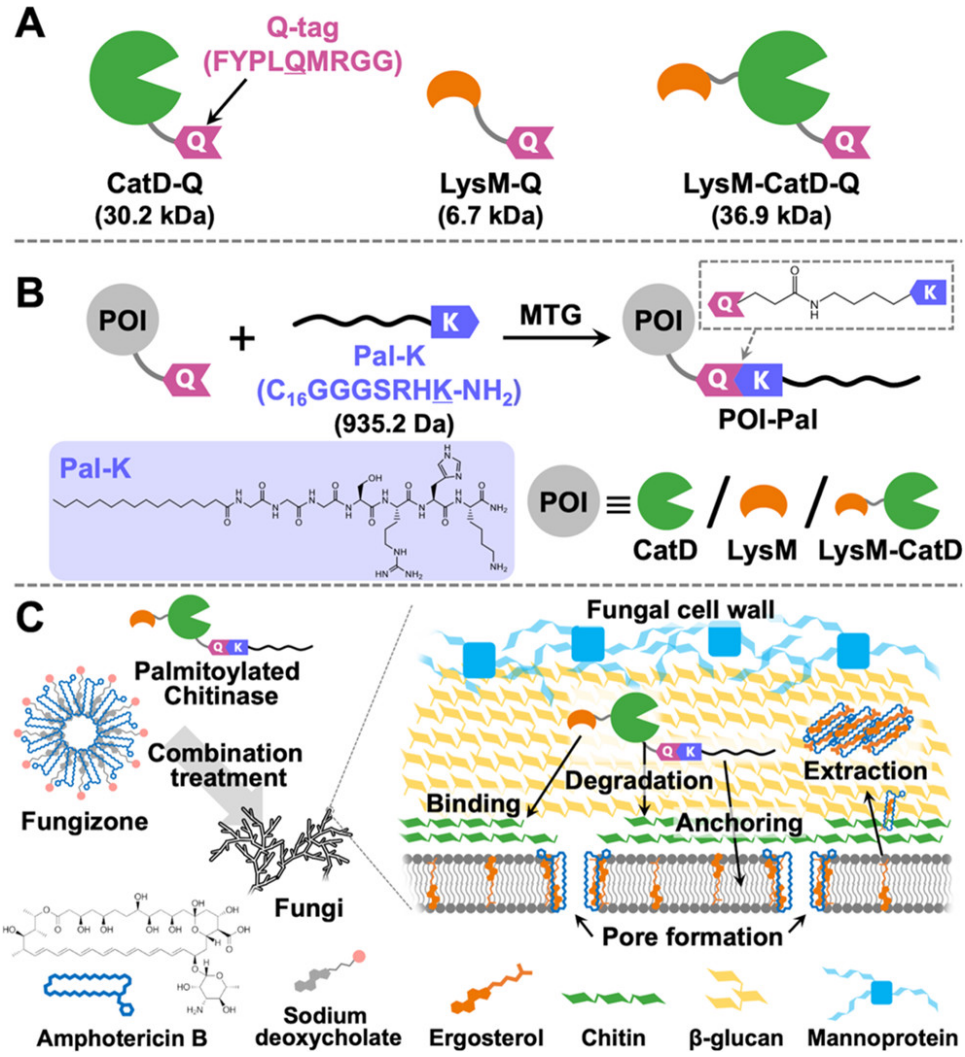

Figure. 2.1. Combined treatment of fungal infections with AMB and chitinases. (A) Schematic illustrations of the chitinase domains from the *P. ryukyuensis* chitinase used in this study. All chitinase domains were tagged with a peptide tag containing an MTG-reactive glutamine residue (Q-tag: FYPLQMRGG) at the C-termini. CatD: catalytic domain; LysM: a ChBD lysine motif. (B) Palmitoylation reaction of the Q-tagged POI catalyzed by MTG. (C) Schematic illustration of the combined treatment of fungi by AMB and palmitoylated chitinases. Fungizone is a commercially available formulation of AMB in which poorly soluble AMB is solubilized by sodium deoxycholate. AMB binds to ergosterol in the cell membrane of fungi and forms pores in the membrane, leading to the leakage of ions. AMB also forms large extracellular aggregates that extract ergosterol from the cell membrane. The palmitoylated chitinase is anticipated to interact with fungi by binding to and degrading the chitin in the cell wall and by anchoring the lipid to the cell membrane. Reproduce with permission from ref [33]. Copyright 2022 American Chemical Society.

2.2 Experimental

2.2.1 Materials.

SDS, glycerol, potassium dihydrogen phosphate, and sodium chloride were purchased from Wako Pure Chemical Industries, Ltd. (Osaka, Japan). Luria–Bertani (LB) broth medium, ammonium peroxodisulfate, 30% acrylamide/bis mixed solution (29:1), tris (hydroxymethyl) aminomethane, tryptone, dried yeast extract, dipotassium hydrogen phosphate, and hydrochloric acid were purchased from Nacalai Tesque, Inc. (Kyoto, Japan). *N*,*N*,*N*′,*N*′-Tetramethylethylenediamine, HisTrap FF crude 5 mL column, HiTrap Q HP column, PD SpinTrap G-25, and Ni Sepharose 6 Fast Flow were purchased from Cytiva (Tokyo, Japan). Amicon Ultra, Amicon Ultra-0.5 mL, and Amicon Ultra-15 mL were purchased from Millipore (Tokyo, Japan). Imidazole was purchased from Sigma-Aldrich (Tokyo, Japan). All chemicals were used without any further purification. The palmitoylated MTG-reactive peptide containing lysine (Pal-K) was synthesized by Fmoc solid-phase peptide synthesis and purified following a previous report[31]. Gibco AMB containing 250 μg of AMB and 205 μg of sodium deoxycholate was purchased from Thermo Fisher Scientific. MTG was expressed as a zymogen bearing the propeptide with mutations of K9R and Y11A in *Escherichia coli* BL21(DE3). A purification tag $(HN)_6$-tag was introduced to the N-terminus of the propeptide, and the tobacco etch virus (TEV) protease recognition sequence (ENLYFQG) was introduced between the propeptide and the matured MTG domain. After brief purification of the MTG zymogen using Ni-NTA column purification, the MTG zymogen was treated with the TEV protease to cleave the propeptide as well as

the $(HN)_6$-tag. The matured MTG was then purified from the eluted fraction of another round of Ni-NTA column purification.

2.2.2 Expression of Chitinase Domains

The author used four types of engineered chitinase domains, namely, LysM-Q, CatD-Q, CatD(E247Q)-Q, and LysM-CatD-Q, from *P. ryukyuensis* chitinase. The amino acid sequences of these proteins are listed Table 2.1. The expression vector of these proteins was constructed using pET22b+, and *E. coli* BL21 (DE3) Star was used as a host for expression. The expression vector was transformed into *E. coli* BL21 (DE3) Star by a heat shock method (42 °C, 30 s), and after 1 h of recovery culture in SOC medium, the cells were cultured on LB agar medium containing 100 μg/mL of ampicillin sodium. The single colony was picked up and inoculated into 5 mL of sterile LB medium containing 100 μg/mL of ampicillin sodium, and then the cells were cultured at 37 °C, 190 rpm for 6 h. The precultured medium was transferred to 500 mL of sterile terrific broth medium containing 100 μg/mL of ampicillin sodium, and then the cells were cultured at 37 °C and 190 rpm until the OD_{600} reached 0.5. Isopropyl-β-D-thiogalactopyranoside was added to the medium to a final concentration of 0.1 mM to induce protein expression, and the cells were further cultured at 18 °C, 190 rpm for 18 h. The cells were collected by centrifugation at 5000*g* for 20 min, and the cell pellets were suspended in Tris-buffered saline (TBS), pH 7.4 and then pelleted again by centrifugation to remove the residual components from the medium. The cell pellets were resuspended in 30 mL of TBS, pH 7.4 and kept at −80°C until purification.

2.2.3 Purification of Chitinase Domains

The frozen cell suspension was thawed on ice, and the cells were lysed by sonication. The cell extract was centrifuged at 20,000 *g* at 4°C for 20 min, and the supernatant containing the target proteins was collected. After filtration by a 0.45 μm syringe filter, the supernatant was injected into a HisTrap FF crude column 5 mL (Cytiva) pre-equilibrated with HisTag binding buffer [20 mM Tris-HCl buffer (pH 7.4), 500 mM NaCl, and 35 mM imidazole]. The column was washed with approximately 50 mL of the HisTag binding buffer, and then the target proteins were eluted by gradient elution of HisTag elution buffer [20 mM Tris-HCl buffer (pH 7.4), 500 mM NaCl, and 500 mM imidazole] from 0 to 100%. The fractions containing the target proteins were collected and desalted into 10 mM Tris-HCl (pH 8.0) using a HiPrep 26/10 desalting column (Cytiva). The desalted solution was then injected into a HiTrap Q HP 5 mL column, which was equilibrated with 10 mM Tris-HCl (pH 8.0). After washing with the buffer until all unbound proteins were eluted out, the target protein was eluted using a gradient of the same buffer containing 500 mM NaCl. The fractions containing the target proteins were collected and concentrated using an ultrafiltration membrane (3 kDa MWCO for LysM-Q and 10 kDa MWCO for CatD-Q and LysM-CatD-Q). The purified proteins were aliquoted and kept at −80°C until use. The protein concentrations were determined by measuring the absorbance at 280 nm and calculating the molar extinction coefficients, which were estimated from the amino acid sequences of each protein.

2.2.4 Chitinase Activity Assays

The chitinase activity against soluble glycol chitin was measured using the procedure of Takashima *et al*[26] with slight modification. A solution of glycol chitin (50 μL; 0.2% w/v) was preincubated in 20 mM acetate buffer (pH 5) at 37 °C for 10 min. Then, 10 μL of chitinase (final concentration of 0.2 μM) was added to each tube. The solution was incubated at 37°C for 15 min, and 1 mL of ferri/ferrocyanide reagent (0.5 g/L potassium ferricyanide/0.5 M sodium carbonate) was added to the reaction[34]. The mixture was heated at 99 °C for 15 min, and then the color change of the solution was measured at 420 nm (UV–vis spectrophotometer V-570, JASCO, Tokyo, Japan). The standard curve for quantification of the generated reducing sugar was made using *N*-acetylglucosamine. Chitinase activity against insoluble chitin was measured using two substrates, α-chitin nanofiber (CNF) and chitin powder. A suspension of 0.2% α-CNF in 20 mM acetate buffer (pH 5) was treated with 1 μM chitinases at 37 °C for 15 min. In the assay using chitin powder, 0.5% chitin powder in 20 mM acetate buffer (pH 5) was treated with 1 μM chitinases at 37 °C for 3 h. The amount of generated reducing sugar was measured as described above.

2.2.5 Palmitoylation of Q-Tagged Proteins with Pal-K by MTG

The conjugation of proteins with Pal-K was conducted in a total reaction volume of 500 μL using a previously reported procedure[31]. Briefly, 100 μM C16-GGGSRHK, 10 μM Q-tagged proteins, 1% *n*-dodecyl-β-D-maltoside (DDM), and 0.1 U/mL MTG were mixed in 10 mM Tris-HCl buffer (pH 7.4) and incubated at 37 °C for 1 h. Then. *N*-ethylmaleimide was added to the solution to a final concentration of 1 mM to quench the MTG reaction.

2.2.6 Purification of Palmitoylated Proteins

Purification of the protein of interest (POI) conjugates was carried out by batch purification using Ni-Sepharose 6 Fast Flow resin as reported by Takahara et al. Briefly, 300 μL of a 50% slurry of Ni-Sepharose resin was equilibrated with HisTag binding buffer (10 mM Tris-HCl, 0.5 M NaCl, 20 mM imidazole, pH 7.4) and added to the solution of palmitoylated proteins. The suspension was mixed by a tube rotator at room temperature for 1 h. The suspension was centrifugated at 2000*g* and 4 °C for 5 min, and the supernatant was removed. The resin was resuspended in 300 μL of HisTag binding buffer and then centrifuged again under the same conditions. This washing step was repeated five times. 90 μL of HisTag elution buffer (20 mM Tris-HCl, 0.5 M NaCl, 1 M imidazole, pH 7.4) was added to the resin to elute the palmitoylated proteins. The suspension was centrifuged at 2000*g* and 4 °C for 5 min, and the supernatant containing the palmitoylated proteins was collected. Finally, the buffer was exchanged into 10 mM Tris-HCl (pH 7.4) using a PD SpinTrap G25 column. The purified palmitoylated proteins were stored in a low-protein-binding tube, PROTEOSAVE (Sumitomo Bakelite Co., Ltd, Tokyo, Japan), and kept at −80 °C until use. The palmitoylation of the proteins was analyzed by SDS-PAGE analysis, and the molecular weight measurements were obtained from MALDI-TOF-MS.

2.2.7 Antifungal Activity Assay of Chitinases with AMB Formulation

The antifungal assays were performed in a 96-plate reader by adding AMB at concentrations from 0 to 5 μM. *T. viride* was added to the antifungal assay at a concentration of 10,000 spores/mL, 1 μM chitinases or Pal-K was added, and the plates were incubated at 25 °C for 60 h. The OD values derived

from the grown fungi were measured either using ImageJ to measure the intensity of the image of each well or using a microplate reader to measure the OD at 630 nm. Images of *T. viride* in a 96-well plate were captured at 60 h of cultivation using a digital camera device. The color images of the 96 well plate were converted to grayscale (8 bits; the gray level range: 0–255) maps to black and white images using ImageJ program (version 1.46) (imagej.nih.gov/ij/download.html). Intensity from each grayscale image was measured with the ImageJ program.

2.3 Result and discussion

2.3.1 Palmitoylation of Q-Tagged Chitinase Domains by MTG

The Q-tagged chitinase domains were conjugated with Pal-K by the MTG reaction. Sodium dodecyl sulfate-polyacrylamide gel electrophoresis (SDS-PAGE) analysis of the palmitoylated proteins showed band shifts to the higher-molecular-weight regions (Figure 2.2A). In all Q-tagged chitinase domains, there was only a single band after the MTG conjugation reaction, suggesting that there was no formation of multiple products. The matrix-assisted laser desorption ionization time-of-flight mass spectrometry (MALDI-TOF-MS) analysis of the palmitoylated chitinase domains showed a shift in the m/z values before and after the conjugation reaction, and the $\Delta m/z$ value was close to the theoretical $\Delta m/z$ value of 917.2 corresponding to modification with a single molecule of Pal-K (Figure 2.2 B-D). These results indicated that although there are 3, 19, and 22 intrinsic glutamine (Gln) residues in LysM-Q, CatD-Q, and LysM-CatD-Q, respectively (Table. 2.1), MTG did not recognize these intrinsic Gln residues and palmitoylation occurred specifically at the reactive Gln residue in the Q-tag. The overall yields of palmitoylated chitinases were less than 20% and the loss of chitinases occurred

during the purification processes. The purified palmitoylated chitinases were relatively stable, and no significant losses were observed during storage in solution form.

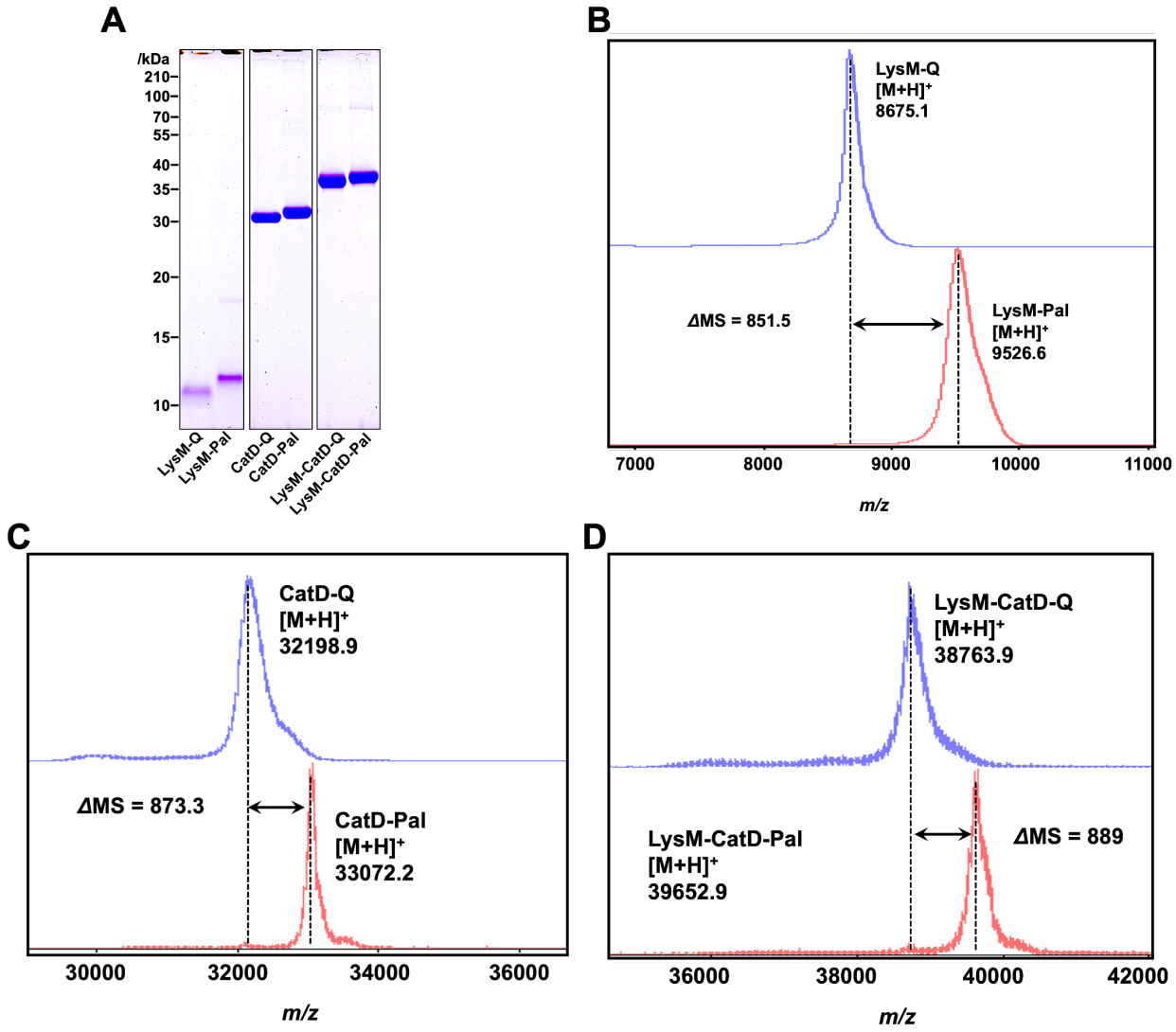

Figure 2.2. Palmitoylation of the Q-tagged chitinase domains. (A) SDS-PAGE analysis results of unmodified chitinase and chitinase modified with Pal-K by MTG. All conjugation reactions were carried out under conditions of 10 μM Q-tagged chitinase domains, 1% DDM, 10 μM Pal-K, and 0.1 U/mL MTG in 10 mM Tris-HCl (pH 8.0) at 37 °C for 1 h. The amount of reducing sugar in the reaction mixture was measured using ferri/ferrocyanide reagent. MALDI-TOF-MS spectra analysis of unmodified and modified of (B) LysM-Q, (C) CatD-Q, and (D) LysM-CatD-Q. The theoretical ΔMS for modification with PAL-K is 917.2 *m/z*. Reproduce with permission from ref [33]. Copyright 2022 American Chemical Society.

Table 2.1 Amino acid sequence of chitinase mutans.

LysM-Q	MCTTYTIKSGDTCYAISQARGISLSDFESWNAGIDCNNLQIGQVVC VSKPSTSTTPSPTPSSSSNGFYPLQMRGGHHHHHH
CatD-Q	MKVFREYIGALYNGVQFTDVPINSGVTFHFILAFAIDYTSAAAAT NGVFNIYWQNSVLTPAAVQAIKAQHSNVKVMVSLGGDTISGSPV QFTATSVSSWVANAVSSLTSLINQYHLDGIDIDYEHFDQVSTSTFV SCIGQLITQLKANNVISVASIAPFDGVESQYTALFGQYSSVIDLVNF QFYSYGAGTSASQYVSLYNTAASKYGGGAKVLASFSTGGVGPAP STVLSACQQLKSSGTLPGIFIFSADGSYASSAKFQYEQQAQTLLTS PSTSTTPSPTPSSSSNGFYPLQMRGGHHHHHH
CatD(E247Q)-Q	MKVFREYIGALYNGVQFTDVPINSGVTFHFILAFAIDYTSAAAAT NGVFNIYWQNSVLTPAAVQAIKAQHSNVKVMVSLGGDTISGSPV QFTATSVSSWVANAVSSLTSLINQYHLDGIDIDYQHFDQVSTSTFV SCIGQLITQLKANNVISVASIAPFDGVESQYTALFGQYSSVIDLVNF QFYSYGAGTSASQYVSLYNTAASKYGGGAKVLASFSTGGVGPAP STVLSACQQLKSSGTLPGIFIFSADGSYASSAKFQYEQQAQTLLTS PSTSTTPSPTPSSSSNGFYPLQMRGGHHHHHH
LysM-CatD-Q	MCTTYTIKSGDTCYAISQARGISLSDFESWNAGIDCNNLQIGQVVC VSKPSTSTTPSPTPSSSSNGKVFREYIGALYNGVQFTDVPINSGVTF HFILAFAIDYTSAAAATNGVFNIYWQNSVLTPAAVQAIKAQHSNV KVMVSLGGDTISGSPVQFTATSVSSWVANAVSSLTSLINQYHLDG IDIDYEHFDQVSTSTFVSCIGQLITQLKANNVISVASIAPFDGVESQ YTALFGQYSSVIDLVNFQFYSYGAGTSASQYVSLYNTAASKYGG GAKVLASFSTGGVGPAPSTVLSACQQLKSSGTLPGIFIFSADGSYA SSAKFQYEQQAQTLLTSPSTSTTPSPTPSSSSNGFYPLQMRGGHHH HHH

The author further examined the chitinolytic activity of the CatD-Q and LysM-CatD-Q mutants toward soluble glycol chitin to examine whether the palmitoylation affected the activity (Figure 2.3A). CatD-Pal and LysM-CatD-Pal exhibited the same level of chitinolytic activity compared with the nonpalmitoylated compounds. When the insoluble substrates, α-chitin and chitin powder, were used as substrates, LysM-CatD-Q exhibited higher chitinolytic activity than CatD-Q because of the chitin-binding ability of the LysM domain (Figure 2.3 B-C). The palmitoylation did not affect the degradation activity toward insoluble chitins for either CatD-Q or LysM-CatD-Q. Therefore, the author concluded

that the palmitoylation of the Q-tagged chitinase domains catalyzed by MTG did not affect the function of either the LysM or CatD domains.

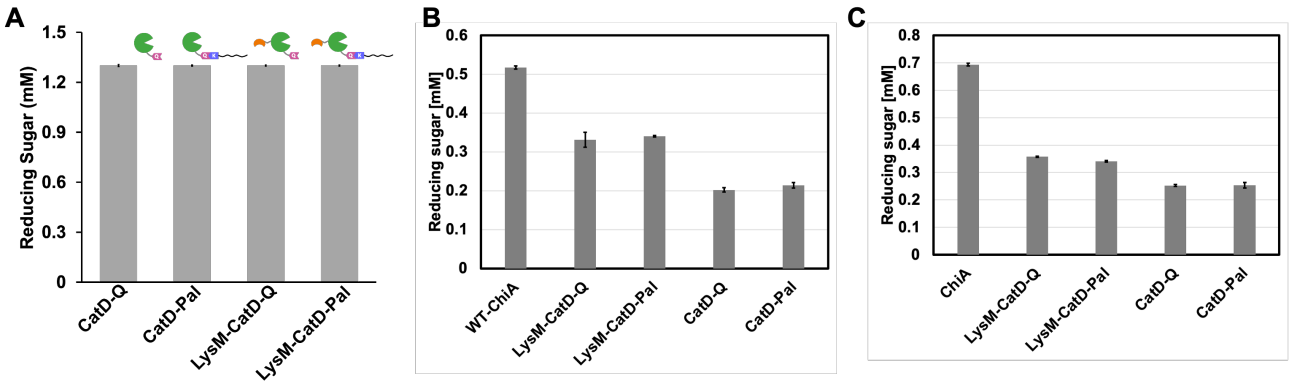

Figure 2.3 Measurement of the amount of reducing sugar generated after degradation of insoluble chitin by chitinases. **A**. The chitinolytic activity of the chitinase domains, with or without palmitoylation toward the soluble chitin substrate, glycol chitin. Glycol chitin solution (0.2% w/v) was treated with 0.2 μM chitinase in 20 mM acetate buffer (pH 5) at 37 °C with shaking at 180 rpm for 15 min. **B**. The chitinase activity of catalytic domain toward 0.2% of the α-CNF substrate using 1 μM of chitinase in 20 mM of acetate buffer (pH 5) at 37°C, with shaking at 180 rpm for 15 minutes. **C**. The degradation of 0.5% chitin powder using 1 μM of chitinase domains in 20 mM of acetate buffer (pH 5) at 37°C, with shaking at 180 rpm for 3 hours. After addition of ferri/ferrocyanide reagent (0.5 g/L potassium ferricyanide/0.5 M sodium carbonate), the solution was heated at 99˚C for 15 min and the then the color change of solution was measured at 420 nm. Reproduce with permission from ref [33]. Copyright 2022 American Chemical Society.

2.3.2 Antifungal Activity of Palmitoylated Chitinase Domains

First, the author investigated the antifungal activity of the Q-tagged chitinase domains and the palmitoylated chitinase domains without AMB. Figure 2.4 shows the results of the antifungal activity assay against *Trichoderma viride*. The unmodified chitinase domains did not inhibit the growth of *T. viride* over the tested concentration range of 0–4 μM. In contrast, all palmitoylated chitinase domains except inactive CatD mutant, CatD(E247Q)-Pal, showed antifungal activity at concentrations ≥1 μM, and the MIC against *T. viride* was estimated to be <2 μM (Figure 2.4 A).

The half-maximal inhibitory concentration (IC_{50}) value of LysM-CatD (without Q-tag) has been previously reported to be approximately 93 μM[26]. The IC_{50} values of LysM and CatD were much higher than that of LysM-CatD and were not able to be determined[26]. Here, the IC_{50} values of LysM-Pal, CatD-Pal, and LysM-CatD-Pal were estimated to be approximately 1 μM (Figure 2.4B). From these results, it was clear that the palmitoylation of the chitinase domains dramatically increased the antifungal activity of the chitinase domains. However, because palmitoylated LysM, CatD, and LysM-CatD all showed a similar level of antifungal activity, the increased antifungal activity might be derived simply from the palmitic acid motif and not from the actions of the chitinase domains. Indeed, while the unmodified CatD(E247Q)-Q did not show any antifungal activity against *T. viride*, the palmitoylated version had antifungal activity but at a lower level compared with active CatD-Pal. Thus, the antifungal activity of the palmitoylated proteins could involve the protein functions of the LysM and CatD domains but was mainly caused by the direct effect of the palmitic acid motif toward *T. viride*.

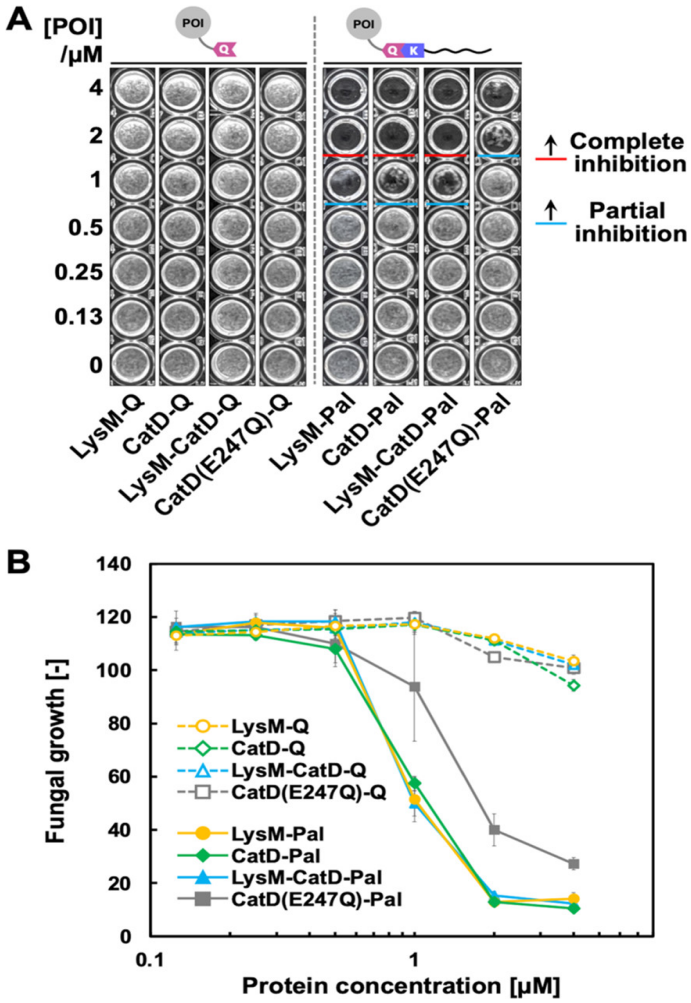

Figure 2.4. Antifungal activity of palmitoylated chitinase domains. (A) 96-well plate after culturing *T. viride* in the presence of 0–4 μM POIs at 25 °C for 60 h. (B) Quantitative measurement results of fungal growth treated with the POIs shown in (A). The optical density of each well was measured from the photograph of the 96-well plate using ImageJ. The IC_{50} values for LysM-Pal, CatD-Pal, LysM-CatD-Pal, and CatD(E247Q)-Pal were estimated from the Rodbard mode curve fitting using ImageJ, and the values were 0.98, 0.96, 0.98, and 1.33 μM, respectively. The error bars represent standard deviation (n = 3). Reproduce with permission from ref [33]. Copyright 2022 American Chemical Society.

2.3.3 Antifungal Activity of CatD-Q and CatD-Pal in Combination with AMB

The antifungal activities of CatD-Q and CatD-Pal in combination with AMB were evaluated, and the results are shown in Figure 2.5. AMB alone inhibited the growth of *T. viride* at concentrations >2.5 μM (Figure 2.5A, lane blank). The addition of 1 μM unmodified CatD-Q enhanced the antifungal activity, and the fungal growth was completely inhibited at an AMB concentration of 1.25 μM. CatD-

Q alone did not inhibit the growth of *T. viride* even at a concentration of 4 μM (Figure 2.4A). Therefore, CatD-Q and AMB acted synergistically to increase the antifungal efficacy. CatD-Pal further increased the antifungal activity compared with CatD-Q, and complete growth inhibition of *T. viride* was achieved at an AMB concentration of 0.63 μM. However, 1 μM CatD-Pal without AMB inhibited the growth of *T. viride* at a comparable level (Figure 2.4 and see Figure 2.7 for comparison), indicating that the synergistic effect of AMB with CatD-Pal is not obvious. This implied that palmitoylation exhibited an inhibitory effect on the antifungal activity of CatD-Q. Note that the palmitoylation did not affect the chitin degradation activity of CatD (Figure 2.3), meaning that the antifungal activity is not directly equivalent to chitin degradation activity. The *T. viride* cells that survived treatment with CatD-Pal showed an aggregated appearance, indicating that the cell walls of *T. viride* were being affected by the CatD and palmitic acid motif (Figure 2.5A, inset). The addition of Pal-K slightly increased the antifungal activity and decreased the cell density (Figure 2.5B); however, the MIC value of AMB was not decreased by the addition of Pal-K alone (Figure 2.5). These results suggested that covalently connecting the palmitic acid and CatD-Q was essential for the antifungal effect of the palmitoyl motif.

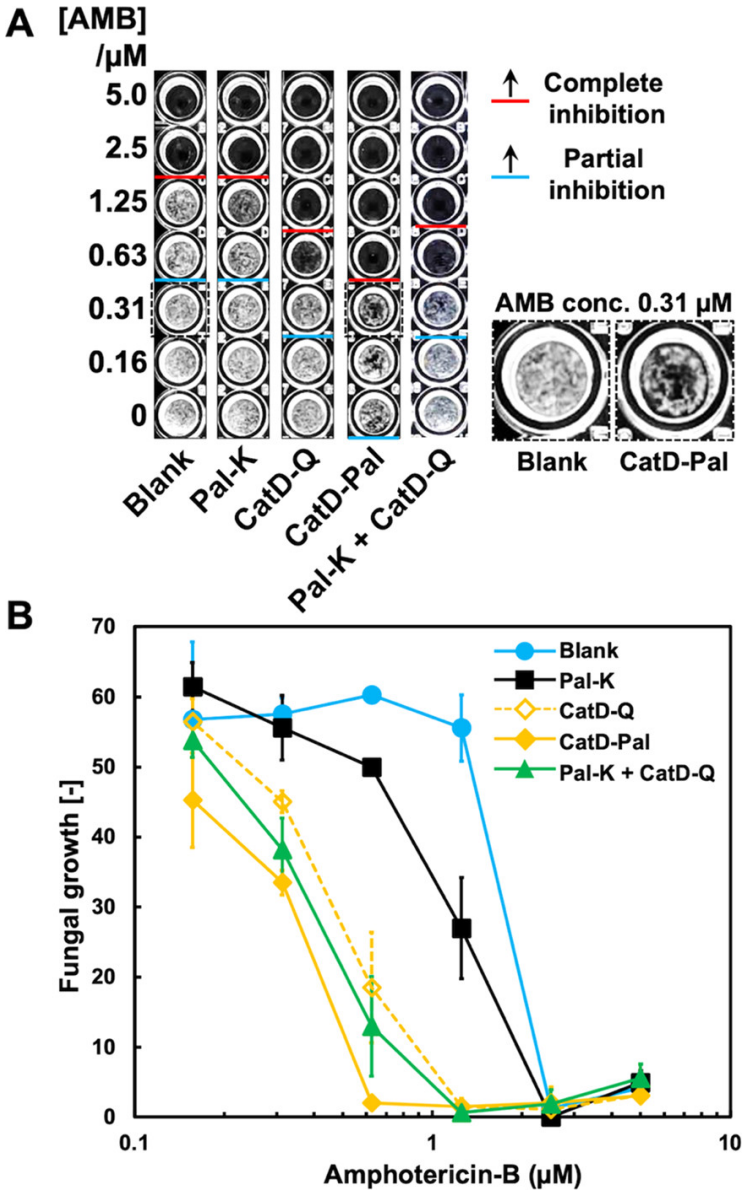

Figure 2.5. Antifungal activity of CatD-Q combined with AMB. (A) Antifungal activity of the unmodified and modified catalytic domain with serial concentrations of AMB. Red lines represent the MIC, and blue lines represent the concentrations at which the growth of *T. viride* was partially inhibited. The enlarged images of wells treated with 0.31 μM AMB and CatD-Pal are shown in the inset. Blank samples are the wells treated solely with AMB. (B) Fungal growth curve of *T. viride* treated with CatD-Q with and without palmitoylation. The fungal growth of each well was estimated as an image intensity by densitometry using ImageJ program. The concentration of CatD-Q was fixed at 1 μM, and all experiments were carried at 25 °C for 60 h (n = 3). The concentration of Pal-K in the sample of CatD-Q + Pal-K was 1 μM. The images of the 96-well plates of all experiments are shown in Figure S2.3. Reproduce with permission from ref [33]. Copyright 2022 American Chemical Society.

2.3.4 Antifungal Activity of Unmodified and Ipidated Chitinase Domains Containing LysM in Combination with AMB

Next, the author evaluated the antifungal activity of unmodified and palmitoylated LysM-Q and LysM-CatD-Q combined with AMB (Figure 2.6). Intriguingly, the palmitoylated LysM-Q, LysM-Pal exhibited the highest antifungal activity among all samples tested (Figure 2.6). The MIC value of AMB with 1 μM LysM-Pal was as low as 0.31 μM, and the growth of *T. viride* was strongly inhibited even at 0.16 μM AMB. Because the MIC value of AMB alone is approximately 2.5 μM, the addition of LysM-Pal enhanced the antifungal activity by an order of magnitude. Unmodified LysM-Q also increased the antifungal activity of AMB at a level comparable to that of CatD-Pal (Figure 2.5A). The combination of Pal-K and LysM-Q slightly reduced the fungal growth, but the MIC value was unchanged, which was consistent with the results for CatD-Q in combination with Pal-K as shown in Figure 2.5. Therefore, the covalent conjugation of Pal-K with the chitinase protein is the key factor for the strong enhancement of antifungal activity in combination with AMB.

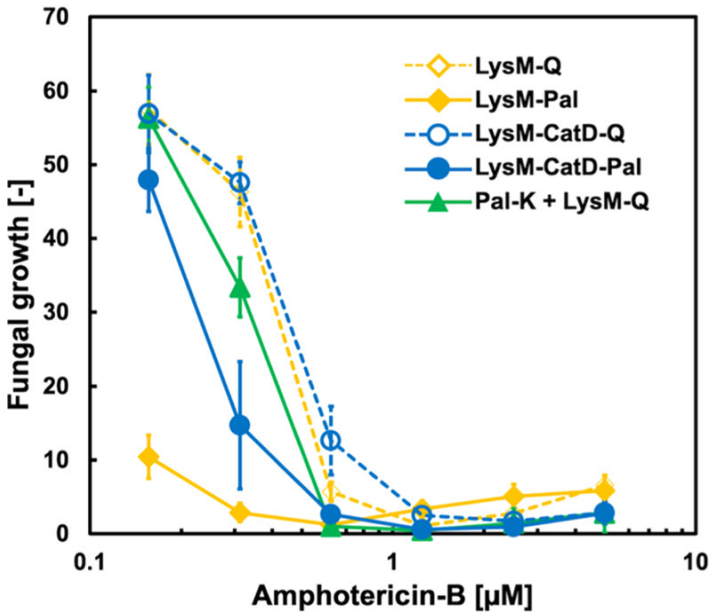

Figure 2.6. Fungal growth curve of *T. viride* treated with palmitoylated and unmodified LysM-Q and LysM-CatD-Q. The fungal growth of each well was estimated as an image intensity by densitometry using ImageJ program. The concentration of protein samples was fixed at 1 μM, and all experiments were carried at 25 °C for 60 h (n = 3). The concentration of Pal-K in the sample of LysM-Q + Pal-K was 1 μM. The images of the 96-well plates of all experiments are shown in Figure 2.7. Reproduce with permission from ref [33]. Copyright 2022 American Chemical Society.

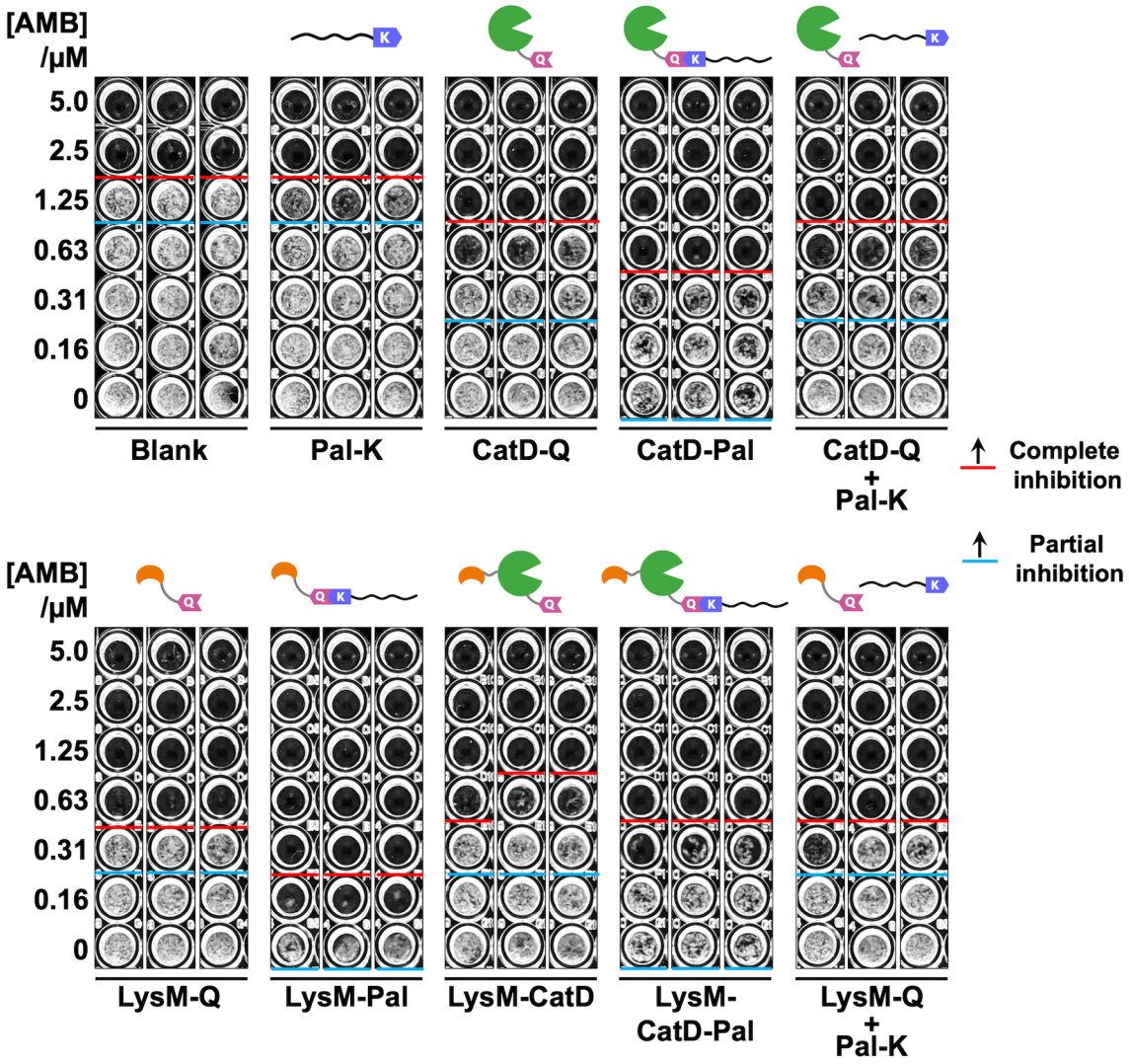

Figure 2.7 The picture of all antifungal activity assay results is shown in Figures 2.5 and 2.6. The experiments were conducted in triplicate (n=3) in 96-well different microplates. Red lines represent the minimum inhibitory concentration (MIC) and blue lines represent the concentrations at which growth of *Trichoderma viride* was partially inhibited. Reproduce with permission from ref [33]. Copyright 2022 American Chemical Society.

One study has reported that conjugation of LysM and CatD domains increased the antifungal activity against fungi compared with the individual domains[35]. Contrary to expectation, treatment with LysM-CatD-Q resulted in a comparable level of antifungal activity to LysM-Q. Moreover, LysM-CatD-Pal showed lower antifungal activity compared with LysM-Pal (Figure 2.6). In contrast, the antifungal activities of LysM-CatD-Q and LysM-CatD-Pal were higher than those of CatD-Q and CatD-Pal, respectively (Figure 2.5). From these results, it can be implied that the antifungal activity of LysM was higher than that of CatD when combined with AMB, and CatD competitively inhibited the antifungal activity of LysM.

To further examine the synergistic antifungal effect of AMB combined with palmitoylated chitinase domains, the author conducted an antifungal activity assay changing the concentrations of both AMB and the palmitoylated chitinase domains (Figure 2.8). Again, LysM-Pal exhibited higher antifungal activity than CatD-Pal and LysM-CatD-Pal, indicating that the presence of CatD decreased the antifungal activity of the LysM domain. LysM-CatD-Pal showed slightly higher antifungal activity than CatD-Pal, as can be seen from the wells treated with 0.62 μM AMB. Therefore, the LysM domain in LysM-CatD-Pal exerted weak antifungal activity. The MIC values of AMB and LysM-Pal alone against *T. viride* were estimated to be approximately 2.5 μM (Figure 2.5) and 2 μM (Figure 2.4), respectively. The combination of 0.31 μM AMB with 0.5 μM LysM-Pal achieved complete inhibition of *T. viride*, indicating that the synergistic antifungal activity of AMB and LysM-Pal resulted in a dramatic reduction in the MIC value.

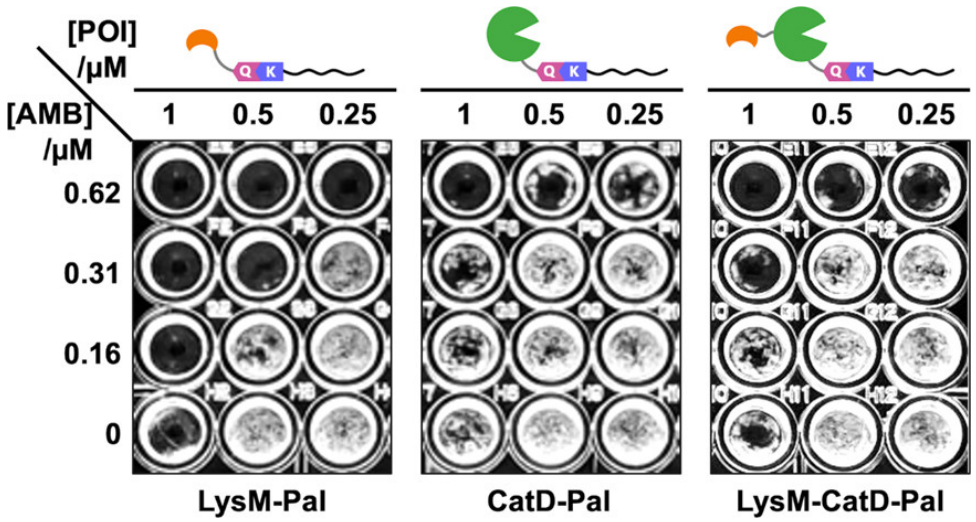

Figure 2.8. Antifungal activity assay using different concentrations of AMB and the palmitoylated chitinases. The concentrations of LysM-Pal, CatD-Pal, and LysM-CatD-Pal were varied in the range 0.25–1 μM, while the concentration of AMB was varied in the range 0–0.62 μM. *T. viride* was cultured in each well at 25 °C for 60 h. Reproduce with permission from ref [33]. Copyright 2022 American Chemical Society.

From this research, the conjugation of chitinase with Pal-K could enhance the antifungal activity, and the chitinase conjugates exhibited a synergistic effect with amphotericin B. Compounds from living organisms often exhibit biological activities and possess the potentials to be used in medical applications[36,37]. Chitinase, a glycoside hydrolase enzyme, has been gaining significant attention as an alternative to commercial antifungal agents due to its specific action on chitin in the fungal cell walls. Recently, several studies on medical applications of chitinases have been reported showing promising results, such as the supernatant of chitinase-producing *Bacillus sp*. A14 showed intense antifungal activity against *Fusarium* sp[38].

In this study, a synergistic antifungal effect was demonstrated with the combination of AMB with palmitoylated chitinase domains, especially LysM-Pal. In previous research, the IC_{50} value of LysM-

CatD against *T. viride* has been reported to be 93 ± 10.9 μM[26]. Here, monomeric LysM-Q, CatD-Q, and LysM-CatD-Q exhibited an enhancement of the antifungal activity of AMB even at a concentration of 1 μM, which was far lower than the individual IC_{50} values, implying that there was a synergistic effect between the antifungal activity of the chitinase domains and AMB (Figure 2.5 and 2.6). All palmitoylated chitinase domains showed the same level of antifungal activity without AMB (Figure 2.4). LysM-Pal exhibited the highest level of antifungal activity enhancement when combined with AMB. However, the CatD-Pal and LysM-CatD-Pal resulted in less synergistic effect with AMB than LysM-Pal (Figure 2.5–2.8). A proposed mechanism for the synergistic effect of LysM-Pal and AMB is summarized in Figure 2.9.

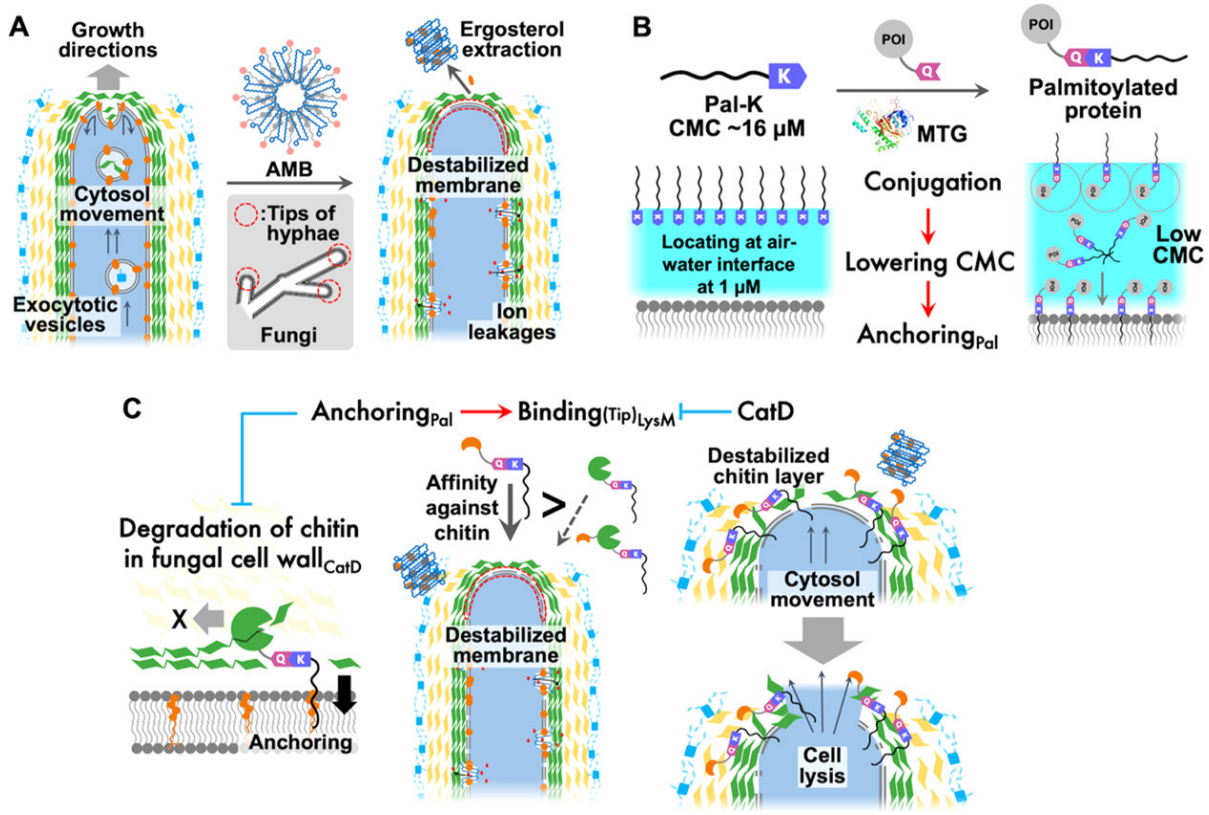

Figure 2.9. Proposed mechanism for the synergistic enhancement of antifungal activity observed with the combination of AMB and palmitoylated chitinase domains. The red lines represent an enhancement effect, and the blue lines represent an inhibitory effect. The subscripts, Pal, CatD, and LysM, represent the molecules that are responsible for the functions to which the subscripts are appended. (A) Destabilization of the cell wall structure by AMB. AMB attacks from the tips of the hyphae where the cell wall structure is being constructed and the cell membrane is exposed. AMB forms pores in the cell membrane by interacting with ergosterol. AMB forms aggregate called sterol-sponges that extract ergosterol from the cell membrane and destabilize the cell membrane, especially at the tip. (B) Conjugation of Q-tagged proteins with Pal-K lowers the CMC of Pal-K, facilitating the anchoring of the palmitic acid motif to the cell membrane of fungi. The CMC value of Pal-K has been reported to be approximately 16 μM[32]. (C) Anchoring of palmitic acid to the cell membrane enhances the binding of LysM to the chitin layer. Palmitoylation could possibly inhibit the movement of CatD and reduce the degradation activity of chitin in the fungal cell wall. It has been reported that fusing CatD to LysM weakens the chitin-binding ability of LysM[24]. LysM-Pal affects the tip of hyphae and destabilizes the chitin layer at the tip where the cell membrane was destabilized by AMB and anchoring of palmitic acid, resulting in cell lysis. Reproduce with permission from ref [33]. Copyright 2022 American Chemical Society.

Possible mechanisms for the antifungal effect against *T. viride* observed in this study are as follows: (1) destabilization of the cell membrane by AMB; (2) anchoring of the palmitic acid motif to the cell membrane; (3) binding of LysM to chitin; and (4) degradation of chitin by CatD. First, AMB affects the cell wall structure of *T. viride* by interacting with the ergosterol in the cellular membrane and forming pores through which intracellular ions leak out. (7) AMB has also been proposed to exert antifungal activity by several modes of action, including the sequestration of ergosterol leading to disruption of the membrane stability[39], the induction of oxidative bursts within fungi by directly acting as a prooxidant, (7) and by causing mitochondrial damage[40]. In addition, a sterol-sponge model[9,10] has been proposed in which AMB forms a self-assembled aggregate, the sterol-sponge, that extracts ergosterol from the cell membrane. The cell wall structures of fungi consist of multilayers of mannoprotein, β-glucan, and chitin and the plasma membrane (Figure 2.1C), and these multilayers are believed to prevent AMB and chitinases from interacting with the plasma membrane and chitins, respectively. In studies using *C. albicans*, one study has reported that AMB binds preferably to the plasma membrane of cells at the budding stage, during which cell wall structures are being generated and loosened[23]. The tips of the fungi hyphae are the sites where cell wall structures are being constructed; thus, the cell membranes at the tip of the hyphae can be exposed. Moreover, the curvature of the plasma membrane at the tip of hyphae is considerably high, thus the plasma membrane at the tip requires high flexibility. Ergosterol is essential for flexibility of the plasma membrane; thus, the presence of ergosterol is particularly critical at the tip of hyphae. Therefore, it can be expected that the

cell membrane at the tips of the hyphae will be affected and destabilized the most by AMB (Figure 2.9A).

The palmitoylated chitinase domains showed antifungal activity toward *T. viride,* and the antifungal activity level was independent of the type of chitinase domains; the IC_{50} values of LysM-Pal, CatD-Pal, and LysM-CatD-Pal were approximately 1 μM (Figure 2.4B). The inactive CatD(E247Q)-Pal showed slightly lower antifungal activity than the other chitinase domains (Figure 2.4), suggesting that the antifungal activity of the palmitoylated chitinase domains was derived mainly from the palmitic acid motif, and the degradation of chitin was not the main factor for the antifungal activity. However, the addition of Pal-K to *T. viride* did not affect the fungal growth (Figures 2.5 and 2.6). This result indicated that Pal-K and the palmitoylated proteins had different antifungal activities, and thus, conjugating Pal-K with a protein was essential for cytotoxicity to be observed. The critical micelle concentration (CMC) of Pal-K is reported to be 16 μM[32]. At concentrations lower than the CMC, amphiphilic molecules are believed to be mainly located at the air-water interface to minimize contact of the hydrophobic domains with the water molecules. In all antifungal activity assays conducted in this research, the concentration of Pal-K was 1 μM; hence, Pal-K must have been mainly located at the air-water interface and was not interacting with the cell membrane of the fungi. At the CMC, amphiphilic molecules will be solubilized within the water phase and start to form micellar structures. A protein conjugated with Pal-K can be regarded as an amphiphilic molecule with a large hydrophilic head group. The size of the hydrophilic groups of the palmitoylated proteins was much larger than that of Pal-K (Figure 2.10); therefore, the concentration at which the air-water

interface will be fully occupied with the palmitoylated proteins should be lower than that for Pal-K (Figure 2.9B).

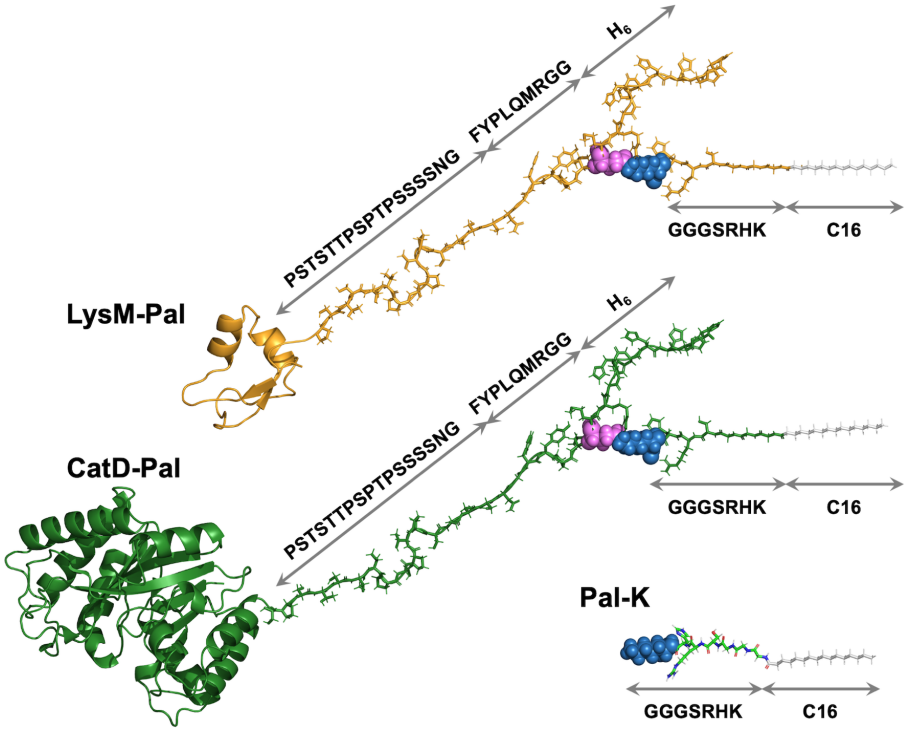

Figure 2.10 The 3-dimensional modeling images of Pal-K, CatD-Pal and LysM-Pal. The protein structures of CatD and LysM were obtained from the PDB(Protein Data Bank) IDs of 4RL3 and 4PXV, respectively. The images were produced with Molecular Operating Environment ™ (MOE) software developed by Chemical Computing Group Inc. (Montreal, Canada). The lysine and glutamine residues in Pal-K and Q-tag were shown as space-filling model with colors of blue and magenta, respectively. Reproduce with permission from ref [33]. Copyright 2022 American Chemical Society.

Dynamic light scattering (DLS) measurements of 1 μM palmitoylated EGFP showed a peak at approximately 50 nm, whereas unmodified EGFP showed a peak at <10 nm[31], indicating the formation of aggregates of palmitoylated EGFP at a concentration of 1 μM. The DLS measurements of LysM-Q and LysM-Pal at a concentration of 1 μM showed that LysM-Pal formed a larger complex than LysM-Q (Figure 2.11), suggesting that the CMC of LysM-Pal is less than 1 μM. The size of the LysM-Pal complex remained stable for 2 days at 25 °C. The palmitoylated chitinase domains were able to anchor

the palmitic acid motif to the cell membrane of fungi because of the higher tendency to aggregate at a lower concentration (lower CMC) compared with Pal-K, and the cytotoxic effects of the palmitic acid motif and chitinase domains were able to be exerted (Figure 2.9B). In the study using lipid bilayer membrane consisting of dioleoylphosphocholine/dipalmitoylphosphocholine (DPPC)/cholesterol, it has been reported that the palmitic acid would facilitate the exclusion of cholesterol from the DPPC-rich phase and decrease the fluidity of the membrane[41]. The antifungal effect by the anchoring of palmitic acid motif is thought to be the result of reduced flexibility of the plasma membrane of fungi, and this mechanism of action is similar to that of ergosterol extraction by AMB.

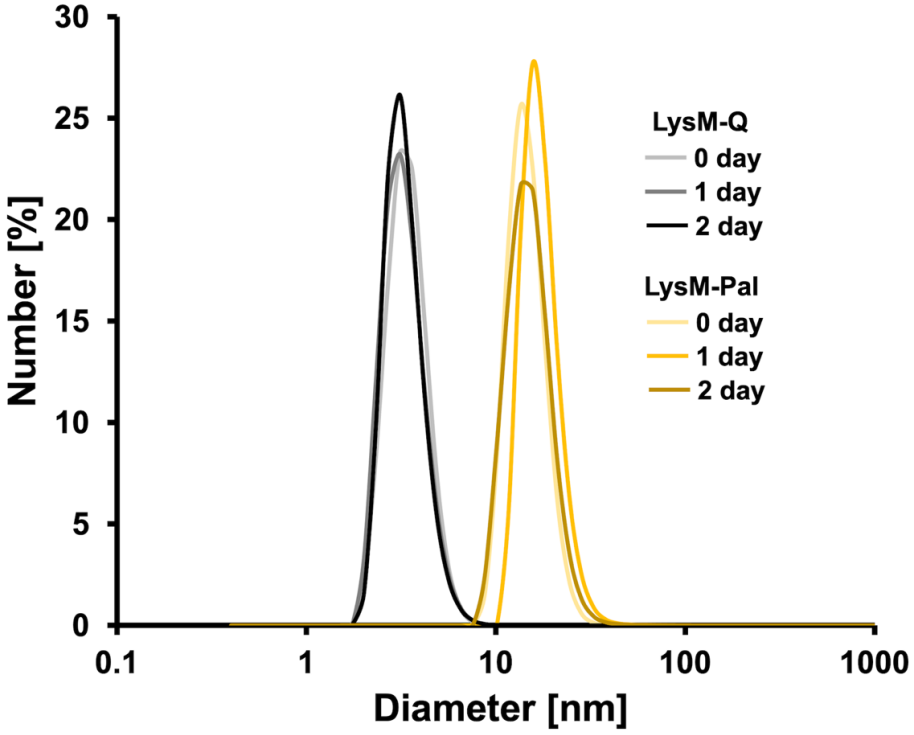

Figure 2.11 Dynamic light scattering measurement on LysM-Q and LysM-Pal. The concentration of LysM-Q and LysM-Pal was fixed at 1 μM. The samples were kept at 25˚C and DLS was measured for 3 days using Zetasizer Nano ZS (Malvern, Worcestershire, UK). Reproduce with permission from ref [33]. Copyright 2022 American Chemical Society.

The hyphae of *T. viride* treated with a tandem trimer of LysM, $LysM_3$, were lysed from the tips and the hyphae treated with $LysM_3$-CatD were lysed from the tips as well as from the lateral wall of hyphae[26]. Importantly, although $LysM_3$ exhibited antifungal activity against *T. viride*, the fusion protein of $LysM_3$ with CatD(E247Q), which lacks chitin degradative activity, showed almost no antifungal activity, indicating that CatD(E247Q) inhibited the activity of $LysM_3$. The LysM tandem dimer has been shown to have stronger binding affinity toward chitin than full-length ChiA, requiring more severe conditions for elution from a chitin column[24]. In the present study, LysM-CatD-Pal exhibited lower enhancement of the antifungal activity than LysM-Pal when combined with AMB (Figures 2.6 and 2.8). From these results, it can be deduced that fusing CatD to LysM removes the ability of LysM to bind to chitin, and this may be one of the reasons why LysM-CatD-Pal had less antifungal activity than LysM-Pal (Figure 2.9C).

Palmitoylation can potentially enhance the binding of LysM to the chitin of fungi by anchoring the palmitic acid motif to the plasma membrane, which is located underneath the chitin layer of the fungi cell wall. The lateral cell wall structures are mature, and thus the chitin layer is covered with layers of mannoproteins and β-glucan. The palmitic acid motif most likely interacts with fungi at the tips of hyphae because the plasma membranes are somewhat exposed there. On the other hand, palmitoylation seemed to reduce the antifungal effect of CatD. The combination of 1 μM of CatD-Pal or LysM-CatD-Pal with AMB showed a synergistic effect of much lower level compared with unmodified CatD-Q or LysM-CatD-Q (Figure 2.5-2.7). The anchoring of palmitic acid to the plasma

membrane might inhibit the movement of CatD, and as a result, the degradation activity of CatD against chitin in the fungi cell wall was diminished.

Takashima *et al*. have proposed a mechanism for how tandem LysM multimers achieve the lysis of *T. viride* at the tips of hyphae. The key point of the proposed mechanism is the bridging of different chitin chains by the LysM multimers[26]. The bridging of chitin chains by a LysM multimer prevents the cell wall at the tip of hyphae from stretching, and as the cell growth continues, the internal cell pressure increases. When the internal cell pressure reaches the limit of the cell, rupture will occur at the tip of the hyphae to lyse the cells. In this model, a covalently connected multimer of LysM is essential. In the present study, monomeric LysM-Pal exerted strong antifungal activity enhancement, which does not fit with the proposed mechanism described above. LysM-Pal might form micellar structures that act as LysM multimers, but it seems unlikely that such LysM assemblies formed by noncovalent interactions would sufficiently bind the chitin chains together. Therefore, we proposed another mechanism for the antifungal action in which LysM binds to the new chitin chains being synthesized at the tips of the hyphae and inhibits the elongation of the chitin chains and/or the packing of the chitin chains. As a consequence of this inhibition, the structure of the chitin layers will be destabilized. In this model, multimers of LysM are not required but strong affinity toward chitin is essential. This model explains why monomeric LysM with low affinity did not show antifungal activity but the tandem LysM multimers with high affinity did. At the tips of the hyphae, the palmitic acid motif of LysM-Pal anchors to the plasma membrane and LysM binds to the chitin. The binding of LysM induces destabilization of the chitin layer at the tips. The plasma membrane at the tips is

destabilized by the effect of AMB and by the anchoring of palmitic acid. In this model, both the chitin layer and the plasma membrane are intensively destabilized at the tips of the hyphae, which can explain why the combination of AMB and LysM-Pal resulted in the highest antifungal activity enhancement of the three types of palmitoylated chitinase domains (Figure 2.9C). Another possible explanation for the difference in antifungal activity of LysM and CatD or LysM-CatD could be the difference in the molecular size. LysM has the smallest molecular size among the chitinase domains tested in this study, and therefore, it might efficiently penetrate into the chitin layer of fungi cell wall and exhibit the antifungal activity the most. Further analysis of the localization of the palmitoylated chitinase domains on fungi will provide more insights into the mechanism of the synergistic effect of AMB and LysM-Pal, which has been discussed in the next chapter.

Combination therapy using antifungal agents that possess different mechanisms of antifungal activity is commonly used in medicine to maximize the treatment efficacy and reduce the amount of required antifungal agents, as well as to prevent the emergence of drug-resistant fungi[42,43,44]. In the present study, we demonstrated that the combination of palmitoylated LysM and AMB exhibited a synergistic effect, and the MIC values of both LysM-Pal and AMB were dramatically reduced compared with the individual agents. We also evaluated the cytotoxicity of LysM-Pal with AMB against mammalian cells, HEK293T (Figure 2.12). The combination of 0.3 μM AMB with 1 μM LysM-Pal, at which the growth of *T. viride* was completely inhibited, showed no cytotoxicity against HEK293T cells, indicating that the formulation of AMB with LysM-Pal is safe. The mechanism for the antifungal activity of AMB and LysM-Pal involved the destabilization of the cell wall structures,

and it is difficult to develop resistance to these types of antifungal agents. Therefore, the formulation of AMB with LysM-Pal could be a safe and effective candidate for the treatment of fungal infections.

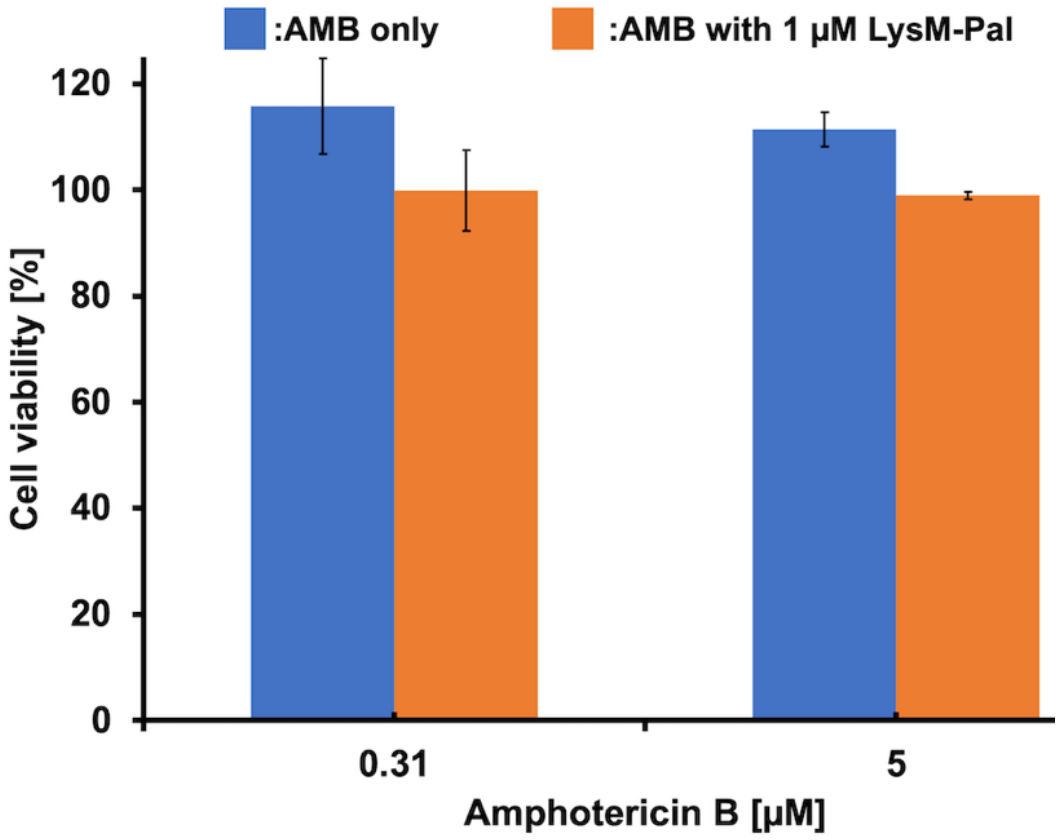

Figure 2.12. Cytotoxicity assay of an amphotericin B (AMB) combination with LysM-Pal against HEK293T cells. The concentration of LysM-Pal was 1 μM, and AMB concentration was varied to 0.31 μM or 5 μM. The cells were seeded in 96 well plates at a density of 5000 cells/well and incubated for 24 h at 37°C in a 5% CO2 incubator; after that, the AMB and LysM-Pal were added to incubate under the same condition. The cell viability was measured using Cell-Counting Kit-8(Dojindo, Tokyo, Japan), and the viability of cells without treatment was set as 100 %. Reproduce with permission from ref [33]. Copyright 2022 American Chemical Society.

2.4 Conclusion

The author has demonstrated a synergistic effect of the palmitoylated chitinase of *P. ryukyuensis* and AMB. LysM-Q, CatD-Q, and LysM-CatD-Q were successfully conjugated with Pal-K using a MTG-mediated, site-specific, cross-linking reaction between lysine in Pal-K and glutamine in the Q-tag. The palmitoylated chitinase domains exhibited strong antifungal activity against *T. viride* with IC_{50} values as low as 1 μM, nearly 2 orders of magnitude lower than the previously reported IC_{50} value of LysM-CatD. The combination of AMB with these palmitoylated chitinase domains resulted in a strong enhancement of the antifungal activity. Intriguingly, the palmitoylated chitin-binding domain, LysM-Pal, showed the largest synergistic effect of the three chitinase domains despite a lack of chitin degradative activity. When 0.5 μM LysM-Pal was combined with AMB, the MIC value of AMB was decreased to 0.31 μM. The palmitoylation of LysM was essential for strong antifungal activity and for a synergistic effect with AMB. The palmitic acid motif of LysM-Pal probably functioned to deliver LysM to the chitin at the tip of the fungal hyphae by anchoring into the plasma membrane, which enhanced the destabilization of the chitin layer by the binding of LysM. The plasma membrane at the tip of the hyphae was destabilized by the extraction of ergosterol by AMB. Because both the chitin layer and the plasma membrane at the tip of the hyphae were damaged by LysM-Pal and AMB, the stability of the tip of hyphae was drastically reduced, resulting in lysis of the fungal cells. Mammalian cells do not have chitin, and therefore LysM is expected to be safe for use in mammals. The combination of LysM with AMB can minimize the dose of AMB required, without any additional risk derived from LysM; thus, we concluded that the combination of LysM-Pal and AMB

could be a promising method for treating fungal infections. Further research on the mechanism of the synergistic effect of LysM-Pal and AMB will provide information toward the development of an ideal formulation of antifungal agent and chitinase.

References

(1) Liu, W.; Yuan, L.; Wang, S. Recent Progress in the Discovery of Antifungal Agents Targeting the Cell Wall. *J. Med. Chem.* **2020**, *63* (21), 12429–12459.

(2) Lionakis, M. S. Primary Immunodeficiencies and Invasive Fungal Infection: When to Suspect and How to Diagnose and Manage. *Curr. Opin. Infect. Dis.* **2019**, 531–537. h

(3) Willyard, C. The drug-resistant bacteria that pose the greatest health threats. *Nature* **2017**, *543*, 15.

(4) Prasad, R.; Shah, A. H.; Rawal, M. K. Antifungals: Mechanism of Action and Drug Resistance. *Adv. Exp. Med. Biol.* **2016**, *892*, 327–349.

(5) Demir, K. K.; Butler-Laporte, G.; Del Corpo, O.; Ekmekjian, T.; Sheppard, D. C.; Lee, T. C.; Cheng, M. P. Comparative Effectiveness of Amphotericin B, Azoles and Echinocandins in the Treatment of Candidemia and Invasive Candidiasis: A Systematic Review and Network Meta-Analysis. *Mycoses* **2021**, *64* (9), 1098–1110.

(6) Bartlett, J. G. Amphotericin B: Time for a New "Gold Standard." *Infect. Dis. Clin. Pract.* **2004**, *12* (2), 149–150.

(7) Mesa-Arango, A. C.; Scorzoni, L.; Zaragoza, O. It Only Takes One to Do Many Jobs: Amphotericin B as Antifungal and Immunomodulatory Drug. *Front. Microbiol.* **2012**, *3* (AUG), 1–10.

(8) Purkait, B.; Kumar, A.; Nandi, N.; Sardar, A. H.; Das, S.; Kumar, S.; Pandey, K.; Ravidas, V.; Kumar, M.; De, T.; Singh, D.; Das, P. Mechanism of Amphotericin B Resistance in Clinical Isolates of Leishmania Donovani. *Antimicrob. Agents Chemother.* **2012**, *56* (2), 1031–1041.

(9) Anderson, T. M.; Clay, M. C.; Cioffi, A. G.; Diaz, K. A.; Hisao, G. S.; Tuttle, M. D.; Nieuwkoop, A. J.; Comellas, G.; Maryum, N.; Wang, S.; Uno, B. E.; Wildeman, E. L.; Gonen, T.; Rienstra, C. M.; Burke, M. D. Amphotericin Forms an Extramembranous and Fungicidal Sterol Sponge. *Nat. Chem. Biol.* **2014**, *10* (5), 400–406.

(10) Lewandowska, A.; Soutar, C. P.; Greenwood, A. I.; Nimerovsky, E.; De Lio, A. M.; Holler, J. T.; Hisao, G. S.; Khandelwal, A.; Zhang, J.; SantaMaria, A. M.; Schwieters, C. D.; Pogorelov, T. V.; Burke, M. D.; Rienstra, C. M. Fungicidal Amphotericin B Sponges Are Assemblies of Staggered Asymmetric Homodimers Encasing Large Void Volumes. *Nat. Struct. Mol. Biol.* **2021**, *28* (12), 972–981.

(11) E., J.; M., B.; W., P.; M., S.; U., B.; C., L.-F.; D., W. Oxidative Stress Response Tips the Balance

in Aspergillus Terreus Amphotericin B Resistance. *Antimicrob. Agents Chemother.* **2017**, *61* (10), 1–14.

(12) Faustino, C.; Pinheiro, L. Lipid Systems for the Delivery of Amphotericin B in Antifungal Therapy. *Pharmaceutics* **2020**, *12* (1), 1–47.

(13) Keyhani, A.; Sharifi, I.; Salarkia, E.; Khosravi, A.; Tavakoli Oliaee, R.; Babaei, Z.; Ghasemi Nejad Almani, P.; Hassanzadeh, S.; Kheirandish, R.; Mostafavi, M.; Hakimi Parizi, M.; Alahdin, S.; Sharifi, F.; Dabiri, S.; Shamsi Meymandi, S.; Khamesipour, A.; Jafarzadeh, A.; Bamorovat, M. In Vitro and in Vivo Therapeutic Potentials of 6-Gingerol in Combination with Amphotericin B for Treatment of Leishmania Major Infection: Powerful Synergistic and Multifunctional Effects. *Int. Immunopharmacol.* **2021**, *101* (PB), 108274.

(14) Santos, J. R. A.; Ribeiro, N. Q.; Bastos, R. W.; Holanda, R. A.; Silva, L. C.; Queiroz, E. R.; Santos, D. A. High-Dose Fluconazole in Combination with Amphotericin B Is More Efficient than Monotherapy in Murine Model of Cryptococcosis. *Sci. Rep.* **2017**, *7* (1), 1–8.

(15) Chudzik, B.; Bonio, K.; Dabrowski, W.; Pietrzak, D.; Niewiadomy, A.; Olender, A.; Malodobry, K.; Gagoś, M. Synergistic Antifungal Interactions of Amphotericin B with 4-(5-Methyl-1,3,4-Thiadiazole-2-Yl) Benzene-1,3-Diol. *Sci. Rep.* **2019**, *9* (1), 1–14.

(16) Takashima, T.; Henna, H.; Kozome, D.; Kitajima, S.; Uechi, K.; Taira, T. CDNA Cloning, Expression, and Antifungal Activity of Chitinase from Ficus Microcarpa Latex: Difference in Antifungal Action of Chitinase with and without Chitin-Binding Domain. *Planta* **2021**, *253* (6), 1–13.

(17) Yano, S.; Kanno, H.; Tsuhako, H.; Ogasawara, S.; Suyotha, W.; Konno, H.; Makabe, K.; Uechi, K.; Taira, T. Cloning, Expression, and Characterization of a GH 19-Type Chitinase with Antifungal Activity from Lysobacter Sp. MK9-1. *J. Biosci. Bioeng.* **2021**, *131* (4), 348–355.

(18) Takashima, T.; Numata, T.; Taira, T.; Fukamizo, T.; Ohnuma, T. Structure and Enzymatic Properties of a Two-Domain Family GH19 Chitinase from Japanese Cedar (Cryptomeria Japonica) Pollen. *J. Agric. Food Chem.* **2018**, *66* (22), 5699–5706.

(19) Toufiq, N.; Tabassum, B.; Bhatti, M. U.; Khan, A.; Tariq, M.; Shahid, N.; Nasir, I. A.; Husnain, T. Improved Antifungal Activity of Barley Derived Chitinase I Gene That Overexpress a 32 KDa Recombinant Chitinase in Escherichia Coli Host. *Brazilian J. Microbiol.* **2018**, *49* (2), 414–421.

(20) Landim, P. G. C.; Correia, T. O.; Silva, F. D. A.; Nepomuceno, D. R.; Costa, H. P. S.; Pereira,

H. M.; Lobo, M. D. P.; Moreno, F. B. M. B.; Brandão-Neto, J.; Medeiros, S. C.; Vasconcelos, I. M.; Oliveira, J. T. A.; Sousa, B. L.; Barroso-Neto, I. L.; Freire, V. N.; Carvalho, C. P. S.; Monteiro-Moreira, A. C. O.; Grangeiro, T. B. Production in Pichia Pastoris, Antifungal Activity and Crystal Structure of a Class I Chitinase from Cowpea (Vigna Unguiculata): Insights into Sugar Binding Mode and Hydrolytic Action. *Biochimie* **2017**, *135*, 89–103.

(21) Khan, A. A.; Alanazi, A. M.; Jabeen, M.; Khan, S.; Malik, A. Additive Potential of Combination Therapy against Cryptococcosis Employing a Novel Amphotericin B and Fluconazole Loaded Dual Delivery System. *Eur. J. Pharm. Sci.* **2018**, *119* (April), 171–178.

(22) Mostafavi, M.; Sharifi, I.; Farajzadeh, S.; Khazaeli, P.; Sharifi, H.; Pourseyedi, E.; Kakooei, S.; Bamorovat, M.; Keyhani, A.; Parizi, M. H.; Khosravi, A.; Khamesipour, A. Niosomal Formulation of Amphotericin B Alone and in Combination with Glucantime: In Vitro and in Vivo Leishmanicidal Effects. *Biomed. Pharmacother.* **2019**, *116* (April).

(23) Grela, E.; Zdybicka-Barabas, A.; Pawlikowska-Pawlega, B.; Cytrynska, M.; Wlodarczyk, M.; Grudzinski, W.; Luchowski, R.; Gruszecki, W. I. Modes of the Antibiotic Activity of Amphotericin B against Candida Albicans. *Sci. Rep.* **2019**, *9* (1), 1–10.

(24) Onaga, S.; Taira, T. A New Type of Plant Chitinase Containing LysM Domains from a Fern (Pteris Ryukyuensis): Roles of LysM Domains in Chitin Binding and Antifungal Activity. *Glycobiology* **2008**, *18* (5), 414–423.

(25) Ohnuma, T.; Onaga, S.; Murata, K.; Taira, T.; Katoh, E. LysM Domains from Pteris Ryukyuensis Chitinase-A: A Stability Study and Characterization of the Chitin-Binding Site. *J. Biol. Chem.* **2008**, *283* (8), 5178–5187.

(26) Takashima, T.; Sunagawa, R.; Uechi, K.; Taira, T. Antifungal Activities of LysM-Domain Multimers and Their Fusion Chitinases. *Int. J. Biol. Macromol.* **2020**, *154*, 1295–1302.

(27) Minamihata, K.; Tanaka, Y.; Santoso, P.; Goto, M.; Kozome, D.; Taira, T.; Kamiya, N. Orthogonal Enzymatic Conjugation Reactions Create Chitin Binding Domain Grafted Chitinase Polymers with Enhanced Antifungal Activity. *Bioconjug. Chem.* **2021**, *32* (8), 1688–1698.

(28) Kim, T. Y.; Nam, Y. R.; Park, J. H.; Lee, D. E.; Kim, H. S. Site-Specific Lipidation of a Small-Sized Protein Binder Enhances the Antitumor Activity through Extended Blood Half-Life. *ACS Omega* **2020**, *5* (31), 19778–19784.

(29) Taguchi, K.; Okamoto, Y.; Matsumoto, K.; Otagiri, M.; Chuang, V. T. G. When Albumin Meets Liposomes: A Feasible Drug Carrier for Biomedical Applications. *Pharmaceuticals* **2021**, *14*

(4), 1–17.

(30) Takahara, M.; Wakabayashi, R.; Minamihata, K.; Goto, M.; Kamiya, N. Design of Lipid-Protein Conjugates Using Amphiphilic Peptide Substrates of Microbial Transglutaminase. *ACS Appl. Bio Mater.* **2018**, *1* (6), 1823–1829.

(31) Takahara, M.; Wakabayashi, R.; Fujimoto, N.; Minamihata, K.; Goto, M.; Kamiya, N. Enzymatic Cell-Surface Decoration with Proteins Using Amphiphilic Lipid-Fused Peptide Substrates. *Chem. - A Eur. J.* **2019**, *25* (30), 7315–7321.

(32) Takahara, M.; Mochizuki, S.; Wakabayashi, R.; Minamihata, K.; Goto, M.; Sakurai, K.; Kamiya, N. Extending the Half-Life of a Protein in Vivo by Enzymatic Labeling with Amphiphilic Lipopeptides. *Bioconjug. Chem.* **2021**, *32* (4), 655–660.

(33) Santoso, P.; Minamihata, K.; Ishimine, Y.; Taniguchi, H.; Komada, T.; Sato, R.; Goto, M.; Takashima, T.; Taira, T.; Kamiya, N. Enhancement of the Antifungal Activity of Chitinase by Palmitoylation and the Synergy of Palmitoylated Chitinase with Amphotericin B. *ACS Infect. Dis.* **2022**, *8*, 1051–1061.

(34) Imoto, T.; Yagishita, K. Activity Measurement of Lysozyme. *Agr. Biol. Chem.* **1971**, *35* (7), 1154–1156.

(35) Wang, N. N.; Gao, K. Y.; Han, N.; Tian, R. Z.; Zhang, J. L.; Yan, X.; Huang, L. L. ChbB Increases Antifungal Activity of Bacillus Amyloliquefaciens against Valsa Mali and Shows Synergistic Action with Bacterial Chitinases. *Biol. Control* **2020**, *142* (November 2019), 104150.

(36) Han, S.; Wang, Z.; Liu, J.; Wang, H. M. D.; Yuan, Q. MiR-29a-3p-Dependent COL3A1 and COL5A1 Expression Reduction Assists Sulforaphane to Inhibit Gastric Cancer Progression. *Biochem. Pharmacol.* **2021**, *188* (145), 114539.

(37) Tseng, C. C.; Lin, Y. J.; Liu, W.; Lin, H. Y.; Chou, H. Y.; Thia, C.; Wu, J. H.; Chang, J. S.; Wen, Z. H.; Chang, J. J.; David Wang, H. M. Metabolic Engineering Probiotic Yeast Produces 3S, 3′S-Astaxanthin to Inhibit B16F10 Metastasis. *Food Chem. Toxicol.* **2020**, *135* (September 2019), 110993.

(38) Cd, D.; Lb, V.; Ma, M.; Md, B. Extracellular Antifungal Activity of Chitinase-Producing Bacteria Isolated From Guano of Insectivorous Bats. *Curr. Microbiol.* **2021**, *78* (7), 2787–2798.

(39) de Kruijff, B.; Demel, R. A. Polyene antibiotic-sterol inreactions in membranes of Acholeplasma laidlawii cells and lecithin liposomes. III. Molecular structure of the polyene antibiotic-cholesterol complexes. Biochim. Biophys. Acta 1974, 339, 57−70.

(40) Shekhova, E.; Kniemeyer, O.; Brakhage, A. A. Induction of Mitochondrial Reactive Oxygen Species Production by Itraconazole, Terbinafine, and Amphotericin B as a Mode of Action against Aspergillus Fumigatus. *Antimicrob. Agents Chemother.* **2017**, *61* (11), 1–14.

(41) Shimokawa, N.; Mukai, R.; Nagata, M.; Takagi, M. Formation of Modulated Phases and Domain Rigidification in Fatty Acid-Containing Lipid Membranes. *Phys. Chem. Chem. Phys.* **2017**, *19* (20), 13252–13263.

(42) Kontoyiannis, D. P. Antifungal Resistance: An Emerging Reality and a Global Challenge. *J. Infect. Dis.* **2017**, *216* (Suppl 3), S431–S435.

(43) Berman, J.; Krysan, D. J. Drug Resistance and Tolerance in Fungi. *Nat. Rev. Microbiol.* **2020**, *18* (6), 319–331.

(44) Montoya, M. C.; Moye-Rowley, W. S.; Krysan, D. J. Candida Auris: The Canary in the Mine of Antifungal Drug Resistance. *ACS Infect. Dis.* **2019**, *5* (9), 1487–1492.

Chapter 3 Controlling the Antifungal Activity of Chitin-Binding Protein by Artificial Lipidation

3.1 Introduction

The ineffectiveness of antifungal drugs in fighting pathogenic fungi has been a scary condition in the health sector. It allows the enhancement of antifungal drug doses, which leads to pathogenic fungal drug resistance issue[1]. Although the victims of fungal infection are not as severe as bacterial infections, recent findings show that pathogenic fungi have aggravated the condition of COVID-19 patients[2,3], exclusively patients with respiratory disorders infected by *Aspergillus fumigatus*[4]. In addition, the case-fatality rate among immunocompromised patients correlated with infection caused by *Candida* strains is still a matter of debate globally that has not been resolved until now[5]. The use of antifungal agents is presently restricted to three primary classes: polyenes, azoles, and echinocandins[6]. The mechanism of action of these antimycotic agents is different in combating fungal pathogens. Polyenes bind to ergosterol in fungal cell membranes, which leads to fungal death. Azoles inhibit the biosynthesis of ergosterol. Echinocandins inhibit the biosynthesis of fungal (1,3)—D-glucan cell walls. Among these antifungal drugs, Amphotericin B (AMB), parts of the polyene's antifungal drugs, has been used widely to treat fungal infection owing to its broad-spectrum antifungal activity towards pathogenic fungi. AMB, in contrast to many other antifungal drugs, almost rarely leads to the development of opportunistic resistance in fungal strains. Fungizone®, which is formulated with deoxycholate acid, has been a mainstay in AMB's product line for a number of years. However, owing to the nephrotoxicity and other adverse effects of Fungizone®, the therapeutic value of this medication

is restricted[7]. In order to circumvent the toxicity-related limits that are associated with AMB[8], liposomal formulations have been brought to the market. Even though these methods are available, they are not widely used because they are too expensive for most medical treatments. In addition, a recent investigation showed that a liposomal AMB formulation led to acute toxicity in female rats[9]. It is abundantly evident that novel antifungal therapies are urgently needed since there is currently a lack of antimycotics available on the market.

The biologically active protein of chitinase has attracted considerable interest. It can be used to replace commercial antifungal medications with low side effects on human cells[10,11] because its mechanism of action targets the chitin in the cell walls of fungi[12]. The degradation of chitin involves two essential parts of chitinase, namely chitin-binding protein and a catalytic domain. These parts have different actions against chitin. Chitin-binding protein and catalytic domain have the function of binding and degrading the chitinous substrate, respectively. As an antifungal candidate, chitin-binding protein is essential in killing the fungal pathogen[12,13] and the authors have reported that a chitin-binding protein (LysM), part of chitinase, isolated from *Pteris ryukyuensis* affected its ability to suppress the *Trichoderma viride* (*T. viride*) growth. The palmitoylation of the CatD-Q, CatD(E247Q)-Q, LysM-CatD-Q, and LysM-Q exhibited a synergistic effect of enhancement of antifungal activity at a low dose (1 uM) combined with the AMB[10]. Even if the palmitoylation of chitinase displayed improvement in antifungal activity, its mechanism of action has not been evaluated yet.

The present study aims to in vitro investigate the role of palmitoylation in the enhancement of LysM activity by observing its localization in fungal cell walls using confocal laser scanning microscopy

(CLSM). In comparison, the LysM was conjugated with lipids comprising of different alkyl chain length (octanoic acid (C8) and dodecanoic acid (C12)) catalyzed by microbial transglutaminase. Both LysM and lipids were engineered by adding the reactive glutamine-tag (Q-tag) and lysine-tag (K-tag), cross-linked by MTG. The author hypothesized that modification of LysM with lipids can easily lead to the insertion of the LysM into the fungal cell wall. Consequently, the LysM can be optimally targeted in the binding of chitin content. This action results in instability of the cell wall and plasma membrane of fungi, by which the fungal cells cannot preserve internal pressure during the growth process or transport electrolytes that contribute to increased cell damage. The process of protein lipidation involves the post- or co-translational attachment of a lipid group to proteins by using a covalent bond. In eukaryotic cells, the interaction of lipidated proteins with specific membranes is made more accessible by the attachment of the lipid group. Protein lipidation is one of the most significant protein modifications because it affects protein distribution, localization, and function. The lipid groups of the proteins facilitate the binding of the proteins to the target membrane. They engage actively in the control of a variety of signaling systems as well as promoting interactions between different protein pairs[14,15]. Using the lipidation strategy, it was observed the anchoring of fluorescent-labeled LysM on the tip of hyphae and the LysM-C12 showed a strong binding affinity to the hyphae compared with LysM-C8 and LysM-Q; meanwhile, LysM-C16 anchors nearly all the fungal cell wall. Furthermore, the lipidated LysM affected the membrane integrity of *T viride*, and eventually, the conjugation of LysM with different alkyl chain length markedly improved the antifungal activity.

3.2 Experimental

3.2.1 Materials

Sodium dodecyl sulfate (SDS), glycerol, potassium dihydrogen phosphate, and sodium chloride were purchased from Wako Pure Chemical Industries, Ltd. (Osaka, Japan). The LB broth medium, ammonium peroxodisulfate, 30% acrylamide/bis mixed solution (29:1), tris(hydroxymethyl) aminomethane, tryptone, dry yeast extract, dipotassium, hydrogen phosphate, and hydrochloric acid were acquired from Nacalai Tesque, Inc. (Kyoto, Japan). N,N,N',N'-tetramethylethylenediamine, HisTrap FF crude 5 mL column, HiTrap Q HP column, PD SpinTrap G-25, and Ni Sepharose 6 Fast Flow were obtained from Cytiva (Tokyo, Japan). Amicon Ultra, Amicon Ultra-0.5 mL, and Amicon Ultra-15 mL were obtained from Millipore (Tokyo, Japan). Imidazole was from Sigma-Aldrich. Slide A-lyzer®mini dialysis and NHS-Fluorescein, Gibco AMB (comprising 250 g of AMB and 205 g of sodium deoxycholate) were obtained from Thermo Fisher Scientific (Walthan, MA USA). All the chemicals were used without additional purification. The lipidated peptide containing MTG-reactive lysine (lipid-K) was prepared and purified using Fmoc solid-phase peptide synthesis as described in Chapter 2. MTG was produced as a zymogen in *Escherichia coli* BL21(DE3) carrying the propeptide with K9R and Y11A mutations[16]. A peptide tag for purification, $(HN)_6$-tag, was added to the N-terminus, and a tobacco etch virus (TEV) protease recognition sequence (ENLYFQG) was added between the propeptide and the matured MTG domain. Following short purification of the MTG zymogen through Ni-NTA column purification, the MTG zymogen was treated with the TEV protease

to cleave the propeptide and the $(HN)_6$-tag. The matured MTG was then purified using the eluted portion of the second round of Ni-NTA column purification.

3.2.2 Conditions of strains, medium, and culture

T. viride was cultured according to the procedure provided by Prof. Toki Taira (The University of Ryukyu). For the conidium collection of *T. viride*, the fungus was cultivated on potato dextrose agar (PDA) plates at room temperature for 3 days. After 3 days, the fungus was suspended in 16% glycerol. The suspension was filtered, and the spores were counted with a disposable cell counting plate (Neuber Type) and microscope (Olympus U-TV1X-2).

3.2.3 Protein production, purification, and lipidation by MTG

The protein production and purification were performed as previously described[10]. In brief, the chitin-binding domain (LysM) was engineered by adding a flexible linker containing glutamine-tag (Q-tag) at the C-terminus to construct Q-tagged LysM (LysM-Q). The recombinant LysM-Q and K-tagged lipids (lipids-K) are cross-linked by MTG in the conjugation reaction to yield lipidated LysM with different alkyl chain lengths (abbreviated as LysM-Cn, n = 8, 12, 16).

3.2.4 Fluorescein labeling of LysM-Q and LysM-Cn

The LysM-Q and LysM-Cn were conjugated to NHS-fluorescein following the procedure provided by the manufacturer. The LysM-Q and LysM-Cn were washed with 20 mM sodium phosphate buffer (pH 7.4). LysM-Q or LysM-Cn were mixed with NHS fluorescein, and they were incubated for 1 h at room temperature in dark conditions. After 1 h, the fluorescently labeled LysM-Q

and LysM-Cn were dialyzed with Slide A-lyzer®mini dialysis to remove unconjugated NHS-fluorescein. The protein concentration was measured using Nanodrop (Spectrophotometer ND-100).

3.2.5 Localization of LysM-Q and LysM-Cn

The localization of fluorescently labeled LysM-Q and LysM-Cn were analyzed on germlings originating from suspensions of $1x10^6$ spores/ml germinated for 16 h. The germinated spores were incubated with 4 uM of LysM-Q or LysM-Cn in the presence and absence of 0.31 uM of AMB for 1 h under conditions at 25 °C, and 180 rpm (Bioshaker M-BR-022UP), then the treated germinated spores were washed with the same buffer to remove unconjugated LysM-Q, LysM-Cn, and AMB. Calcofluor-White (CFW) staining was used as a control to identify the chitin layer on fungal cell walls.

3.2.6 Membrane integrity assay

The germinated spores were treated with 1 uM of LysM-Q or LysM-Cn combined with 0.65 uM of AMB or without AMB, and they were incubated at 25°C, 180 rpm for 4 h. After 4h, the 0.1 uM of propidium iodide (PI) dye was added and continued incubation for 10 minutes, then they were washed with 20 mM sodium phosphate buffer (pH 7.4).

3.2.7 In vitro analysis of the biological activity of LysM-Cn with amphotericin B

The antifungal activity of LysM-Q and LysM-Cn in combination with AMB or without AMB was performed according to our previous report. Briefly, in a 96-well plate reader, antifungal experiments were carried out with varying doses of amphotericin B (AMB), ranging from 0 to 5 M. Following the addition of *T. viride* to the antifungal test at a concentration of 10,000 spores/mL, 1 uM of LysM-Q or

LysM-Cn was added to the plates, and then the plates were incubated at 25°C for 60 h. The optical density (OD) values obtained from the growing fungus were either measured by using ImageJ to measure the intensity of the image of each well. A digital camera was used to take pictures of the *T. viride* at 60 h in a 96-well plate. ImageJ application (version 1.46; imagej.nih.gov/ij/download.html) was used to change the color pictures of the 96-well plate to grayscale (8 bits; the gray level range: 0–255) maps, which were then transformed to black and white photos. With the help of the ImageJ application, the intensity of each grayscale picture was evaluated.

3.3 Results and Discussion

3.3.1 Lipidation of LysM-Q by MTG

First, LysM-Q and Lipid-K were site-specifically conjugated by MTG (Figure. 3. 1A). The lipid conjugation of LysM-Q was performed by mixing lipid-K, LysM-Q, DDM, and MTG in 10 mM Tris-HCl buffer (pH 7.4) at 37 °C for 60 min. As shown in Figure. 3. 1B, the result of SDS-PAGE showed that the LysM-Q was conjugated entirely to the lipid and there were slight differences in molecular weight between unmodified and modified LysM-Q in each case. According to the amino acid sequences of LysM-Q, the molecular weight of those conjugates with different alkyl chain lengths should be around 7.5 kDa (LysM-C8), 7.6 kDa (LysM-C12), and 7.6 kDa (LysM-C16) and the results were correlated with the SDS-PAGE results.

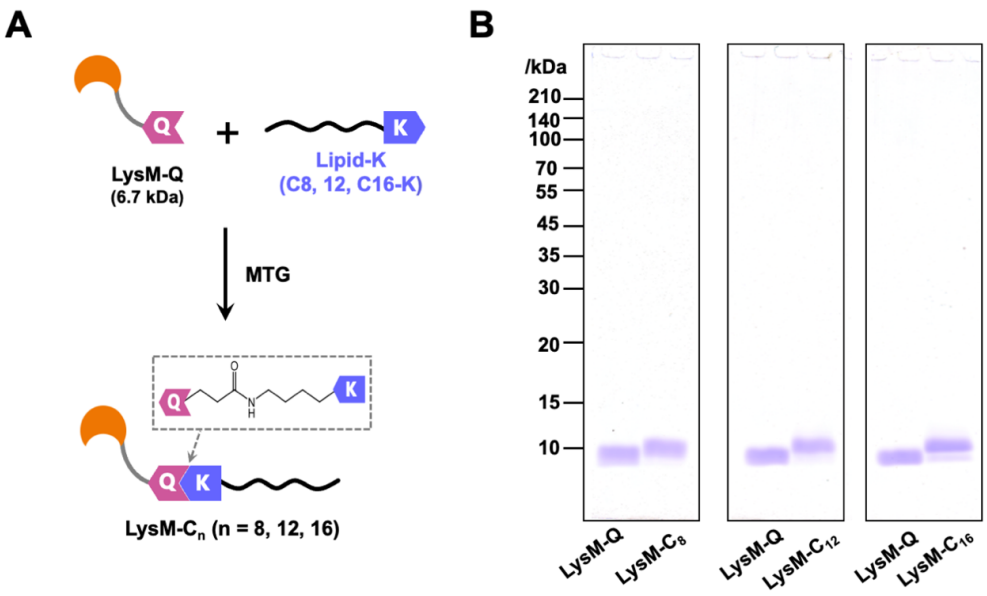

Figure. 3. 1. Bioconjugation of LysM-Q with different alkyl chain length of lipids catalyzed by microbial transglutaminase (MTG). **A**. Schematic illustration of lipidated LysM-Q. **B**. SDS-PAGE analysis result of bioconjugation of LysM-Q with lipid by MTG. All bioconjugation procedures were conducted as in previous research.

3.3.2 In vitro Antifungal Activity Test of LysM-Q and LysM-Cn combined with AMB or without AMB

The results of antifungal activities of LysM-Q and LysM-Cn in combination with AMB or without AMB were shown in Figure 3. 2. At more than 2.5 μM dosages, *T. viride* growth was inhibited by AMB alone (Figure. 3. 2A). The addition of 1 μM unmodified LysM-Q to 1.25 μM AMB completely prevented the fungal growth, whereas the LysM-Q independently did not impede the growth of *T. viride.* Consequently, LysM-Q and AMB cooperated synergistically to enhance antifungal activity. Surprisingly, the lipidation of LysM-Q markedly improved the antifungal activity. Compared with LysM-Q, LysM-Cn resulted in an even more significant increase in antifungal activity. Complete growth inhibition of *T. viride* was reached at a combination of AMB at a concentration of 0.63 μM with LysM-C8, LysM-C12, and LysM-C16 at a concentration of 1 μM. On the contrary, at a

concentration of AMB in the range of 0.16-0.31 μM, the fungus growth was observed at around 45%-49% for LysM-C8 and 16%-21% for LysM-C12 (Figure 3. 2B); meanwhile, LysM-C16 still perfectly inhibited the fungus growth, depicted by the homogenous black well-plates (Figure. 3. 2A), indicating that there was no fungal growth. In the case without AMB, the LysM-C16 showed the best antifungal activity, suppressing 97.3% of the fungus growth (fungal growth value at 3.7%). Intriguingly, the LysM-C12 without AMB remarkably exhibited good antifungal activity compared with LysM-C8, with a fungal growth value of 20.8% (inhibition value 79.2%) and 44.9% (inhibition value 55.1%), respectively. These findings were surprising because LysM-C12 exhibited an enhancement in antifungal activity close to the level of LysM-C16. Next, to gain further insight into this phenomenon, the effect of different concentrations of LysM-Cn in inhibiting the *T. viride* growth was investigated.

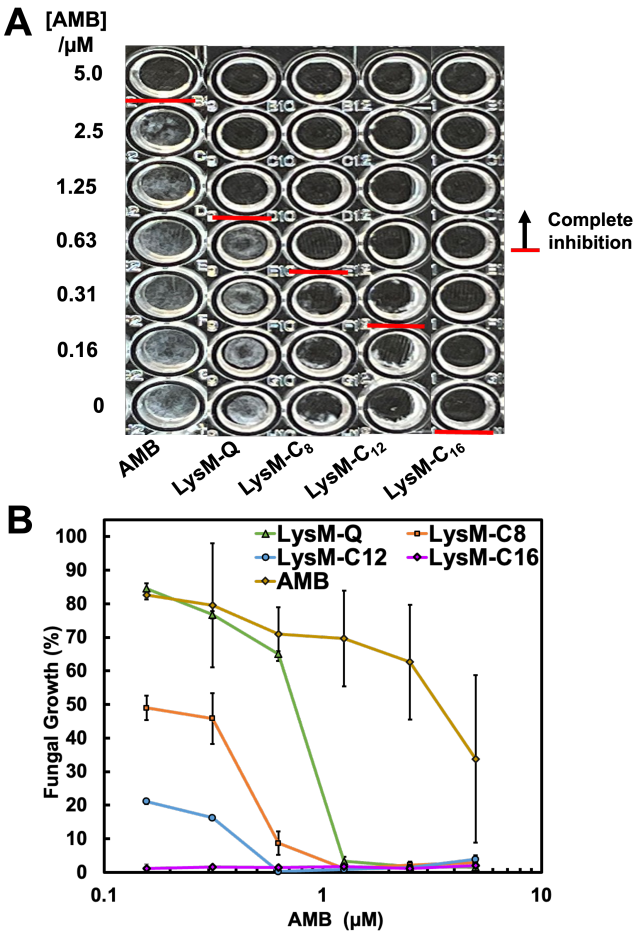

Figure. 3. 2. Comparative antifungal activity of LysM-Cn against *Trichoderma viride*. Antifungal activity was evaluated in vitro in a 96-well plate at 25°C for 60 h. *T. viride* was treated with 1 µM of LysM-Cn and 0-5 µM of amphotericin B. Using ImageJ; the optical density of an image of a 96-well plate was measured to estimate the growth curve of the fungus. As 100% growth, the intensity of the grayscale picture of wells without AMB ([AMB = 0]) was utilized. The error bar displays the standard deviation (n = 3).

In the course of investigation of the antifungal properties of AMB and lipidated LysMs, an experiment was conducted in which the amounts of both of these components were altered. This was done with the intention of gaining better comprehension of the synergistic antifungal action generated when AMB is coupled with lipidated LysMs (Figure. 3. 3). Again, LysM-C16 exhibited greater antifungal activity than LysM-C12 and LysM-C8. The LysM-C16 (1 µM) in the presence of AMB (0.625 µM) inhibited the *T. viridie* growth up to 93.7% (fungal growth at 6.3%). Even if the

concentration of LysM-C16 at 0.5 μM, the fungus growth was still suppressed up to 84.3%. In the case of LysM-C12 and LysM-C8 at 1 μM AMB, the fungal growth of *T. viride* was observed at 31.6% and 54.8%, respectively. Meanwhile, LysM-C12, and LysM-C8 with a concentration of 0.5 μM, the fungus can be grown at around 41.1% and 63.5%, respectively. In the case without AMB, the fungus growth was detected at 16.7%, 43.3%, and 56.6% when 1 μM of LysM-C16, LysM-C12, and LysM-C8 was used, respectively. Otherwise, at 0.1 μM AMB, *T. viride* can be grown at a value of 43.9%, 46%, and 68.4%, respectively. These results suggest that the modification with palmitic acid affected the antifungal activity of the LysM domain. These findings also supported the synergistic antifungal action of AMB and LysM-Pal with a significant reduction in the MIC value.

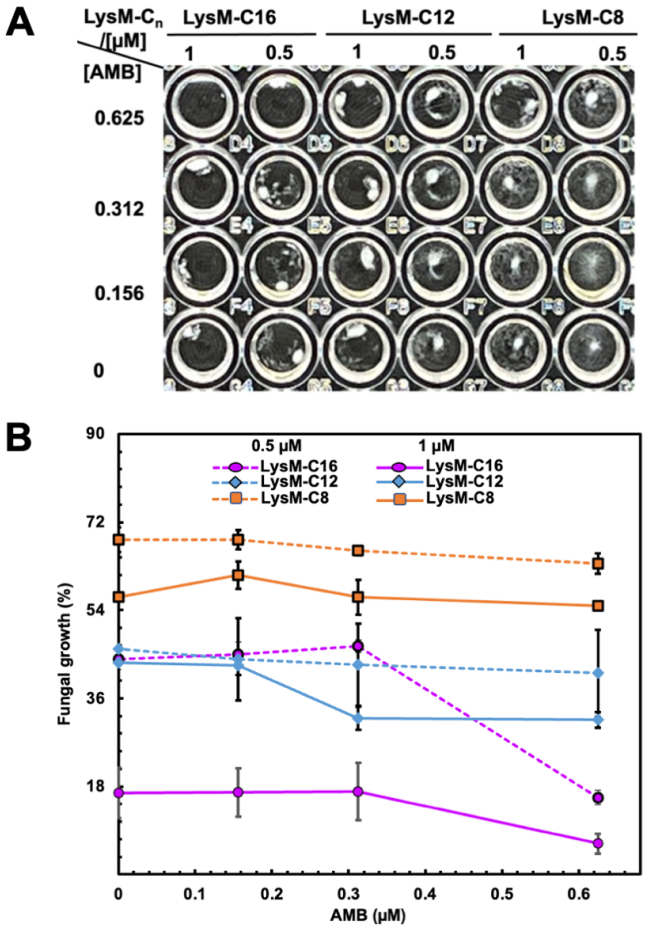

Figure. 3. 3. The comparison of antifungal activity with different dosages of AMB and lipidated LysM. LysM and LysM-Cn concentrations varied at 0.5 uM and 1 uM, whereas AMB concentrations ranged from 0 to 0.62 M. In each well, *T. viride* was treated with LysM-Q or LysM-Cn combined with AMB or without AMB at 25 °C for 60 hours.

The discovery would not have been attainable without the interaction of the two antifungal drugs with the fungal cell wall. It is suggested that an increase in the hydrophobicity of LysM-Cn conjugates contributed to an enhanced contact between LysM and the surface of the fungal cell wall. Namely, artificial lipidation would control the distribution of LysM-Cn into the cell wall or anchor to the cellular membrane of the fungus. After the initial contact between LysM and the outer membrane, the increased surface area of LysM that has been conjugated with lipids caused a rise in the volume and surface area

of the outer leaflet of the fungal cell membrane while it may not affect the inner leaflet. This mismatch may cause a curvature in the lipid bilayer, which in turn leaded to a rupture of the cellular membrane, resulting in a greater antifungal activity.

3.3.2 Effect of LysM-Q and LysM-Cn combined with AMB on the localization in the cell wall and on the membrane integrity of T. viridie hyphae

Next, the distribution and protein localization inside the mycelia of the fungal cell wall was studied by using confocal laser scanning microscopy (CLSM). The LysM-Q and LysM-Cn were labeled with NHS-fluorescein (Figure. 3. 4 and Figure. 3. 5). Calcofluor white (CFW), a dye that specifically binds to the chitin layer, was used as a control to stain the chitin in the fungal cell wall to visualize how much and/or where chitin is present (as blue fluorescence). Figure. 3. 4 and Figure 3. 5 demonstrated that the lipid modification led to an increase in the anchoring of LysM to the surface of the fungus, which suggests that lipidated LysM showed a stronger affinity for the fungus than LysM-Q did (green color). The location of LysM seemed to be altered (Figure. 3. 4), and a more fluorescent signal from the tip of the fungal hyphae was noticed from LysM. AMB probably affected the structure of the fungal cell wall; as a result, the pattern of LysM localization was altered. Intriguingly, the LysM-C12 combined with AMB exhibited the highest fluorescent intensity towards the tips of *T. viride* hyphae, implying an enhancement of the affinity to the cell wall. In the case of LysM-C16, nearly all the cell walls of *T. viride* hyphae were labeled, indicating that the modification of LysM-Q with palmitic acid improved the anchoring of LysM-Q on the cell membrane of fungi.

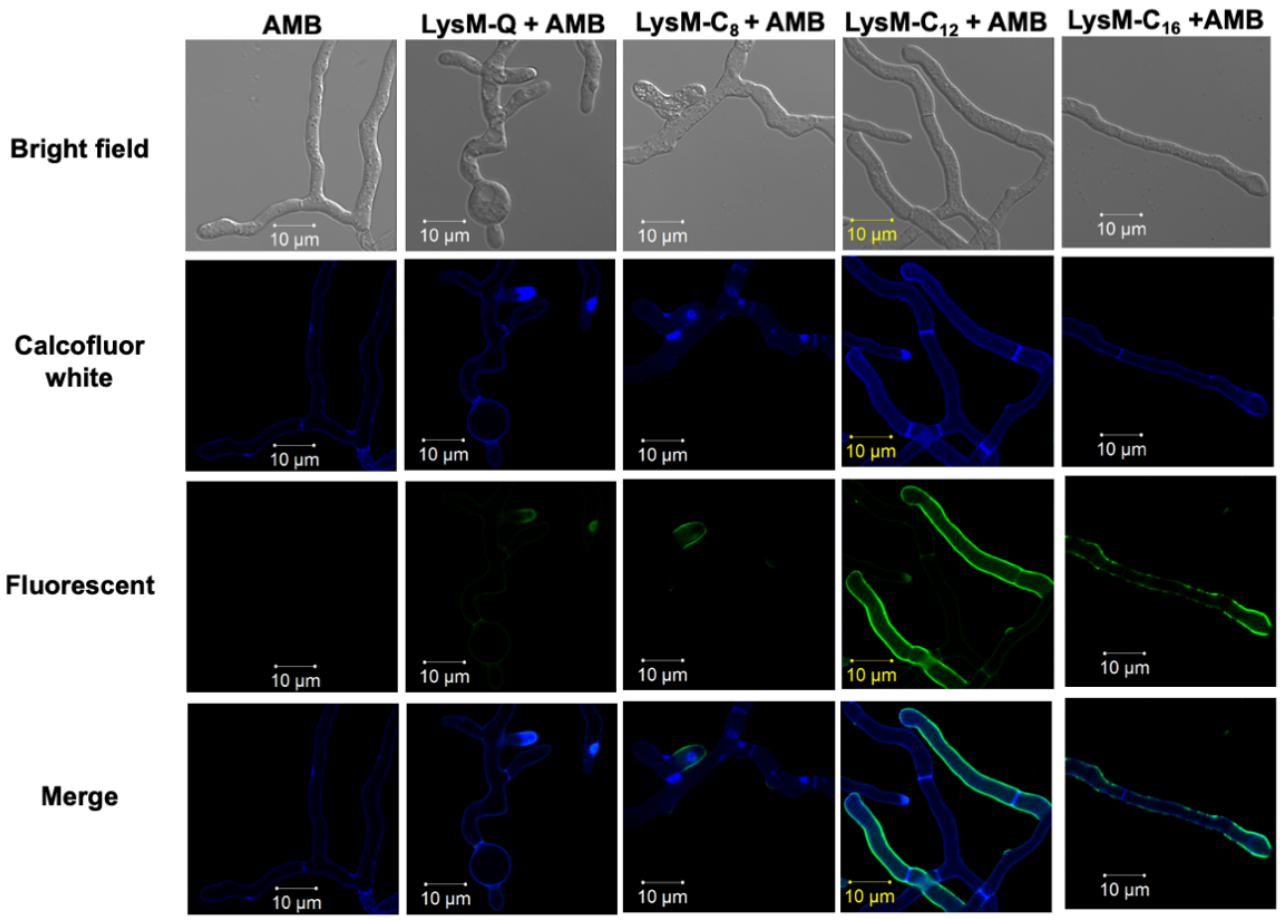

Figure. 3. 4. The confocal laser scanning microscopy (CLSM) analysis of LysM-Q and LysM-C_n localization on *Trichoderma viride*. The LysM-Q and LysM-C_n were conjugated with NHS-fluorescent. The *Trichoderma viride* were germinated for 16 h and treated with AMB (0.31 uM) and LysM-Q or LysM-C_n for 1 h. It was washed with 20 mM sodium phosphate buffer (pH 7.4) to remove unconjugated fluorescent.

Then, the localization of LysM-Q and LysM-Cn was further evaluated without AMB (Figure. 3. 5). The lipidation of LysM-Q showed a high binding ability with the fungal cell wall, and the LysM-C12 displayed vigorous critical activity while the LysM-C16 anchored all the fungal cell walls. From the picture of LysM-Q only, we could see that the lysis at the tip of *T. viride* by exhibiting the leaking out of cytosolic components from the fungal cell. These results correlated with a previous research[17], showing the mechanism of action of Lysine motif multimers (LysMn) acted on the tips of fungal hyphae. In addition, Taira *et al*. demonstrated that the fluorescent protein could be identified in the

septa, lateral walls, and tips of the hyphae of *Trichoderma* sp. when the fungus was treated with FITC-labeled RSC-a[18]. Based on the literature review, this is the first report investigating the effect of anchoring of chitin-binding domain modified with lipids on fungal cell walls.

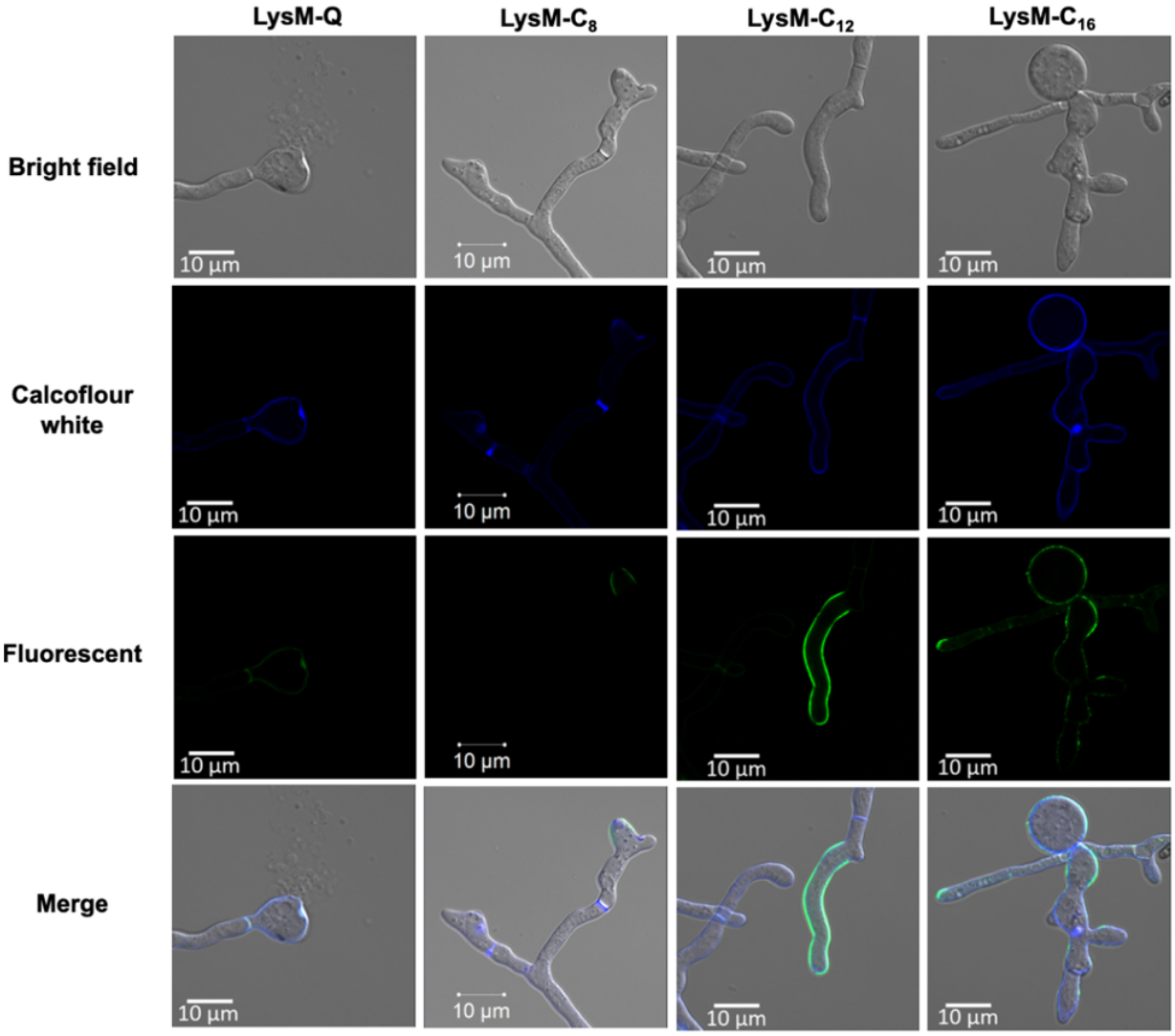

Fig. 3. 5. The confocal laser scanning microscopy (CLSM) analysis of LysM-Q and LysM-C_n localization on *Trichoderma viride*. The LysM-Q and LysM-C_n were conjugated with NHS-Fluorescent. The *Trichoderma viride* were germinated for 16 h and treated with LysM-Q or LysM-C_n for 1 h, and it was washed with 20 mM sodium phosphate buffer (pH 7.4) to remove unconjugated fluorescent.

In order to examine the integrity of the membrane upon the treatment with LysM-Q or LysM-Cn conjugates, they were incubated with *T. viride* at a concentration of 1 µM, either in combination with

AMB (0.65 uM) or without AMB. The fluorescence of PI was seen on the mycelium (Figure. 3. 6). It was revealed that the length of alkyl chains of lipid moiety influenced membrane integrity, with strong fluorescence was found for LysM-C16, LysM-C16+AMB, LysM-C12, LysM-C12+AMB, and AMB alone. The conjugates that included palmitic acid were combined with AMB showed the highest PI fluorescence on the mycelium. This phenomenon might be due to the change in the membrane structure caused by anchoring LysM-Cn and the insertion of AMB into fungal membrane cells, resulting in membrane damage. AMB and LysM have different mechanisms of action in targeting the fungal cell. AMB is a membrane-acting drug that binds to the ergosterol at fungal membrane cells; meanwhile, LysM is a cell wall-binding protein targeted at the chitin part in the fungal cell walls located near the cell membrane of fungi. It is possible that an increase in the permeability of the fungal cell membrane resulted in the loss of membrane functions, ultimately leading to the cell's death. This permeability enhancement may result from several different mechanisms, such as depolarization, the disruption of lipid domain structure, the formation of holes, or an internal electrochemical gradient imbalance[19,20]. All these mechanisms might potentially contribute suppressing to *T. viride* growth, treated with LysM-Cn combined with AMB.

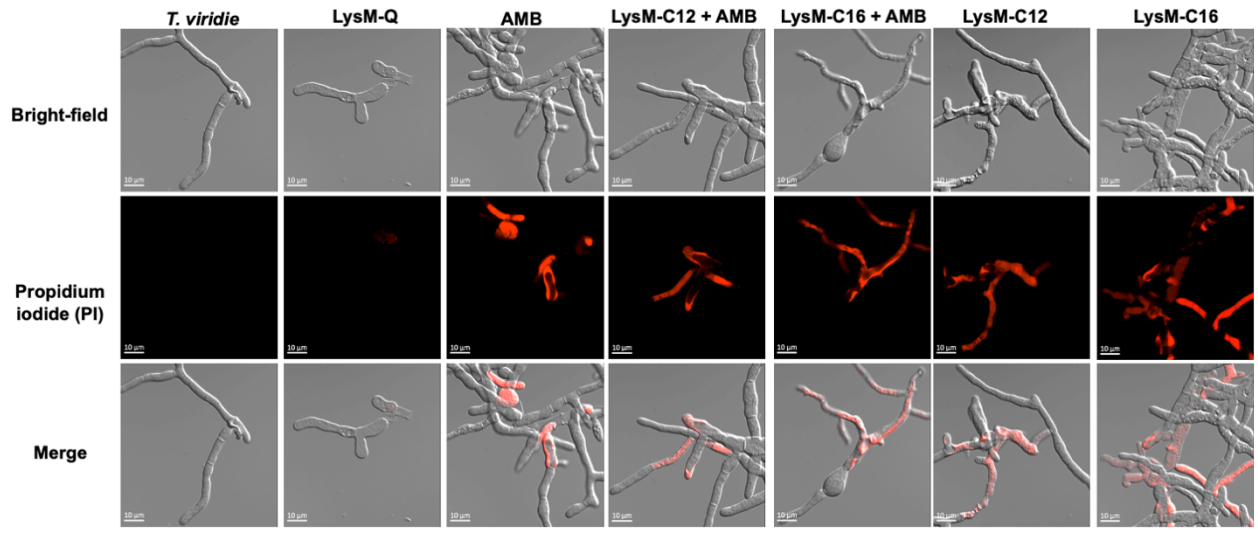

Fig. 3. 6. The effect of LysM-C12 or LysM-C16 combined with AMB and without AMB on membrane integrity of *T. viride***.** *T. viride* was treated with 1 µM of LysM-C12 or LysM-C16 and 0.625 µM of AMB at 37 ºC for 5 hours. The propidium iodide (PI) was added at 0.1 µM and incubated for 10 minutes; then, it was washed with 20 mM sodium phosphate buffer (pH 7.4) to remove unconjugated PI before CLSM analyses.

3.4 Conclusion

In this chapter, the localization of the chitin-binding protein of *Pteris ryukyuensis* was successfully observed in the fungal cell walls of *T. viride*. The labeled LysM with NHS-Fluorescent and PI staining confirmed that the lipidated LysM could enhance the anchoring ability of LysM to the fungal cell wall, and it affected the membrane integrity of fungus. LysM-C12 and LysM-C16 exhibited a strong binding affinity to the fungal cell wall compared with LysM-C8 and LysM. Interestingly, the conjugation of LysM-Q with C-12 and C-16 showed good antifungal activity compared with LysM-C8 and LysM-Q only. At the concentration of 1µM without AMB, these conjugates showed an inhibition value against *T. viride* growth at 96.3% (LysM-C16), 79.2% (LysM-C12), 55.1% (LysM-C8), and 7.6% (LysM-Q. In addition, the observation of LysM-Q conjugates (1 µM) activity combined with AMB exhibited the enhancement of antifungal activity with a minimum inhibitory concentration (MIC) value of 0.625

μM. These combinations could fully suppress the *T. viride* growth. The findings obtained in this study are well correlated with the improved staining of fluorescein-labeled LysM-Cn, in which the action of LysM depends on the alkyl chain length of attached lipids.

References

(1) Fisher, M. C.; Alastruey-Izquierdo, A.; Berman, J.; Bicanic, T.; Bignell, E. M.; Bowyer, P.; Bromley, M.; Brüggemann, R.; Garber, G.; Cornely, O. A.; Gurr, S. J.; Harrison, T. S.; Kuijper, E.; Rhodes, J.; Sheppard, D. C.; Warris, A.; White, P. L.; Xu, J.; Zwaan, B.; Verweij, P. E. Tackling the Emerging Threat of Antifungal Resistance to Human Health. *Nat. Rev. Microbiol.* **2022**, *0123456789*.

(2) Ayalon, O.; Cohen, M. J.; Orenbuch-Harroch, E.; Sviri, S.; van Heerden, P. V.; Korem, M. Invasive Fungal Infections in Critically Ill COVID-19 Patients in a Large Tertiary University Hospital in Israel. *J. Crit. Care* **2022**, *69*, 154004.

(3) Lai, C. C.; Yu, W. L. COVID-19 Associated with Pulmonary Aspergillosis: A Literature Review. *J. Microbiol. Immunol. Infect.* **2021**, *54* (1), 46–53.

(4) Jiang, Z.; Chen, S.; Zhu, Q.; Xiao, Y.; Qu, J. COVID-19-Associated Pulmonary Aspergillosis in a Tertiary Care Center in Shenzhen City. *J. Infect. Public Health* **2022**, *15* (2), 222–227.

(5) Lee, Y.; Puumala, E.; Robbins, N.; Cowen, L. E. Antifungal Drug Resistance: Molecular Mechanisms in Candida Albicans and Beyond. *Chem. Rev.* **2021**, *121* (6), 3390–3411.

(6) Li, Y.; Sun, L.; Lu, C.; Gong, Y.; Li, M.; Sun, S. Promising Antifungal Targets against Candida Albicans Based on Ion Homeostasis. *Front. Cell. Infect. Microbiol.* **2018**, *8* (SEP), 1–13.

(7) Cavassin, F. B.; Baú-Carneiro, J. L.; Vilas-Boas, R. R.; Queiroz-Telles, F. Sixty Years of Amphotericin B: An Overview of the Main Antifungal Agent Used to Treat Invasive Fungal Infections. *Infect. Dis. Ther.* **2021**, *10* (1), 115–147.

(8) Laniado-Laborín, R.; Cabrales-Vargas, M. N. Amphotericin B: Side Effects and Toxicity. *Rev. Iberoam. Micol.* **2009**, *26* (4), 223–227.

(9) Wang, D.; Zhang, W.; Ju, J. X.; Wang, L. J.; Huang, R. Y.; Xu, Y. F.; Zhang, H. L.; Qi, J. L. Gender Differences in Acute Toxicity, Toxicokinetic and Tissue Distribution of Amphotericin B Liposomes in Rats. *Toxicol. Lett.* **2021**, *338* (November 2020), 78–84.

(10) Santoso, P.; Minamihata, K.; Ishimine, Y.; Taniguchi, H.; Komada, T.; Sato, R.; Goto, M.; Takashima, T.; Taira, T.; Kamiya, N. Enhancement of the Antifungal Activity of Chitinase by Palmitoylation and the Synergy of Palmitoylated Chitinase with Amphotericin B. *ACS Infect. Dis.* **2022**, *8*, 1051–1061.

(11) Abu-Tahon, M. A.; Isaac, G. S. Anticancer and Antifungal Efficiencies of Purified Chitinase Produced from Trichoderma Viride under Submerged Fermentation. *J. Gen. Appl. Microbiol.* **2020**, *66* (1), 32–40.

(12) Ohnuma, T.; Onaga, S.; Murata, K.; Taira, T.; Katoh, E. LysM Domains from Pteris

Ryukyuensis Chitinase-A: A Stability Study and Characterization of the Chitin-Binding Site. *J. Biol. Chem.* **2008**, *283* (8), 5178–5187.

(13) Minamihata, K.; Tanaka, Y.; Santoso, P.; Goto, M.; Kozome, D.; Taira, T.; Kamiya, N. Orthogonal Enzymatic Conjugation Reactions Create Chitin Binding Domain Grafted Chitinase Polymers with Enhanced Antifungal Activity. *Bioconjug. Chem.* **2021**, *32* (8), 1688–1698.

(14) Mejuch, T.; Waldmann, H. Synthesis of Lipidated Proteins. *Bioconjug. Chem.* **2016**, *27* (8), 1771–1783.

(15) Ray, A.; Jatana, N.; Thukral, L. Lipidated Proteins: Spotlight on Protein-Membrane Binding Interfaces. *Prog. Biophys. Mol. Biol.* **2017**, *128*, 74–84.

(16) Sato, R.; Minamihata, K.; Ariyoshi, R.; Taniguchi, H.; Kamiya, N. Recombinant Production of Active Microbial Transglutaminase in E. Coli by Using Self-Cleavable Zymogen with Mutated Propeptide. *Protein Expr. Purif.* **2020**, *176* (August), 105730.

(17) Takashima, T.; Sunagawa, R.; Uechi, K.; Taira, T. Antifungal Activities of LysM-Domain Multimers and Their Fusion Chitinases. *Int. J. Biol. Macromol.* **2020**, *154*, 1295–1302.

(18) Taira, T.; Ohnuma, T.; Yamagami, T.; Aso, Y.; Ishiguro, M.; Ishihara, M. Antifungal Activity of Rye (Secale Cereale) Seed Chitinases: The Different Binding Manner of Class i and Class Ii Chitinases to the Fungal Cell Walls. *Biosci. Biotechnol. Biochem.* **2002**, *66* (5), 970–977.

(19) Lee, H.; Hwang, J. S.; Lee, J.; Kim, J. Il; Lee, D. G. Scolopendin 2, a Cationic Antimicrobial Peptide from Centipede, and Its Membrane-Active Mechanism. *Biochim. Biophys. Acta - Biomembr.* **2015**, *1848* (2), 634–642.

(20) Lee, W.; Lee, D. G. Fungicidal Mechanisms of the Antimicrobial Peptide Bac8c. *Biochim. Biophys. Acta - Biomembr.* **2015**, *1848* (2), 673–679.

Chapter 4 Preparation of amphotericin B-loaded hybrid liposomes and the integration of chitin-binding proteins for enhanced antifungal activity

4.1 Introduction

Fungal infection correlated with other diseases is a global problem; for example, invasive pulmonary aspergillosis has been reported to cause acute respiratory distress in 19.6%–33.3% of COVID-19 patients with acute respiratory distress syndrome[1]. Invasive aspergillosis is a fungal infection caused by *Aspergillus* species, especially *A. fumigatus*. The annual morbidity and mortality caused by this pathogen are constantly increasing because of the limited antifungal drugs available to fight the infection[2,3]. The emergence of antifungal drug-resistant fungi is also a critical issue, and recent studies showed that *A. fumigatus* may be resistant to several commercial antifungal drugs[4,5]. Amphotericin B (AMB), which is isolated from *Streptomyces nodosus* in 1954, is another widely used antifungal because of its broad-spectrum activity against pathogenic fungi, including yeasts and molds[6].

AMB, which is a membrane-acting drug, kills pathogenic fungi by various molecular mechanisms. The commonest mechanism of action is the interaction of AMB with ergosterol in the fungal cell membrane[7]. AMB binds the ergosterol, causing membrane pore formation, loss of intracellular ions, and cell death. Using a micellar formulation may improve the solubility of AMB; however, it has caused nephrotoxicity and hypokalemia in patients infected by fungi[8]. Therefore, the second generation of AMB-based drugs, such as AmBisome®, was introduced, based on liposomal

formulations. These formulations are believed to be safer than fungizone (the conventional commercial formulation in which AMB is solubilized by using sodium deoxycholate). Liposomes have been widely used as drug carriers because of their biocompatibility, and their capability to encapsulate bioactive hydrophobic molecules have proven their potential for the therapy and prevention of infectious diseases[9]. Since a recent study has shown that a liposomal AMB formulation caused acute toxicity in female rats[10], new approaches have been developed to minimize the toxicity of AMB, but there remains room for further development[11-13]. One of the best approaches is the combination of AMB with other natural antifungal compounds; this strategy shows promising results with decreased toxicity[14,15].

The enzyme chitinase (EC. 3.2.1.14) is considered a potent, low-toxicity antifungal candidate because of its specificity toward chitin, which is present in the fungal cell wall but absent in humans. A class IV chitinase isolated from *Anacardium occidentale* L. was reported to exhibit antifungal activity toward the phytopathogenic fungus *Lasiodiplodia theobromae*, potentially inhibiting its growth by degrading the hyphae[16]. Notably, Medhat and George reported that *Trichoderma viride* chitinase was nontoxic to the human HeLa and HepG2 cell lines, even at a high concentration of chitinase (>120 µg/mL). This chitinase was reported to inhibit the growth of *Fusarium oxysporum* f. sp. *lycopersici race* 3 at 2.13 mg/mL[17].

In pharmaceutical applications, lipids have been utilized to enhance the function of antimicrobial reagents and the lipidation of antimicrobial peptides have been of great interest to increase the bioavailability in recent years[18,19]. However, little information is available on the effect of lipidation

of antifungal proteins possibly due to the difficulty in scalable preparation. To circumvent the problem, we established an enzymatic method to site-specifically attach a lipid-peptide conjugate with a recombinant protein, and found that a model green fluorescent protein modified with a myristoyl or palmitoyl moiety exerted the strong anchoring ability to mammalian cell surface[20]. In this context, our previous study, we focused on the conjugation of a palmitoyl moiety to the *C*-terminus of biologically active domains of chitinase from *Pteris ryukyuensis*[21]. Interestingly, the antifungal activity of the chitin-binding domain (LysM) of *P. ryukyuensis* chitinase, which has a pivotal role in inhibiting the fungal growth[22], was markedly enhanced when palmitoylated and combined with a conventional AMB formulation. On the basis of our recent findings, here, we shifted from a micellar formulation of AMB to a liposomal formulation[23] to decrease the possible side effects. To understand the properties of AMB-loaded liposomal formulations (AMB-LFs) combined with LysM, we prepared different types of hybrid liposomes, including AMB and sodium deoxycholate, and characterized them with regard to size, surface charge, and activity against the mold *T. viride* (Fig. 1). Our results suggest that the combination of neutral AMB-LF with LysM is effective in decreasing the amount of AMB required to suppress fungal growth, and the combination with LysM-Pal shows strong antifungal activity independent of the type of liposome used.

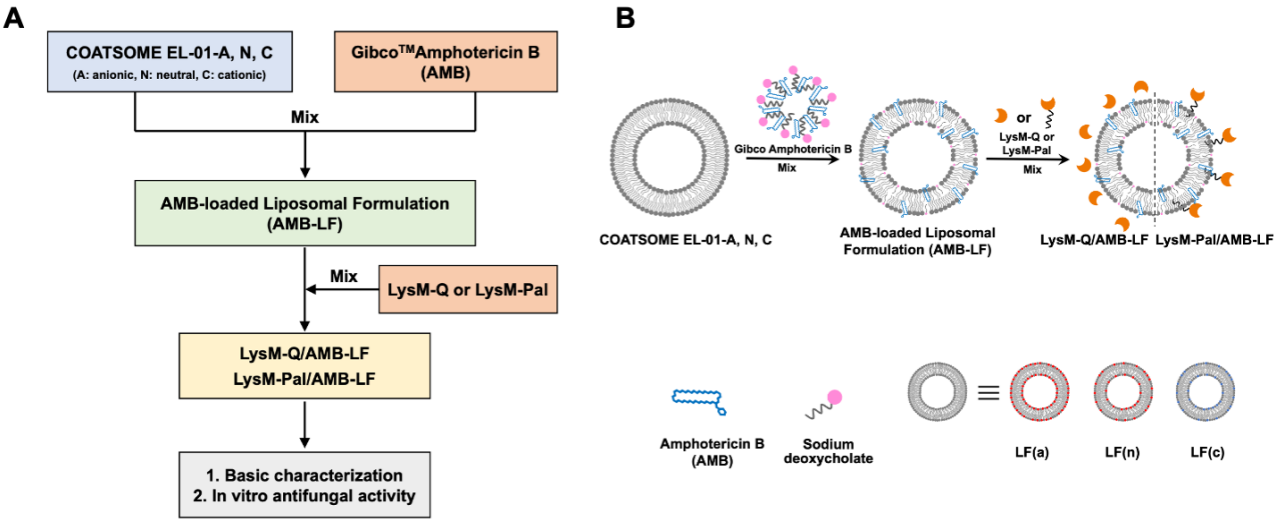

Figure 4.1. (A) Flowchart of the preparation and characterization of amphotericin B (AMB)-loaded liposomal formulations (AMB-LFs). **(B)** Schematic illustration of the preparation of AMB-LFs having different surface charges, with or without integration of engineered chitin-binding domains (LysM-Q or LysM-Pal). AMB-LF(a), LF(n) and LF(c) stand for those prepared by mixing AMB with COATSOME EL-01-A, -N and -C, respectively. The red and blue headgroups of lipids represent the anionic and cationic charges of L-α-dipalmitoyl phosphatidyl glycerol (DPPG) and stearyl amine, and the gray shows L-α-dipalmitoyl phosphatidyl choline (DPPC). Reproduce with permission from ref[26]. Copyright 2022 Elsevier.

4.2 Materials and Methods

4.2.1 Materials

Gibco™ Amphotericin B (containing 250 µg of AMB and 205 µg of sodium deoxycholate as a solubilizer) was purchased from Thermo Fisher Scientific. Three different types of commercial liposomes were purchased from NOF Corporation (Japan): neutral liposomes (COATSOME EL-01-N) containing 54 µmol L-α-dipalmitoyl phosphatidyl choline (DPPC), 40 µmol cholesterol (CHOL), and 6 µmol L-α-dipalmitoyl phosphatidyl glycerol (DPPG); anionic liposomes (COATSOME EL-01-A) containing 30 µmol DPPC, 40 µmol CHOL, and 30 µmol DPPG; and cationic liposomes (COATSOME EL-01-C) containing 52 µmol DPPC, 40 µmol CHOL, and 8 µmol stearyl amine (SA).

Sodium dodecyl sulfate, glycerol, potassium dihydrogen phosphate, and sodium chloride were purchased from Wako Pure Chemical Industries, Ltd. (Osaka, Japan). Luria-Bertani broth, ammonium peroxodisulfate, 30% acrylamide/*bis*-acrylamide mixed solution (29:1), tris(hydroxymethyl)aminomethane, tryptone, dried yeast extract, dipotassium hydrogen phosphate, and hydrochloric acid were purchased from Nacalai Tesque, Inc. (Kyoto, Japan). All chemicals were used without any further purification. Amicon®Ultra centrifugal concentrators (100-kDa cutoff, 0.5 mL) were purchased from Millipore (Tokyo, Japan). The palmitic acid-peptide conjugate comprising of an MTG-reactive Lys-containing peptide (C16-GGGSRHK) was synthesized by a standard Fmoc peptide synthesis (MTG)[20]. Recombinant microbial transglutaminase (MTG)[25], and a chitin-binding LysM domain from *P. ryukyuensis* with an MTG-reactive Gln-containing tag (LysM-Q)[21] were prepared using *Escherichia coli* BL21(DE3) in accordance with the procedures described in our previous reports. LysM was engineered by fusing a Gln-containing peptide (FYPLQMRGG) at the *C*-terminus to yield LysM-Q. LysM-Q and C16-GGGSRHK were cross-linked by MTG to prepare a palmitoylated LysM domain (LysM-Pal).

4.2.2 Preparation of AMB-LFs

The overall process of the preparation and characterization of AMB-LFs is shown in Fig. 1. AMB-LF(a), AMB-LF(n), and AMB-LF(c) indicate those prepared using COATSOME EL-01-A, COATSOME EL-01-N, and COATSOME EL-01-C, respectively. The AMB-LFs with different surface charges were prepared as follows. First, each liposome (anionic, neutral, or cationic) was prepared in 20 mM NaPi (pH 7.4) in a separate tube following the manufacturer's protocol. Then,

Gibco™ Amphotericin B was added to the aqueous solution of each liposome. Each solution was mixed by gently inverting the test tube several times. The resultant solutions of AMB-LFs for dynamic light scattering (DLS) and antifungal activity analyses contained 5.0 μM AMB, 9.1 μM sodium deoxycholate, and 47.6 μM total lipids in 20 mM NaPi (pH 7.4). When combining an AMB-LF with LysM-Q or LysM-Pal, the final concentration of LysM-Q or LysM-Pal was adjusted to 1.0 μM.

4.2.3 Characterization of AMB-LFs

The size and zeta potential of the AMB-LFs at 25°C were analyzed by DLS measurement using a Zetasizer Nano ZS (Malvern, Worcestershire, UK). The encapsulation efficiency of AMB in the liposomal formulations was determined as follows: We prepared an aqueous solution of AMB-LF containing 100 μM AMB, 183 μM sodium deoxycholate, and 951 μM total lysosomal lipids in 20 mM NaPi (pH 7.4). Each sample of AMB-LF (300 μL) was placed in a 100-kDa cutoff centrifugal filter (Amicon®Ultra) and centrifuged at 7,500 × *g* for 5 min. Then, 300 μL of the aqueous buffer solution was added to the filter to recover the remaining liposomal formulation. The concentration of AMB encapsulated in AMB-LFs was calculated by measuring the absorbance at 330 nm in the recovered solution using a NanoDrop instrument (Thermo Fisher Scientific) by referring a calibration curve separately prepared for each sample.

4.2.3 Antifungal activity assay

Antifungal assays were performed in 96-well plates by using serial dilutions of AMB-LFs, LysM-Q/AMB-LFs, or LysM-Pal/AMB-LFs. *T. viride* was added to each well at 10,000 spores/mL, and the plates were incubated at 25°C for 60 h. The OD values at 630 nm (arising from grown fungi) were

measured using a microplate reader. Images of *T. viride* in the plates were captured using a digital camera. The color images were converted to grayscale (8 bits; gray level range: 0 to 255) using ImageJ software (version 1.46; https://imagej.nih.gov/ij/download. html) and the intensity of each grayscale image was measured to determine the amount of fungus that was present.

4.2.4 Data analysis

GraphPad Prism 6 (GraphPad Software, La Jolla, CA, U.S.A) was used for statistical analysis, and the data were expressed as a mean ± standard deviation (SD). One-way analysis of variance was used to assess the type of liposomal formulations and the antifungal activities. An unpaired *t*-test was used to evaluate the effect of liposomal combination with AMB. Significant differences were analyzed by Tukey's HSD posthoc test for multiple comparisons (* $p < 0.05$, ** $p < 0.01$).

4.3 Results and discussion

4.3.1 Characterization of AMB-LFs by DLS analysis

First, the authors evaluated the particle size and zeta potential of AMB-LFs. Figure 4.2 and Table 4.1 show the results of DLS measurements of different types of AMB-free liposomes and AMB-loaded liposomes. The AMB-free liposomes had similar sizes, approximately 140–150 nm. The zeta potential of all the samples was negative, but the magnitude of the charge depended on the lipid composition. The charge of AMB-LF(a) was the greatest (−64.9 mV), while that of AMB-LF(c) was the smallest (−20.7 mV), plausibly because of the presence of SA in the latter. AMB-LF(n) showed an intermediate charge (−50.5 mV). An unpaired *t*-test of the zeta potential for AMB encapsulation into the liposome showed that the LF(a) vs AMB-LF(a) and LF(c) vs AMB-LF(c) did not show a significant difference,

whereas the zeta potential of LF(n) vs AMB-LF(n) has a significant difference ($p < 0.05$). The one-way analysis of variance (ANOVA) of liposomal formulations exhibited that the LF(a) vs LF(c) and LF(c) vs LF(n) gave a significant difference ($p < 0.01$). Mixing LFs with Gibco™ Amphotericin B resulted in a slight decrease on the particle size in all cases (Table 4.1), but it had little influence on the size distribution for AMB-LF(a) or AMB-LF(n) (Figure. 4.2). However, in the case of AMB-LF(c), a wider size distribution with an increased PDI value was observed, suggesting that the incorporation of AMB and sodium deoxycholate affected the integrity of the liposomal formulation. The negative charges of the LFs were mitigated by the incorporation of AMB, plausibly because of the presence of a primary amino group in AMB. These results suggest that AMB and its solubilizer sodium

deoxycholate were successfully integrated, and the hybrid liposomal formulations AMB-LF(a) and AMB-LF(n) were obtained successfully.

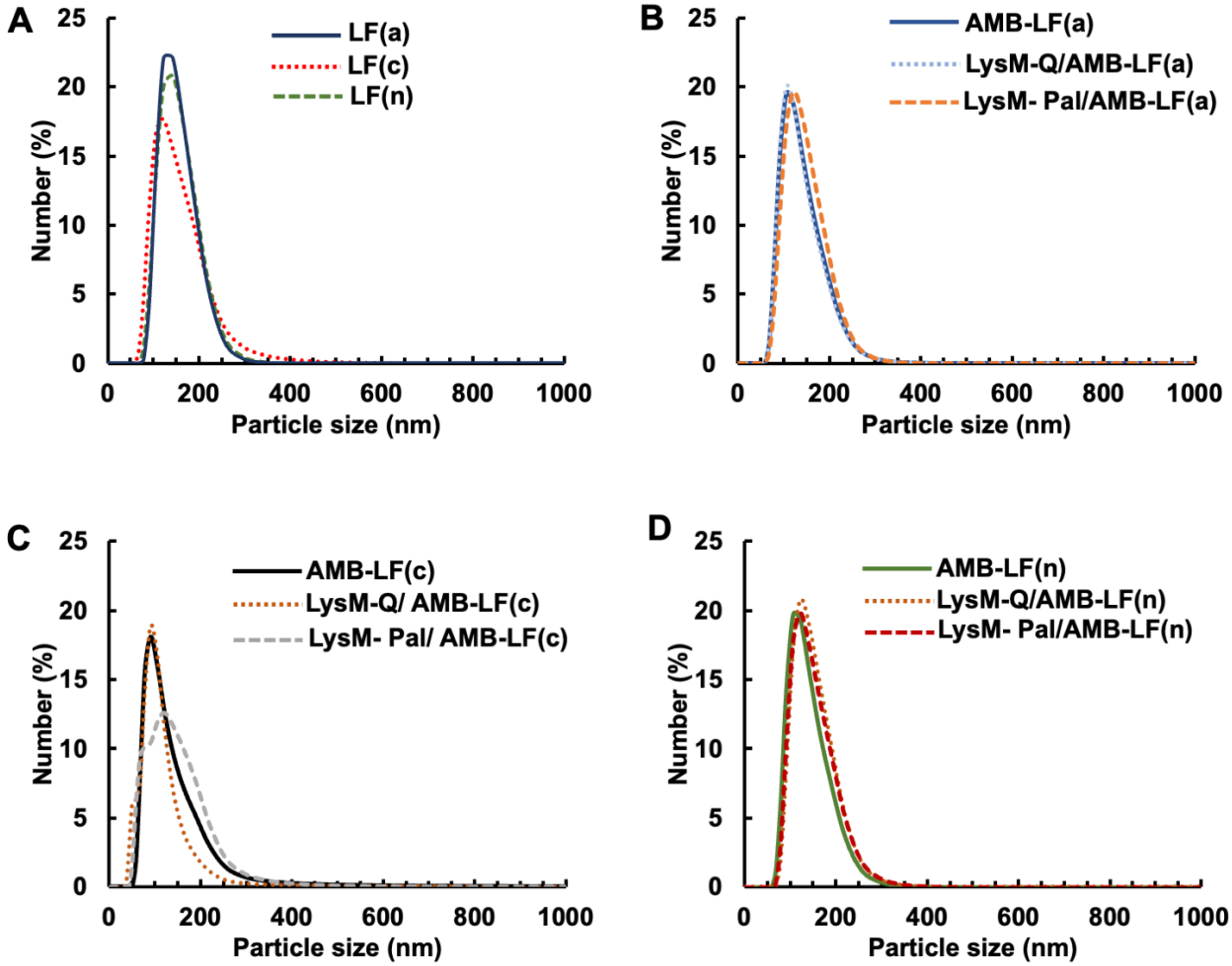

Figure 4.2. Dynamic light scattering analysis of AMB-free liposomes (A) and AMB-LFs with different surface charges: (B) AMB-LF(a), (C) AMB-LF(c), and (D) AMB-LF(n). Reproduce with permission from ref[26]. Copyright 2022 Elsevier.

Table. 4.1. Size and zeta potential of three kinds of liposomes (anionic, cationic, and neutral), and combination of liposome-loaded amphotericin B (AMB). Reproduce with permission from ref[26]. Copyright 2022 Elsevier.

Antifungal reagent	Size (Z-average) (nm)	Polydispersity Index (PDI)	Zeta potential (mV)
LF(a)	167.0 ± 2.5	0.04 ± 0.02	-64.9 ± 2.9
AMB-LF(a)	163.6 ± 1.9	0.10 ± 0.03	-63.0 ± 3.2
LF(c)	143.6 ± 8.7	0.21 ± 0.02	-20.7 ± 1.6
AMB-LF(c)	119.8 ± 25.4	0.36 ± 0.05	-18.4 ± 1.9
LF(n)	173.1 ± 2.7	0.05 ± 0.03	-50.5 ± 2.0
AMB-LF(n)	170.5 ± 0.4	0.15 ± 0.04	-41.6 ± 1.6

The AMB encapsulation of each liposomal formulation was quantified (Figure. 4.3). Free Gibco™ Amphotericin B, which is a micellar formulation, would be expected to pass through a 100-kDa cutoff centrifugal filter membrane. AMB-LF(a) and AMB-LF(n) retained >75% of the initial loaded AMB after one round of filtration, and approximately half of the initially loaded AMB after three rounds of filtration. However, in the case of AMB-LF(c), approximately 75% of the initially loaded AMB was lost after the first filtration, indicating that AMB was not stably incorporated in AMB-LF(c), consistent with the DLS analysis (Table 4.1). These results suggest decreased integrity of LFs containing SA and AMB, both of which possess a primary amino group, because of electrostatic repulsion.

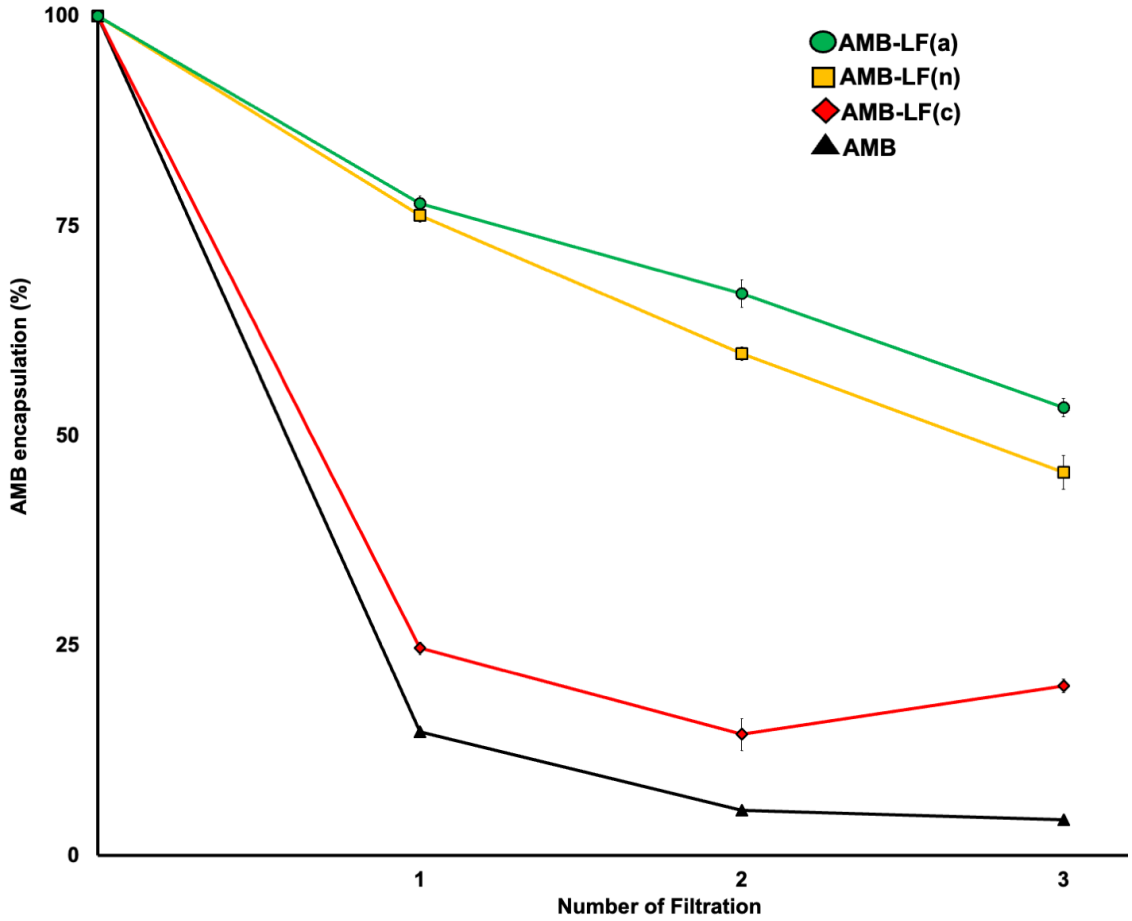

Figure 4.3. Encapsulation efficiency of AMB in AMB-LFs. The encapsulation efficiency of Amphotericin B-loaded Liposomes. The encapsulation of AMB into liposome was conducted using a 100 kDa cut-off ultrafiltration filter (Amicon®Ultra) under condition 7,500 × g for 5 min. The concentration of AMB-Liposome Formulation (AMB-LF) was measured spectrophotometrically at 330 nm by using NanoDrop (Thermo Fisher Scientific). All experiments were conducted in triplicate (n = 3). Reproduce with permission from ref[26]. Copyright 2022 Elsevier.

Next, recombinant LysM-Q and LysM-Pal were mixed with AMB-LFs. No marked change in size distribution was observed after mixing LysM-Q with AMB-LF(a) or AMB-LF(n), while the size of LysM-Pal/AMB-LF(a) and LysM-Pal/AMB-LF(n) were 170.0 nm and 177.7 nm, respectively, showing a slight increase in size by the incorporation of LysM-Pal (Fig. 4.2). In contrast, however, AMB-LF(c) was seemingly destabilized by the incorporation of LysM-Pal. The theoretical isoelectric

point of LysM-Q is 6.99, thus it is negatively charged at pH 7.4. It is plausible that electrostatic interaction between LysM-Pal and SA could disrupt the self-assembled liposomal formulation. On the basis of the results above, AMB-LF(a) and AMB-LF(n) were selected for further study.

4.3.2 Antifungal activity of AMB-LFs and the effect of integration of LysM

The authors evaluated the antifungal activity of AMB-LFs against *T. viride* in a 96-well plate format (Figure. 4.4). Fungal growth was partially inhibited by AMB-LFs with AMB concentration 5.0 μM, and there was no difference between AMB-LF(a) and AMB-LF(n) (Figure. 4.4A). The inhibition of fungal growth by AMB-LFs was clearly enhanced in the presence of LysM-Q (LysM-Q/AMB-LFs), prepared by simple mixing of an aqueous solution of LysM-Q (1.0 μM) with the AMB-LFs. The minimum inhibitory concentration (MIC) of AMB in LysM-Q/AMB-LF(n) was slightly lower than that in LysM-Q/AMB-LF(a), suggesting that the difference in the surface charge of AMB-LFs affected the performance in suppression of fungal growth because the particle sizes of AMB-LF(a) and AMB-LF(n) were similar (Table 4.1).

The one-way ANOVA was performed to analyze the differences between the antifungal liposomal formulations and significant differences were analyzed by Tukey's HSD posthoc test for multiple comparisons (Figure. 4.4B). At 1.25 uM AMB, the antifungal activity of AMB-LF(a) was significantly enhanced in the combination with LyM-Q ($p < 0.01$), suggesting the synergistic action of LysM-Q with AMB-LF(a). The difference in the antifungal activities of LysM-Q/AMB-LF(n), LysM-Pal/AMB-LF(a), and LysM-Pal/AMB-LF(n) was not significant. At 0.16 uM AMB, LysM-Pal/AMB-LF(a) and LysM-Pal/AMB-LF(n) exhibited marked antifungal activities, and they showed significant

differences towards AMB-LF(a), AMB-LF(n), LysM-Q/AMB-LF(a) and LysM-Q/AMB-LF(n) ($p < 0.01$), indicating that incorporation of LysM-Pal into the AMB-LFs markedly lowered the dose of AMB required for fungal inhibition, while LysM-Pal/AMB-LF(a) and LysM-Pal/AMB-LF(n) exhibited comparable performance with MIC values of 0.31 μM for both. Comparing LysM-Q/AMB-LF(a) with LysM-Pal/AMB-LF(a), the effect of adding the palmitoyl moiety to LysM-Q resulted in an approximately 15-fold decrease in the dose of AMB required to inhibit the fungal growth. Because the effect of LysM-Pal was similar when it was incorporated with either AMB-LF(a) or AMB-LF(n), the integration of LysM-Pal to AMB-loaded liposomes was dominant in the observed phenomenon. Therefore, we suggest that the functionalization of liposomal drug formulations with cell wall-binding proteins is an effective way to target pathogenic fungi with enhanced antifungal activity, and further study is needed to validate the concept for practical applications. This study also illustrates one way to approach biointerfaces, by designing artificial bioconjugates that can be tethered to an artificial membrane (i.e., liposomes) as well as functioning at a natural cell surface (i.e., the fungal cell wall)[25].

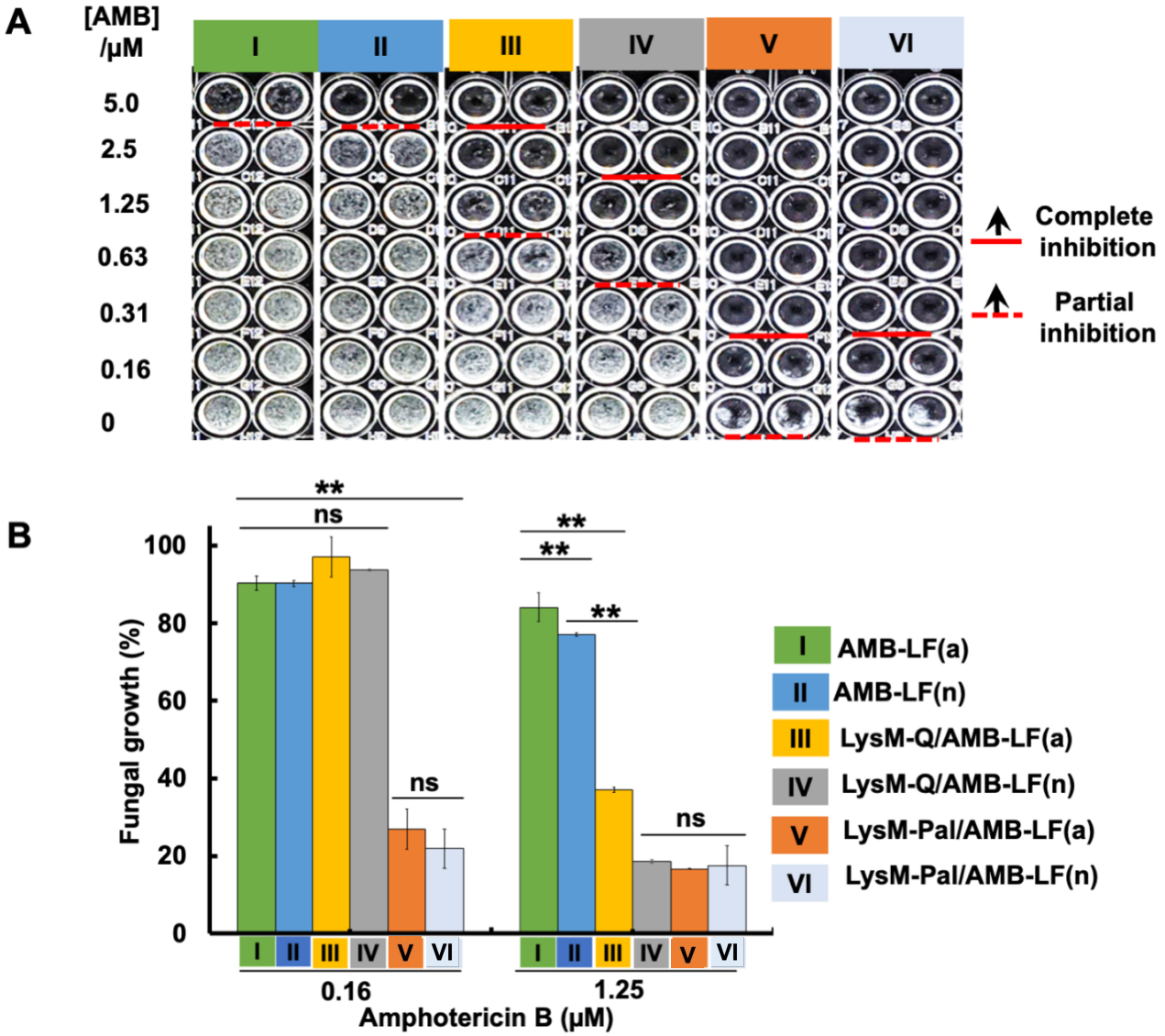

Figure 4.4. Antifungal activity of AMB-LFs. (A) Antifungal activity of AMB-LFs with or without engineered chitin-binding domains (LysM-Q or LysM-Pal). Image of a 96-well plate after culturing *Trichoderma viride* in the presence of AMB-LFs at 25°C for 60 h. (B) Fungal growth suppression by AMB-LFs. The fungal growth of each well was estimated from the photograph of the 96-well plate using ImageJ software. The intensity of grayscale image of wells without AMB ([AMB] = 0) was used as 100% growth. The error bars represent the standard deviation ($n = 2$). $^{**}p < 0.01$, ns = not significant. Reproduce with permission from ref[26]. Copyright 2022 Elsevier.

References

(1) Lai, C. C.; Yu, W. L. COVID-19 Associated with Pulmonary Aspergillosis: A Literature Review. *J. Microbiol. Immunol. Infect.* **2021**, *54* (1), 46–53.

(2) Zakaria, A.; Osman, M.; Dabboussi, F.; Rafei, R.; Mallat, H.; Papon, N.; Bouchara, J. P.; Hamze, M. Recent Trends in the Epidemiology, Diagnosis, Treatment, and Mechanisms of Resistance in Clinical Aspergillus Species: A General Review with a Special Focus on the Middle Eastern and North African Region. *J. Infect. Public Health* **2020**, *13* (1), 1–10.

(3) Paulussen, C.; Hallsworth, J. E.; Álvarez-Pérez, S.; Nierman, W. C.; Hamill, P. G.; Blain, D.; Rediers, H.; Lievens, B. Ecology of Aspergillosis: Insights into the Pathogenic Potency of Aspergillus Fumigatus and Some Other Aspergillus Species. *Microb. Biotechnol.* **2017**, *10* (2), 296–322.

(4) Escribano, P.; Rodríguez-Sánchez, B.; Díaz-García, J.; Martín-Gómez, M. T.; Ibáñez-Martínez, E.; Rodríguez-Mayo, M.; Peláez, T.; García-Gómez de la Pedrosa, E.; Tejero-García, R.; Marimón, J. M.; Reigadas, E.; Rezusta, A.; Labayru-Echeverría, C.; Pérez-Ayala, A.; Ayats, J.; Cobo, F.; Pazos, C.; López-Soria, L.; Alastruey-Izquierdo, A.; Muñoz, P.; Guinea, J.; Sánchez-Yebra, W.; Sánchez-Gómez, J.; Lozano, I.; Marfil, E.; Muñoz de la Rosa, M.; García, R. T.; Castro, C.; López, C.; Castelló-Abietar, C.; Costales, I.; Serra, J. L.; Jiménez, R.; Echeverría, C. L.; Pérez, C. L.; Megías-Lobón, G.; Lorenzo, B.; Sánchez-Reus, F.; Martín, M. T.; Vidal, I.; Sánchez-Hellín, V.; Ibáñez, E.; Pemán, J.; Fajardo, M.; Gómez, E.; Serrano, J.; Rodríguez, B.; Zvezdanova, E.; Gómez-Núñez, A.; Leiva, J. G.; Machado, M.; Sánchez-Romero, I.; García-Rodríguez, J.; Luis del Pozo, J.; Vallejo, M. R.; Ruiz de Alegría-Puig, C.; Vicente, D.; Fernández-Torres, M.; Hernáez-Crespo, S. Azole Resistance Survey on Clinical Aspergillus Fumigatus Isolates in Spain. *Clin. Microbiol. Infect.* **2021**, *27* (8), 1170.e1-1170.e7.

(5) Satish, S.; Perlin, D. S. Echinocandin Resistance in Aspergillus Fumigatus Has Broad Implications for Membrane Lipid Perturbations That Influence Drug-Target Interactions . *Microbiol. Insights* **2019**, *12*, 117863611989703.

(6) Cavassin, F. B.; Baú-Carneiro, J. L.; Vilas-Boas, R. R.; Queiroz-Telles, F. Sixty Years of Amphotericin B: An Overview of the Main Antifungal Agent Used to Treat Invasive Fungal Infections. *Infect. Dis. Ther.* **2021**, *10* (1), 115–147.

(7) Baginski, M.; Sternal, K.; Czub, J.; Borowski, E. Molecular Modelling of Membrane Activity of Amphotericin B, a Polyene Macrolide Antifungal Antibiotic. *Acta Biochim. Pol.* **2005**, *52* (3), 655–658. https://doi.org/10.18388/abp.2005_3426.

(8) Laniado-Laborín, R.; Cabrales-Vargas, M. N. Amphotericin B: Side Effects and Toxicity. *Rev.*

Iberoam. Micol. **2009**, *26* (4), 223–227.

(9) Nisini, R.; Poerio, N.; Mariotti, S.; De Santis, F.; Fraziano, M. The Multirole of Liposomes in Therapy and Prevention of Infectious Diseases. *Front. Immunol.* **2018**, *9* (FEB), 155.

(10) Wang, D.; Zhang, W.; Ju, J. X.; Wang, L. J.; Huang, R. Y.; Xu, Y. F.; Zhang, H. L.; Qi, J. L. Gender Differences in Acute Toxicity, Toxicokinetic and Tissue Distribution of Amphotericin B Liposomes in Rats. *Toxicol. Lett.* **2021**, *338* (November 2020), 78–84.

(11) Fuentefria, A. M.; Pippi, B.; Dalla Lana, D. F.; Donato, K. K.; de Andrade, S. F. Antifungals Discovery: An Insight into New Strategies to Combat Antifungal Resistance. *Lett. Appl. Microbiol.* **2018**, *66* (1), 2–13.

(12) Chang, Y. L.; Yu, S. J.; Heitman, J.; Wellington, M.; Chen, Y. L. New Facets of Antifungal Therapy. *Virulence* **2017**, *8* (2), 222–236.

(13) Campitelli, M.; Zeineddine, N.; Samaha, G.; Maslak, S. Combination Antifungal Therapy: A Review of Current Data. *J. Clin. Med. Res.* **2017**, *9* (6), 451–456.

(14) Chudzik, B.; Bonio, K.; Dabrowski, W.; Pietrzak, D.; Niewiadomy, A.; Olender, A.; Malodobry, K.; Gagoś, M. Synergistic Antifungal Interactions of Amphotericin B with 4-(5-Methyl-1,3,4-Thiadiazole-2-Yl) Benzene-1,3-Diol. *Sci. Rep.* **2019**, *9* (1), 1–14.

(15) Khan, M. S. A.; Malik, A.; Ahmad, I. Anti-Candidal Activity of Essential Oils Alone and in Combination with Amphotericin B or Fluconazole against Multi-Drug Resistant Isolates of Candida Albicans. *Med. Mycol.* **2012**, *50* (1), 33–42.

(16) Oliveira, S. T.; Azevedo, M. I. G.; Cunha, R. M. S.; Silva, C. F. B.; Muniz, C. R.; Monteiro-Júnior, J. E.; Carneiro, R. F.; Nagano, C. S.; Girão, M. S.; Freitas, C. D. T.; Grangeiro, T. B. Structural and Functional Features of a Class VI Chitinase from Cashew (Anacardium Occidentale L.) with Antifungal Properties. *Phytochemistry* **2020**, *180* (April).

(17) Abu-Tahon, M. A.; Isaac, G. S. Anticancer and Antifungal Efficiencies of Purified Chitinase Produced from Trichoderma Viride under Submerged Fermentation. *J. Gen. Appl. Microbiol.* **2020**, *66* (1), 32–40.

(18) Grimsey, E.; Collis, D. W. P.; Mikut, R.; Hilpert, K. TEMPORARY REMOVAL: The Effect of Lipidation and Glycosylation on Short Cationic Antimicrobial Peptide. *Biochim. Biophys. Acta - Biomembr.* **2020**, *1862* (8), 183195.

(19) Rounds, T.; Straus, S. K. Lipidation of Antimicrobial Peptides as a Design Strategy for Future Alternatives to Antibiotics. *Int. J. Mol. Sci.* **2020**, *21* (24), 1–15.

(20) Takahara, M.; Mochizuki, S.; Wakabayashi, R.; Minamihata, K.; Goto, M.; Sakurai, K.; Kamiya, N. Extending the Half-Life of a Protein in Vivo by Enzymatic Labeling with Amphiphilic Lipopeptides. *Bioconjug. Chem.* **2021**, *32* (4), 655–660.

(21) Santoso, P.; Minamihata, K.; Ishimine, Y.; Taniguchi, H.; Komada, T.; Sato, R.; Goto, M.; Takashima, T.; Taira, T.; Kamiya, N. Enhancement of the Antifungal Activity of Chitinase by Palmitoylation and the Synergy of Palmitoylated Chitinase with Amphotericin B. *ACS Infect. Dis.* **2022**, *8*, 1051–1061.

(22) Takashima, T.; Sunagawa, R.; Uechi, K.; Taira, T. Antifungal Activities of LysM-Domain Multimers and Their Fusion Chitinases. *Int. J. Biol. Macromol.* **2020**, *154*, 1295–1302.

(23) Ulrich, A. S. Biophysical Aspects of Using Liposomes as Delivery Vehicles. *Biosci. Rep.* **2002**, *22* (2), 129–150.

(24) Sato, R.; Minamihata, K.; Ariyoshi, R.; Taniguchi, H.; Kamiya, N. Recombinant Production of Active Microbial Transglutaminase in E. Coli by Using Self-Cleavable Zymogen with Mutated Propeptide. *Protein Expr. Purif.* **2020**, *176* (August), 105730.

(25) Hori, K.; Yoshimoto, S.; Yoshino, T.; Zako, T.; Hirao, G.; Fujita, S.; Nakamura, C.; Yamagishi, A.; Kamiya, N. Recent Advances in Research on Biointerfaces: From Cell Surfaces to Artificial Interfaces. *J. Biosci. Bioeng.* **2022**, *133* (3), 195–207.

(26) Pugoh Santoso., Takuya Komada., Yugo Ishimine., Hiromasa Taniguchi., Kosuke Minamihata., Masahiro Goto., Toki Taira., Noriho Kamiya. Preparation of amphotericin B-loaded hybrid liposomes and the integration of chitin-binding proteins for enhanced antifungal activity**,** *J Biosci Bioeng.* **2022.**

Chapter 5. Conclusion

5.1 Summary

The increasing cases of fungal infection and the emergence of antifungal drug-resistant fungi have been priority health concerns globally. The annual prevalence of morbidity and mortality caused by fungal infection gradually increases due to the ineffectiveness of antifungal drugs in combating pathogenic fungi and their toxicity toward human cells. Amphotericin B (AMB), a polyene antifungal group, is a gold standard antifungal drug widely used to treat fungal infections because of its broad-spectrum activity in combating the fungal pathogen. However, AMB has been reported to possess a nephrotoxicity level in humans due to its low solubility in water. The strategy to reduce the limitation of AMB has been developed until the combination with other antimycotic agents shows promising results by decreasing its toxicity. The combination of AMB with the biologically active compound is one of the best strategies to suppress pathogenic fungi because it exhibits a low side effect on humans. Chitinase is a potential candidate that can be considered a combination agent with AMB because chitinase catalyzes the hydrolysis of chitin, of which a major component of fungal cell wall. The chitinase consists of two essential domains: chitin-binding and a catalytic domain. The chitin-binding domain, like a LysM from the fern *Pteris ryukyuensis*, and the catalytic domain have the function to bind the chitin and hydrolysis of chitinous substrate, respectively. A study showed that deletion of LysM domain could decrease the antifungal activity, and the arrangement of tandem LysM can increase the antifungal activity. In this study, I investigated the role of LysM by conjugating it with a lipid by

microbial transglutaminase (MTG)-catalyzed cross-linking and found that marked increase in the antifungal activity in suppressing the fungal growth of *Trichoderma viride*.

In chapter 2, the role of the chitin-binding domain (LysM) and catalytic domain (CatD) and those combinations (LysM-CatD) in the antifungal activity were investigated. All the recombinant proteins were engineered by adding a glutamine-containing peptide (Q-tag) at the C-terminus to yield LysM-Q, CatD-Q and LysM-CatD-Q to facilitate the site-specific cross-linking catalyzed by MTG. I demonstrated a synergistic effect of the palmitoylated chitinase of *P. ryukyuensis* and AMB. LysM-Q, CatD-Q, and LysM-CatD-Q were successfully conjugated with a palmitoylated-peptide substrate with MTG-reactive Lys (Pal-K) by MTG. The palmitoylated chitinase domains exhibited strong antifungal activity against *T. viride* with IC_{50} values as low as 1 μM, nearly 2 orders of magnitude lower than the previously reported IC_{50} value of LysM-CatD. The combination of AMB with these palmitoylated chitinase domains resulted in a strong enhancement of the antifungal activity. Intriguingly, the palmitoylated chitin-binding domain, LysM-Pal, showed the highest synergistic effect of the three chitinase domains despite a lack of chitin degradative activity. The palmitic acid motif of LysM-Pal probably functioned to deliver LysM to the chitin at the tip of the fungal hyphae by anchoring into the plasma membrane, which enhanced the destabilization of the chitin layer by the binding of LysM. Because both the chitin layer and the plasma membrane at the tip of the hyphae were damaged by LysM-Pal and AMB, the stability of the tip of hyphae was drastically reduced, resulting in lysis of the fungal cells. Mammalian cells do not have chitin, and therefore LysM is expected to be safe for use in mammals.

In chapter 3, based on the results with LysM-Q in the preceding chapter, I discussed the effect of the alkyl chain length of lipids such as octanoic acid (C8), dodecanoic acid (C12), and palmitic acid (C16) on the antifungal activity and their localization in the fungal cell wall. The lipid-peptide substrates with different alkyl chain length (C8-K, C12-K and C16-K) were synthesized with the addition of peptide sequence containing MTG-reactive lysine. Both LysM-Q and lipid-conjugated peptides were successfully crosslinked by MTG to yield lipidated LysMs (LysM-C8, -C12 and -C16) then tested the enhancement of antifungal activity when combined with AMB. Intriguingly, LysM-C12 and -C16 showed better antifungal activity compared with that of LysM-C8. Fluorescently labeled LysM-lipids confirmed their localization in the fungal cell wall. The confocal laser scanning microscopy (CLSM) showed that LysM-C12 and LysM-C16 exhibited much better penetration through the fungal cell wall compared with LysM-C8 and unmodified LysM-Q, suggesting the potential of protein delivery to the fungal cells through artificial lipidation. These findings were correlated with the antifungal activity of lipidated LysMs, by which its action depends on the alkyl chain length of lipids.

In chapter 4, the liposomal formulation was applied to encapsulate the Gibco™ Amphotericin B, a commercial amphotericin B solubilized into sodium deoxycholate, to prepare hybrid liposomal formulations. Furthermore, the formulation was combined with the LysM-Pal, and its antifungal activity was observed against *Trichoderma viride*. Hybrid liposomal formulations with different surface charges were prepared by combining a commercially available reagents to explore key factors in the antifungal activity. The characterization of AMB-loaded liposomal formulations (AMB-LFs),

including particle size distribution and zeta potential, showed that anionic and neutral AMB-LFs could stably encapsulate AMB. The combination of either anionic or neutral AMB-LFs with unmodified LysM decreased the minimum inhibitory concentration (MIC) of AMB. The combination of neutral AMB-LF with LysM-Pal resulted in a further decrease in the MIC compared with that of the neutral AMB-LF alone. The results obtained demonstrated the potential utility of lipid-based liposomal formulations of AMB combined with lipid-modified proteinaceous binders to tackle fungal infections.

5.2 Outlook and future prospects

As a direct result of a rise in the number of cancer patients treated with cytotoxic chemotherapeutic medications, which result in immunodeficiency, the number of patients who are immunocompromised has seen a substantial increase in recent years, and it allows for to use of high doses of drugs, leading the emerging threat of pathogens resistant to drugs. In addition, patients who have had procedures such as organ transplantation, catheterization, dialysis, or complex operations, are HIV positive, or are receiving therapy in an intensive care unit are at an increased risk of contracting a deadly fungal infection. Patients' most prevalent fungal infections are *Candida*, and *Aspergillus* species. There is a significant burden of fungal infections, and the advent of antibiotic resistance highlights the need for developing antifungal medication that is both more effective and cost-effective. Few antifungal medicines, mostly polyenes, and azoles constitute the whole of the treatment arsenal available to combat invasive fungal infections (triazoles). AMB is a prototypical example of a membrane-acting polyene antifungal drug with a wide range of activity. The effectiveness of AMB in warding off fungal infections is, without a shadow of a doubt, incomparable to that of any other medicine now on the

market. However, AMB formulation with deoxycholate acid, a conventional AMB, is accompanied by acute side effects, such as nausea and fever, as well as dose-related renal toxicity, which can occur in fifty to ninety percent of patients. Because of this, the patient must be hospitalized so that the vital monitoring of the drug's plasma level may occur. Consequently, there is an urgent need for the development of AMB that enhances the therapeutic index while simultaneously reducing toxicity. There are several strategies to eliminate the toxicity of AMB. Still, the strategies that introduce in the literature are still debated. One possibility the strategy can be accepted is a combination of the AMB with biologically active protein, like chitinase. Chitinase is believed safer than the combination with a chemical compound because the mode of action of chitinase is specifically targeted to degrade the chitin content on the cell walls of pathogenic fungi. Because the chitinase only acts with chitin, the possible toxicity will not occur. In this Ph.D. thesis, artificially lipidated chitinase has proven to improve antifungal activity at a low dose and decrease the AMB concentration, reducing AMB toxicity. The lipidation of proteins has attracted much attention because the lipidation of proteins dramatically alters their intrinsic functionalities, such as the pharmacologic properties of drugs. In addition, conjugation catalyzed by MTG provides the advantage of maintaining protein performance because it is suitable in a buffer solution adapted to human organ conditions. Based on the results in this thesis, the MTG-catalyzed conjugation reaction of Q-tagged chitinases and K-tagged lipids in a site-specific manner is a promising strategy for further application as a novel antifungal reagent. Considering the potential results from this thesis, the author also suggests evaluating the potency of lipidated chitinase with other antifungal drugs and investigating their activity using pathogenic fungi,

such as *Candida, Aspergillus*, and *Fusarium* strains. These fungi have significantly contributed to the threat to human health, livestock, and agriculture sectors.

ACKNOWLEDGEMENTS

To begin with, I would like to express my deepest appreciation to my advisor, Prof. Noriho Kamiya, for his guidance and support during the Ph.D. program at Kyushu University. It has been a tremendous pleasure and joy to have you as my academic adviser. Your clever but comprehensible ideas and great work ethic have inspired me in research activities and in everyday life. Under your guidance, I experienced significant growth in my knowledge, abilities, attitude, and self-assurance, which enabled me to become a better scientist. I would also want to thank my co-advisor, Prof. Masahiro Goto, for his assistance, counsel, and encouragement during my Ph.D. studies. I appreciate the insightful insights and perspective you provided throughout my time in this laboratory. I am really honored to be a part of Goto-Kamiya Laboratory. In addition, I would like to thank Prof. Hiroyuki Ijima for serving as the thesis adviser and as a member of the thesis committee. I really value your constructive recommendations, insightful questions, and insightful remarks.

I would like to thank Prof. Toki Taira and his colleagues from Ryukyu University, who assisted me in analyzing and teaching me how to interpret the antifungal activity test. I would like to thank Assistant Prof. Kosuke Minamihata, who helped me write the journal, and for his suggestion for my research. I would like to thank Assistant Prof. Rie Wakabayashi for helping me with the lab activity. Also, I would like to thank Mr. Ryo Sato and Mr. Hiromasa Taniguchi, who assisted me in the experiment of recombinant protein and protein purification, and I would like to thank and appreciate Mr. Takuya Komada for his immense contribution to the part of my thesis. I also gratefully thank my

admirable best friends, Mas Hendra and Mba Diah, who always have a way of making me happy and supporting me in all aspects.

I am appreciative to the Japanese Ministry of Education, Culture, Sport, and Technology (MEXT) for offering a scholarship. It has been an honor to have a chance for me as a MEXT scholar. Many individuals have contributed to the achievement of my Ph.D. study, Dr. Yopi and Prof. Uju from BRIN and IPB are to be thanked for introducing me to Kamiya-sensei. This great chance to join GK-Lab would not exist without your confidence and generosity. In addition, I would like to thank the Indonesian GK-Lab members (Mas Adroit, Kang Dani, Mas Wahyu, Mba Tyas, Mba Ainul, and Ghazian) for their support and collaboration. Thanks for the support, camaraderie, foreign students, and lab mates (Cai, Shihab, Moshikur, Rashed, Nabila, and others). Additionally, I would like to thank every member of GK-Lab and staff at Faculty Engineering, whom I cannot name individually, for their continual support, kind welcome, and wonderful experiences shared throughout my time in Japan. Lastly, I would like to thank my mother, father, brother, and sister for their unwavering support and many letters of encouragement about my professional pursuits. Exclusively for my father, who passed away in covid-19 pandemic, and my mother, I presented this Ph.D. to you. Even though you never get a formal education, you always want me to study until the doctoral level. Thank you for everything. Alhamdulillah, all praise is due to Allah, the omnipotent God who always protects, guides, and blesses my life. I give you thanks with each breath I take.

Fukuoka, July 2022

Pugoh Santoso